



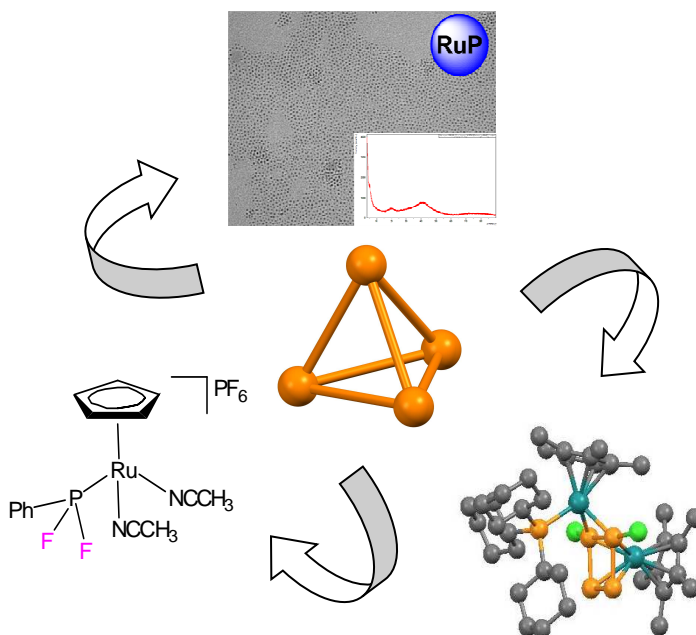
UNIVERSITÀ  
DEGLI STUDI  
FIRENZE

## DOTTORATO DI RICERCA IN SCIENZE CHIMICHE

CICLO XXVIII

COORDINATORE Prof. ANDREA GOTI

### SOME ADVANCES IN LOW VALENT PHOSPHORUS CHEMISTRY: FLUOROPHOSPHINES, NAKED POLYPHOSPHORUS COMPOUNDS AND METAL PHOSPHIDE NANOPARTICLES



#### **Dottorando**

Dott. Fuencisla Delgado Calvo

#### **Tutori**

Dr. Maria Caporali  
Dr. Maurizio Peruzzini





UNIVERSITÀ  
DEGLI STUDI  
FIRENZE

DOTTORATO DI RICERCA IN  
SCIENZE CHIMICHE

CICLO XXVIII

COORDINATORE Prof. ANDREA GOTI

SOME ADVANCES IN LOW VALENT PHOSPHORUS CHEMISTRY:  
FLUOROPHOSPHINES, NAKED POLYPHOSPHORUS COMPOUNDS AND  
METAL PHOSPHIDE NANOPARTICLES

Settore Scientifico Disciplinare CHIM/03

**Dottorando**

Dott. Fuencisla Delgado Calvo

---

*(firma)*

**Tutori**

Dr. Maria Caporali

---

*(firma)*  
Dr. Maurizio Peruzzini

---

*(firma)*

**Coordinatore**

Prof. Andrea Goti

---

*(firma)*

Anni 2013/2015



*A mi familia*



*“I was taught that the way of progress  
is neither swift nor easy”*

Marie Curie (1867-1934)





# Table of contents

## Chapter 1: Introduction

1.1 Overview	1
1.2 The element Phosphorus	3
1.2.1 Allotropes of elemental phosphorus	3
1.3 Reactivity of white phosphorus	7
1.3.1 Activation of P <sub>4</sub> by main group element	9
1.3.2 Activation of P <sub>4</sub> by transition metals	11
1.4 Phosphines and related compounds	27
1.4.1 Electronic and steric properties	28
1.4.2 Halophosphines	30
1.5 Metal phosphides	31
1.6 Aims of the thesis	33

## Chapter 2: XtalFluor-E, the key to ruthenium-coordinated fluorophosphines from phosphorous oxyacids

2.1 Overview	39
2.2 Introduction	41
2.3 Direct deoxofluorination of P-oxyacids	43
2.4 Synthesis and characterization of [CpRu(PPh <sub>3</sub> ) <sub>2</sub> (PF <sub>2</sub> R)]X	44
2.5 Synthesis and characterization of [Cp <sup>R</sup> Ru(CH <sub>3</sub> CN) <sub>3-x</sub> (PhPF <sub>2</sub> ) <sub>x</sub> ]PF <sub>6</sub>	48
2.6 Synthesis and characterization of [η <sup>6</sup> -( <i>p</i> -cym)RuCl <sub>2</sub> (PhPF <sub>2</sub> )]	51
2.7 Conclusions	53
2.8 Experimental section	54

### **Chapter 3: Activation of P<sub>4</sub> mediated by ruthenium(II) complexes**

3.1 Overview	69
3.2 Activation of P <sub>4</sub> by ruthenium(II) complexes: State-of-the-art	71
3.3 Activation and functionalization of white phosphorus by [Cp* <i>Ru</i> PCy <sub>3</sub> X] (X = Cl, Br, I)	74
3.3.1 Synthesis and characterization of [ <i>Cp</i> * <i>Ru</i> (PCy <sub>3</sub> )](μ <sub>2</sub> ,η <sup>2:4</sup> P <sub>4</sub> Cl <sub>2</sub> ){ <i>Ru</i> Cp* }	74
3.3.2 Synthesis and characterization of [ <i>Cp</i> * <i>Ru</i> (PCy <sub>3</sub> )](μ <sub>2</sub> ,η <sup>2:4</sup> P <sub>4</sub> Br <sub>2</sub> ){ <i>Ru</i> Cp* }	79
3.3.3 Activation of P <sub>4</sub> with [Cp* <i>Ru</i> PCy <sub>3</sub> I]	84
3.4 Conclusions	88
3.5 Experimental section	89

### **Chapter 4: Synthesis, characterization and preliminary catalytic studies of white phosphorus-based ruthenium phosphide “RuP” nanoparticles**

4.1 Overview	97
4.2 Introduction	99
4.3 Synthesis and characterization of RuP NPs	101
4.4 Catalytic tests	110
4.5 Conclusions	112
4.6 Experimental section	112

<b>Appendix</b>	119
<b>Curriculum vitae</b>	123

## **Introduction**

### **1.1 Overview**

In this introductory chapter different points related to the phosphorus chemistry will be mentioned. The opening section reports a general description of the element phosphorus and its allotropic modifications before taking into detailed consideration the reactivity of white phosphorus, emphasizing on the production of organophosphorus compounds through catalytic processes involving the activation of  $P_4$  mediated by transition metal complexes. The second section reports a brief introduction about the importance of phosphines ligands in catalysis, particularly addressing the role of fluorophosphine ligands. Finally, the last section deals with the synthesis of metal phosphides nanoparticles, which are of great interest on diverse fields, particularly in catalysis, aiming at  $P_4$ -derived metal phosphide nanoparticles.

## *Chapter 1*

## 1.2 The element Phosphorus

Phosphorus (P) is a chemical element whose name is derived from the Greek φώς ‘phos’ meaning “light” and φόρος ‘phoros’ meaning “bearer”. It is the 11<sup>th</sup> element most abundant on the earth and it is essential to all life. The average human body contains about 650 grams of P. It is necessary for the formation and maintenance of bones and teeth in all vertebrates, mainly in the form of hydroxyapatite  $[\text{Ca}_{10}(\text{PO}_4)_6(\text{OH})_2]$ . Phosphorus, as phosphate form, is vital at cellular level. It is a key structural component of DNA and RNA, being part of the backbone of the molecule, sugar phosphates form the helical structure of every molecule. It provides the orientation of the phospholipids and, consequently, the structural characteristics of the cell membrane. ATP (adenosine triphosphate) is the principal molecule responsible of the intracellular energy transport.<sup>1,2</sup>

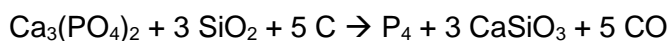
### 1.2.1 Allotropes of elemental phosphorus

Phosphorus as elemental form has different allotropes: white, red, violet and black.<sup>3</sup>

**White phosphorus**  $[\text{P}_4]$  is the most common and reactive and the least stable allotrope of phosphorus. It is a waxy white or yellowish solid, with a characteristic garlic smell and it is highly flammable when it is in contact with air. Industrially, production of white phosphorus uses the Boyle process, see **Scheme 1.1.**, where phosphate rocks are reacted with silica (melting agent) and coke (reducing agent) in an electric furnace at 1400–1500 °C. At these temperature, phosphate anion is reduced to

## Chapter 1

phosphorus vapor  $P_2$ , which is condensed into solid  $P_4$  under water,<sup>4</sup> the suitable medium used to store it avoiding its violent oxidation or air combustion. Besides, different methods of purification of white phosphorus are used.



**Scheme 1.1.** Industrial production of white phosphorus.

White phosphorus has a unique structure formed by discrete tetrahedral tetraatomic molecules with P-P distances of 2.21 pm and P-P-P angle of  $60^\circ$ , see **Figure 1.1**. Depending on the temperature and pressure, three modifications of white phosphorus ( $\alpha$ -,  $\beta$ -,  $\gamma$ -) are possible.  $\alpha$ - $P_4$  form occurs at room temperature as a body-centered cubic plastic crystal with  $P_4$  molecules dynamically rotating around their centers of gravity.  $\beta$ - $P_4$  form exhibits an hexagonal crystal structure, whose molecules have fixed orientations. It is stable at room temperature and pressure higher than 1.0 GPa or at temperatures below 197 K and ambient pressure. Instead,  $\gamma$ - $P_4$ , triclinic modification, is also stable at low temperature but up to 160 K.<sup>5</sup>

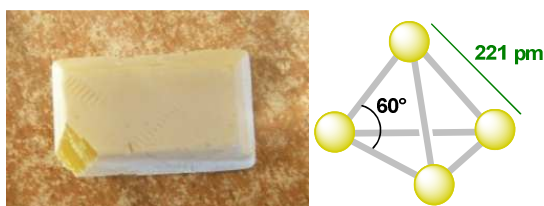


**Figure 1.1.** a) solid white phosphorus. b) tetrahedral structure of white phosphorus.

White phosphorus melts at a temperature of  $44^\circ C$ . When  $P_4$  is heated upon  $800^\circ C$ , dissociation on phosphorus vapor containing diatomic  $P_2$

## Chapter 1

molecules starts, being this latter the thermodynamically stable form at temperatures above 1200 °C. At temperatures above 2000 °C, the diphosphorus molecule is dissociated into atomic phosphorus.<sup>6</sup>

White phosphorus is extremely toxic, hepatic and renal damages are observed as well as blood disorders, such as anemia and leucopenia.<sup>7</sup> Besides, in the 19<sup>th</sup> and early 20<sup>th</sup>, prolonged exposures to white phosphorus without proper safeguards in matches industry led to a bone osteonecrosis in the jaws, chronic disease commonly called “Phossy jaw”.<sup>8</sup>

**Red phosphorus [P<sub>n</sub>]** is an amorphous polymeric material, made of long chains of phosphorus atoms, much more stable, less reactive, less toxic and easy to handle. It ignites exposed to air at temperatures only above 240 °C or by a strong impact or friction at room temperature. It oxidizes slowly at room temperature emitting phosphorescence. Red phosphorus can be prepared exposing white phosphorus to sunlight or on heating at 250-350 °C, using iodine as catalyst. It can be transformed into white phosphorus after heating up to 260 °C.<sup>9</sup> It is a component of striking surfaces for safety matches.<sup>10</sup>

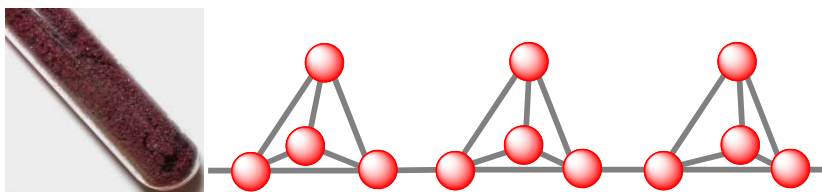


**Figure 1.2.** Molecular chain structure of red phosphorus.

**Violet phosphorus**, also called ‘Hittorf phosphorus’, is a crystalline monoclinic or rhombohedral allotrope. It is also much less reactive than

## Chapter 1

white phosphorus and it is not conductor of the electricity. It is obtained after heating red phosphorus for a long time at 530 °C. It can also be prepared by dissolving white phosphorus in molten lead at 500 °C. It does not ignite below 400°C, it is not poisonous and does not glow in the air.<sup>11</sup>

**Black phosphorus** is the most stable allotrope of phosphorus and the least reactive. It can be prepared from white phosphorus at high pressure,<sup>12</sup> using mercury as catalyst,<sup>13</sup> or liquid bismuth<sup>14</sup> or from red phosphorus.<sup>15,16</sup> Black phosphorus has high density. It crystallizes in orthorhombic form at standard conditions consisting of parallel puckered double layers.<sup>17</sup> Optical,<sup>18</sup> semiconducting,<sup>19</sup> properties of black phosphorus have been described.



**Figure 1.3.** Crystals of black phosphorus.

As graphite, black phosphorus can be exfoliated either by Scotch tape method or by liquid phase exfoliation, producing a 2D material, named phosphorene. Exfoliated few-layer black phosphorus see **Figure 1.4.**, are very sensitive to air, moisture and light, studies on its degradation are in progress, meanwhile a variety of applications as in FET (field effect transistors), solar cell, lithium and sodium ion batteries, or gas sensors have been demonstrated.<sup>20</sup>



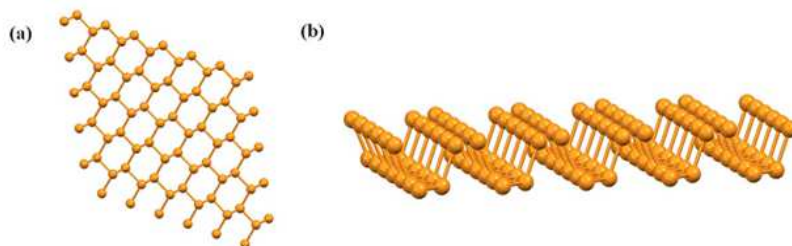
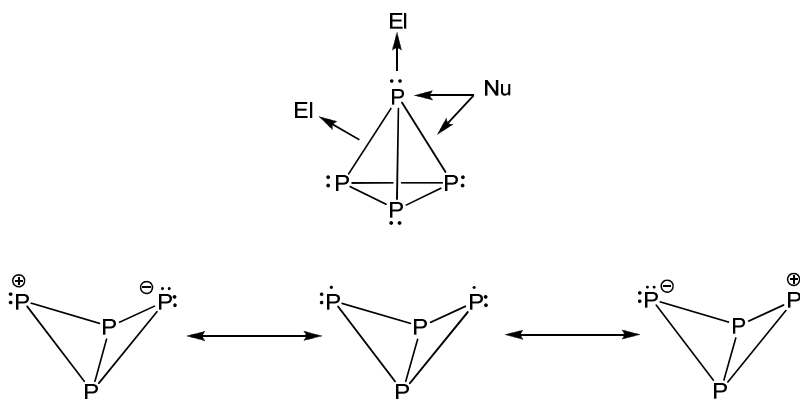


**Figure 1.4.** Single layer black phosphorus a) top view b) side view.<sup>21</sup>

### 1.3 Reactivity of white phosphorus

The high reactivity and instability of  $P_4$  is related to the high bond strain energy of the tetrahedron cage.<sup>22</sup> The general reactivity pattern of  $P_4$  is shown in **Scheme 1.2.**, electron lone pairs at the P apexes and the filled  $\sigma$ -orbital of the P-P bonds are the places of main nucleophilicity where the outer electrophile is directed.

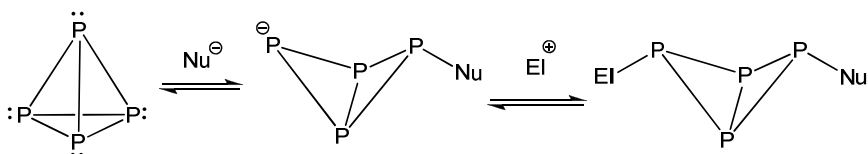


**Scheme 1.2.** Reactivity pattern of white phosphorus in the presence of electrophiles and nucleophiles.

## Chapter 1

*Ab initio* calculations on the protonation of  $P_4$  cage were reported<sup>23</sup> showing the favored protonation is carried out at a vertex of the  $P_4$  molecule, followed by an edge protonation. Besides, computational methods to calculate the basicity of  $P_4$  in gaseous phase were described revealing that the stability of  $H^+$  bridged opened P-P edge structure is  $45.2 \text{ kJ mol}^{-1}$  more than an apex-attached molecule.<sup>24</sup>

White phosphorus may react with electrophiles only in the presence of a previously added nucleophile. Indeed, after a nucleophilic species has promoted the cleavage of a P-P bond of the  $P_4$  cage a site with electron density, as shown in **Scheme 1.3.**, is generated at the opposite wing, which is then prone to react with an electrophile. Strong nucleophiles drive the equilibrium to the right, while the reaction of  $P_4$  with a weak nucleophile is pushed onwards by the presence of an electrophile.

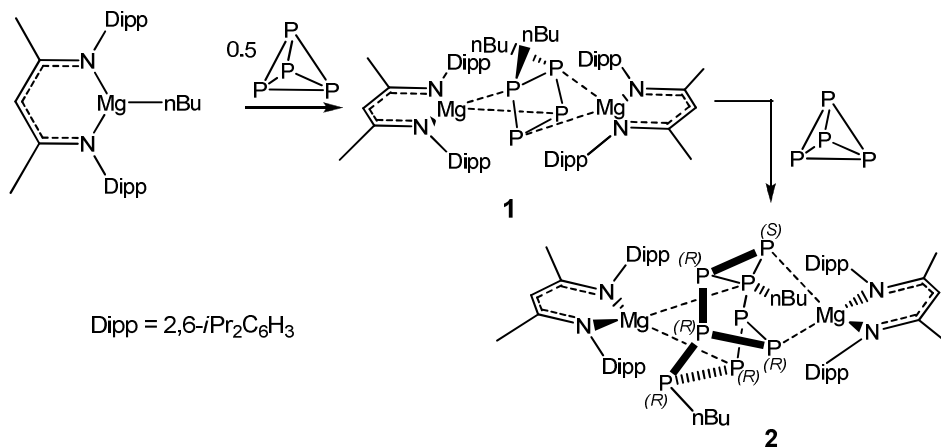


**Scheme 1.3.**

The nucleophilic attack on white phosphorus by main group element or transition metals has historically been one of the most studied methods of white phosphorus derivatization and will be discussed in the following sections.

### 1.3.1. Activation of P<sub>4</sub> by main group element

Activation of white phosphorus by alkali metals gives the formation of alkali metal phosphide or oligophosphides, depending on the conditions and the stoichiometry of the reaction. The reactivity of half equivalent of white phosphorus with the organomagnesium complex  $[(L^{\text{Dipp}})\text{Mg}(n\text{-Bu})]$  ( $L^{\text{Dipp}} = 2,6\text{-}i\text{PrC}_6\text{H}_3$ ) was recently studied<sup>25</sup> and led to the formation of a new dinuclear complex  $[(L^{\text{Dipp}})\text{Mg}]_2[n\text{-Bu}_2\text{P}_4]$  (**1**) bearing a non-planar functionalized dianion,  $[n\text{-Bu}_2\text{P}_4]^{2-}$  as shown in **Scheme 1.4**. By adding to the starting organomagnesium reagent a stoichiometric amount of P<sub>4</sub> and keeping for one week at room temperature, the dimer  $[(L^{\text{Dipp}})\text{Mg}]_2[n\text{-Bu}_2\text{P}_8]$  (**2**) containing the cluster dianion  $[n\text{-Bu}_2\text{P}_8]^{2-}$  was isolated. The latter could be obtained as well by heating  $[(L^{\text{Dipp}})\text{Mg}]_2[n\text{-Bu}_2\text{P}_4]$  for 2 days.

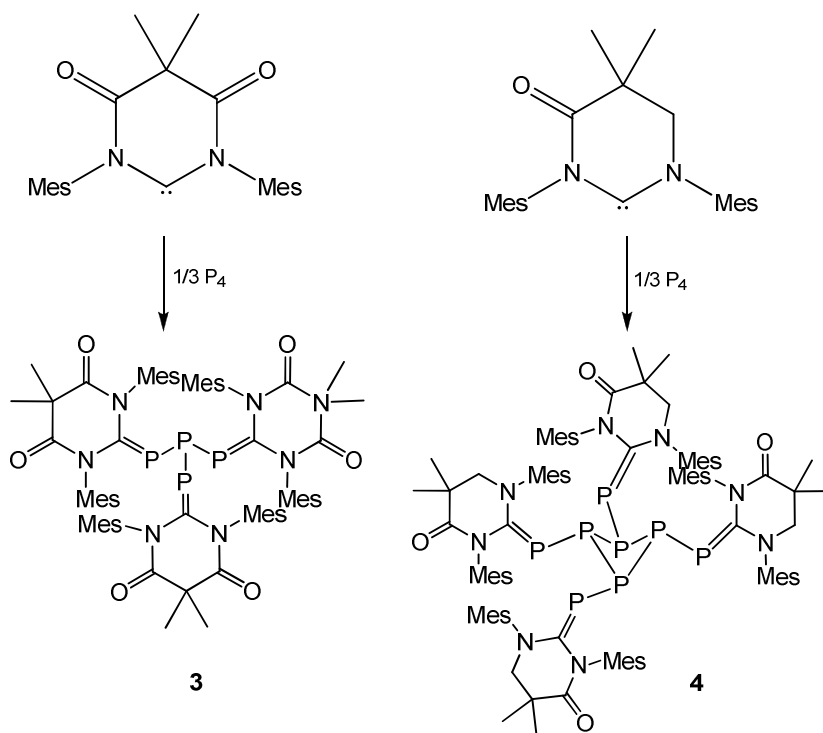


**Scheme 1.4.** P<sub>4</sub> activation with an organomagnesium complex.

Intriguing studies from the group of Guy Bertrand, highlight carbenes as highly potential candidate to activate white phosphorus affording its fragmentation or re-aggregation. Carbonyl-decorated carbenes (**CDCs**)

## Chapter 1

are a kind of carbenes containing different number of carbonyl groups in different positions in the backbone. They are very reactive and the activation of white phosphorus is analog to the N-heterocyclic carbenes (NHCs), the most nucleophilic carbenes, which lead to the formation of  $P_{12}$ -containing compound capped by two NHC ligands.<sup>26</sup> In case of CDCs,<sup>27</sup> the electrophilicity of the carbenes influences the product. For a weakly electrophilic carbene, the linear  $P_4$ -diphosphene **3** is formed while using a strongly electrophilic carbene the  $P_8$  cluster **4** is obtained. (Scheme 1.5.)

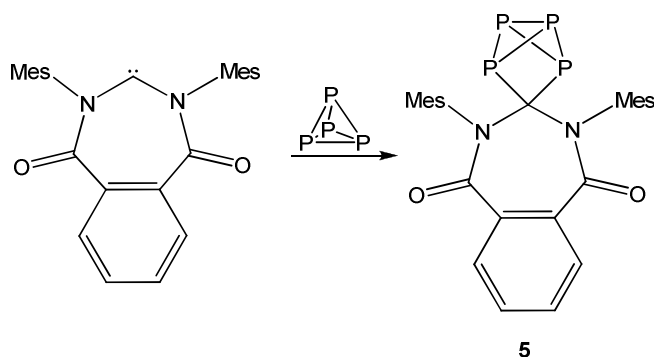


**Scheme 1.5.** Reaction of white phosphorus with carbonyl-decorated carbenes.

In case of electrophilic cyclic six-membered diamido carbenes, (DACs) a donor stabilized  $P_8$  unit can be prepared from white phosphorus. This  $P_8$

## Chapter 1

cluster, as for **4**, could also be prepared with the less electrophilic cyclic (alkyl)(amino) carbenes (CAACs) if  $P_4$  is in excess, suggesting that the outcome of the reactions of carbenes with white phosphorus could be influenced by stoichiometry,<sup>28</sup> in contrast with the  $P_4$ -bearing molecules favor the diastereoselective formation of two phosphorus-carbon bonds. In addition, the reaction of white phosphorus with the extremely electrophilic seven-membered cyclic benzamidocarbene shown in **Scheme 1.6**. led to the isolation of an organophosphorus derivatives where  $P_4$  has a butterfly geometry **5**, resembling the eta-2 coordinated towards a metal center.<sup>29</sup>



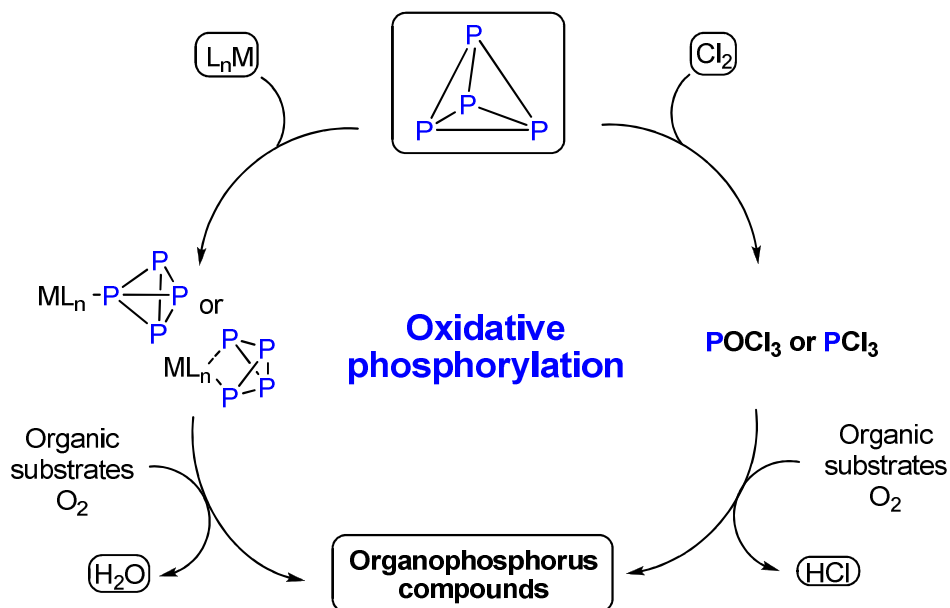
**Scheme 1.6.** Reaction of seven membered cyclic benzamidocarbene with white phosphorus.

### 1.3.2 Activation of $P_4$ by transition metals

After the discovery in the 70's that metal complexes can coordinate, activate and transform white phosphorus, a period of intensive research on the topic associated with transition metal-mediated activation of  $P_4$  started.

## Chapter 1

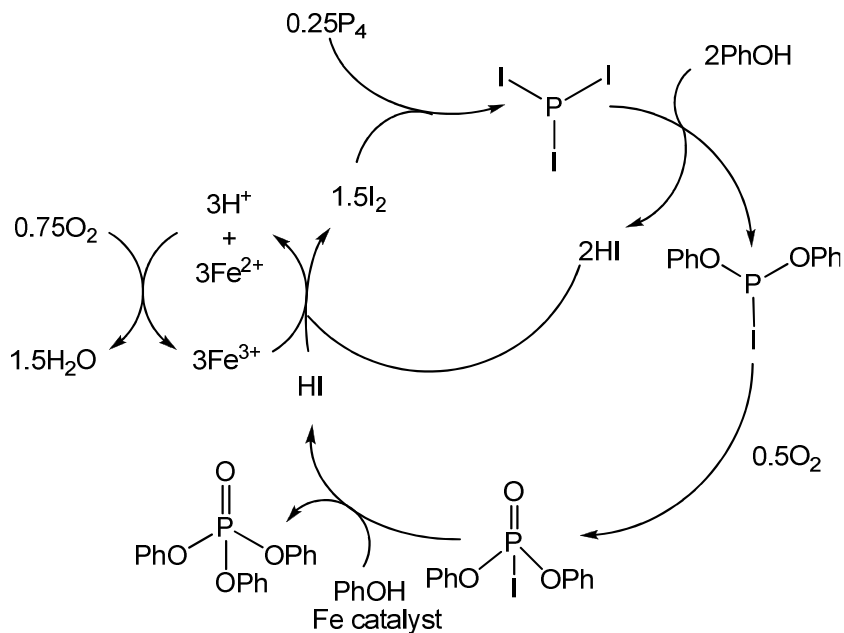
As summarized by the right side of **Scheme 1.7.**, white phosphorus is nowadays the starting material to synthesize most of the organophosphorus compounds, by following the chlorination route. This encompasses the reaction of white phosphorus with chlorine to afford either  $\text{PCl}_3$  or  $\text{POCl}_3$ ; in a following step the phosphorus chlorides are used to carry out the phosphorylation of an organic substrate to eventually afford the desired organophosphorus derivative. This worldwide used industrial technology is environmentally harmful because requires large quantities of  $\text{Cl}_2$  and a huge amount of  $\text{HCl}$  is formed as by-product, requiring high cost for its proper disposal. For this reason, the ideal, environmentally friendly process that may combine directly white phosphorus and an organic compound, could be a catalytic process, mediated by a transition metal complex as shown in the left side of **Scheme 1.7.** In the latter route, a metal-mediated catalytic process would involve the presence of oxygen as mild oxidant and would produce water as a by-product.<sup>30</sup>



**Scheme 1.7.** Traditional (right) and catalytic (left) routes to synthesized organophosphorus compounds

A relevant contribution on this regard comes from Kilian *et al.*<sup>31</sup>, who recently found out that  $P_4$  can react with phenol in aerobic conditions in the presence of iodine and  $Fe(acac)_3$  as catalyst affording quantitative conversion to triphenyl phosphate and producing as by-product only water. Mechanistic studies were carried out to understand the reaction pathway and in particular the rate-limiting steps in order to optimize the process. Iodine, also used in catalytic amount, served to oxidize  $P_4$  to P(III) by forming  $PI_3$ . Additionally, it was observed that the reaction did not proceed under anaerobic conditions, being oxygen indispensable first to oxidize P(III) to P(V) in the catalytic step where  $PI_3$  reacted with phenol. Secondly,  $O_2$  was responsible for the re-oxidation of the by-product HI back to iodine, as shown in **Scheme 1.8**. The reaction, carried out at 80 °C and with a loading of 25 mol%  $Fe(acac)_3$ , was applied

successfully also to functionalized phenols giving high conversion and very good selectivity.



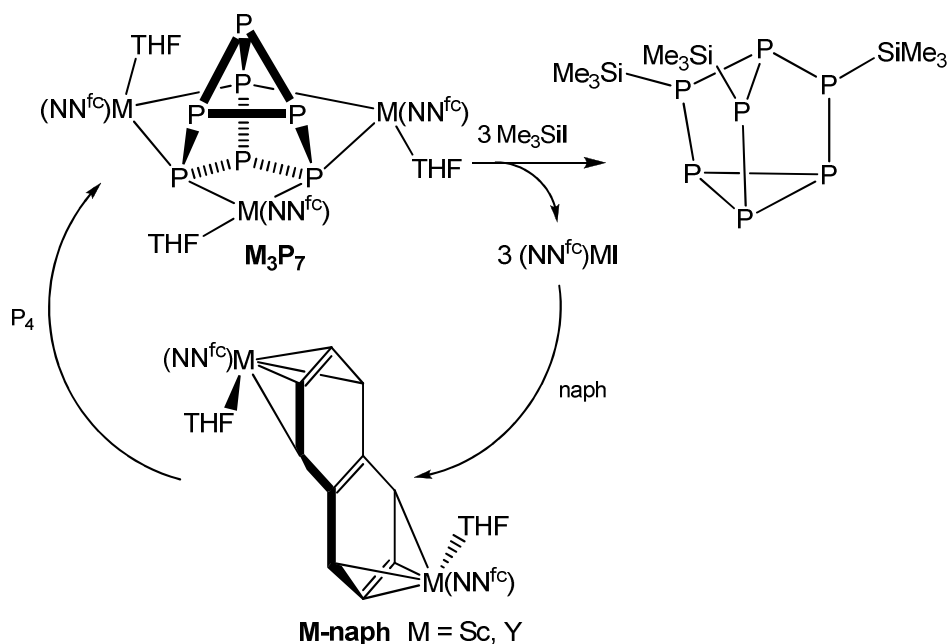
**Scheme 1.8.** Iron-catalyzed aerobic reaction of white phosphorus with phenol.

The feasibility of a catalytic process, in which white phosphorus is selectively and quantitatively converted into highly valuable phosphines was shown by Cummins<sup>32</sup> who published a niobium-mediated catalytic cycle producing phosphorus-rich organic molecules from  $P_4$  through activation, functionalization, and transfer reactions.

Recently, Diaconescu and co-workers<sup>33</sup> explored the activation of white phosphorus in the presence of early transition metals aiming to the development of a catalytic protocol to transform  $P_4$  directly into organophosphorus compounds. The direct reaction of  $P_4$  with group 3 metal complexes,  $[(NN^{fc})Sc]_2(\mu-C_{10}H_8)$   $[(Sc_2-naph)]$  and



$[(\text{NN}^{\text{fc}})\text{Y}(\text{THF})]_2(\mu\text{-C}_{10}\text{H}_8)$  [ $\text{Y}_2\text{-naph}$ ], where  $\text{NN}^{\text{fc}} = 1,1'$ - $\text{fc}(\text{NSi}^t\text{BuMe}_2)_2$ ,  $\text{fc} = \text{ferrocenylene}$ ,  $\text{naph} = \text{naphthalene}$  ( $\mu\text{-C}_{10}\text{H}_8$ ), leads to the formation of a polyphosphide cage,  $\text{P}_7^{3-}$ , also known as Zintl anion, which behave as a ligand for scandium and yttrium, see **Scheme 1.6**. Reaction of both  $\text{Sc}_3\text{P}_7$  and  $\text{Y}_3\text{P}_7$  with three equivalents of  $\text{Me}_3\text{SiI}$  gave  $(\text{Me}_3\text{Si})_3\text{P}_7$  and yielded as by-product the salt scandium/yttrium iodide, which can coordinate the ferrocenylene and naphthalene ligands yielding back the arene complex capable of further activating an equimolar amount of  $\text{P}_4$  closing the catalytic cycle, as shown in **Scheme 1.9**. This constitutes the first example of transferring the Zintl anion  $[\text{P}_7]^{3-}$  to an organic species and establishes a synthetic cycle for the direct transformation of  $\text{P}_4$  into an organophosphorus cage.

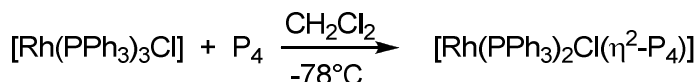


**Scheme 1.9.** Catalytic cycle mediated by either scandium or yttrium.

## Chapter 1

Organophosphorus compounds have a plethora of applications. They are used in agriculture, as pesticides or herbicides, in catalytic processes as ligands towards metal centers, in the industry of lubricants, flame retardants and additives for plastic materials and are becoming more and more important in different biological fields with special attention to antiviral compounds and specific drugs for the treatment of bone tissue diseases. Military and nuclear industry applications complete the large scenario of uses of organophosphorus compounds. Therefore, there is a great interest on the development of eco-friendly pathways for the preparation of such derivatives, in particular the search for catalytic processes that blends P<sub>4</sub> with organic substrates, represents a very important target for industry. This has stimulated several academic and industrial research teams to study the activation of P<sub>4</sub> by a metal complex, in stoichiometric ratio, thus mimicking the initial step of a possible catalytic cycle capable of affording specific organophosphorus derivatives from elemental phosphorus and organic substrates.

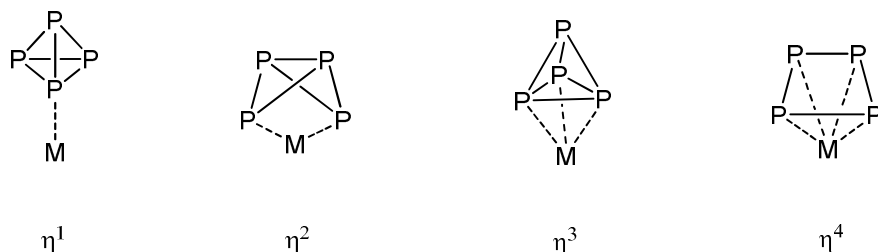
Since the discovery in 1971 by Ginsberg and Lindsell that P<sub>4</sub> can react with the Wilkinson complex<sup>34</sup> affording the first transition metal complex containing white phosphorus as a ligand [Rh(PPh<sub>3</sub>)<sub>2</sub>Cl(η<sup>2</sup>-P<sub>4</sub>)] **6**, see **Scheme 1.10.**, the reactivity of P<sub>4</sub> towards a variety of transition metal fragments has been studied.



**Scheme 1.10.** Synthesis of [Rh(PPh<sub>3</sub>)<sub>2</sub>Cl(η<sup>2</sup>-P<sub>4</sub>)]

## Chapter 1

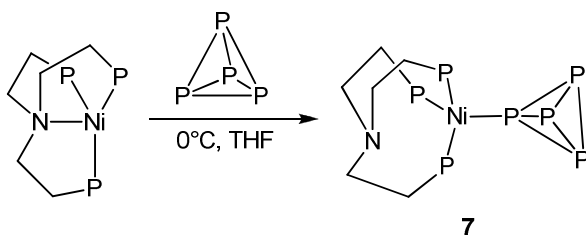
Various coordination topologies of white phosphorus towards the metal center have been elucidated and are summarised in **Scheme 1.11**.



**Scheme 1.11.** Coordination modes of P<sub>4</sub> towards a transition metal.

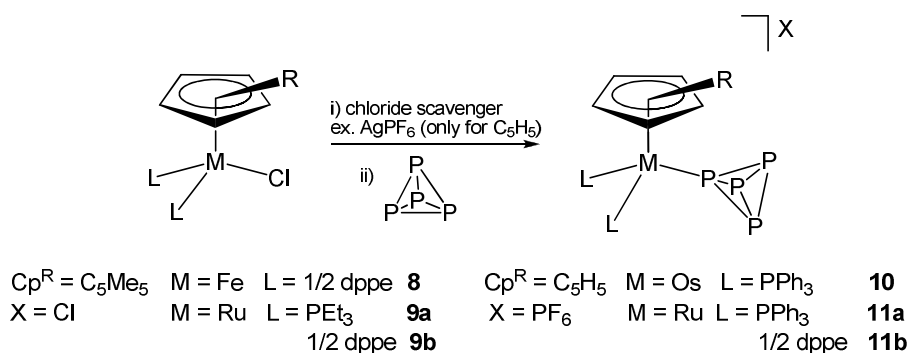
Some representative examples on the activation of white phosphorus mediated by late transition metal fragments showing the different coordination modes will be described below.

The first complex containing the intact  $\eta^1$ -P<sub>4</sub> ligand was prepared by Sacconi *et al.*<sup>35</sup> By reacting the trigonal pyramidal complex [(NP<sub>3</sub>)Ni] where [NP<sub>3</sub> = N(CH<sub>2</sub>CH<sub>2</sub>PPh<sub>2</sub>)<sub>3</sub>] with P<sub>4</sub> at 0 °C, a N-Ni decoordination took place while white phosphorus enters into the coordination sphere of nickel as monohapto *tetrahedro*-tetraphosphorus ligand forming the product [(NP<sub>3</sub>)Ni( $\eta^1$ -P<sub>4</sub>)] **7** (**Scheme 1.12.**) where a tetrahedral geometry around the metal is achieved.



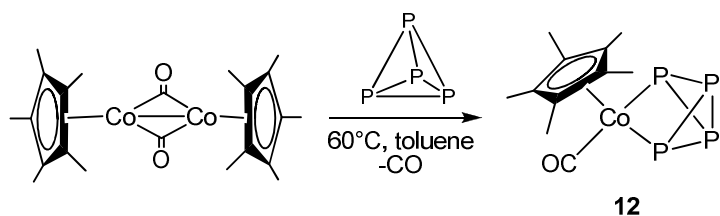
**Scheme 1.12.** Preparation of [(NP<sub>3</sub>)Ni( $\eta^1$ -P<sub>4</sub>)]

After the work of Sacconi, Stoppioni and Peruzzini have successfully carried out the coordination of white phosphorus as an intact *tetrahedro*- $\eta^1$ -P<sub>4</sub> ligand towards a variety of metals including rhenium, cobalt, rhodium, iron, ruthenium and osmium. Of particular interest, the synthesis of metal complexes of formula [Cp<sup>R</sup>M(L)<sub>2</sub>( $\eta^1$ -P<sub>4</sub>)]<sup>+</sup> (Cp<sup>R</sup> = C<sub>5</sub>Me<sub>5</sub>, M = Fe, L = 1/2 dppe **8**; M = Ru, L = PEt<sub>3</sub> **9a**, dppe **9b**.<sup>36</sup> Cp<sup>R</sup> = C<sub>5</sub>H<sub>5</sub>, M = Os, L = PPh<sub>3</sub> **10**;<sup>37</sup> M = Ru, L = PPh<sub>3</sub> **11a**,<sup>38</sup> 1/2 dppe **11b**<sup>39</sup>) was carried out in mild conditions as shown in **Scheme 1.13**. Complexes bearing Cp ligand need firstly the abstraction of the chloride ligand by the action of a chloride scavenger as AgOTf or TlPF<sub>6</sub>, followed by the addition of P<sub>4</sub>. These compounds, although may be manipulated in the air without decomposition, are not stable towards traces of water, because the P<sub>4</sub> moiety a complicated metal-mediated hydrolytic process resulting in the formation of PH<sub>3</sub>, which coordinates to ruthenium and free oxyacids, including H<sub>3</sub>PO<sub>3</sub>, H<sub>3</sub>PO<sub>2</sub>, and, likely, H<sub>3</sub>PO. On the other hand, the addition of a chloride scavenger is not necessary for complexes bearing Cp\*, where the chloride ligand is easily displaced by P<sub>4</sub>. Unexpectedly, these latter complexes are stable towards hydrolysis at room temperature.



**Scheme 1.13.** Synthesis of complexes [Cp<sup>R</sup>M(L)<sub>2</sub>( $\eta^1$ -P<sub>4</sub>)]<sup>+</sup>.

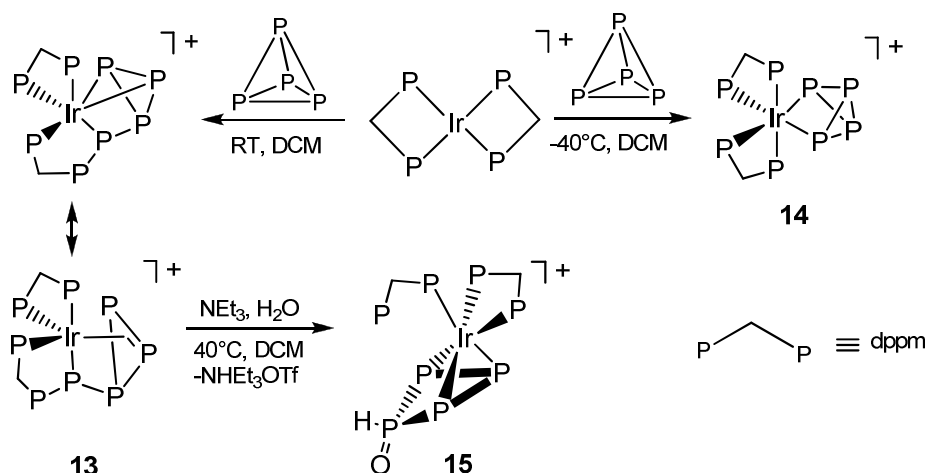
As reported above, after the first complex bearing  $P_4$  as a dihapto ligand,  $[\text{Rh}(\text{PPh}_3)_2\text{Cl}(\eta^2\text{-P}_4)]$ , was prepared by Ginsberg, analog rhodium and iridium complexes containing phosphines other than triphenylphosphine were prepared.<sup>34</sup> As shown in **Scheme 1.14.**, Scherer *et al.*<sup>40</sup> prepared the complex  $[\text{Cp}^*\text{Co}(\eta^2\text{-P}_4)(\text{CO})]$  **12** by thermolysis of the dimer  $[\text{Cp}^*\text{Co}(\mu\text{-CO})_2]$  in the presence of an excess of white phosphorus at  $60^\circ\text{C}$  and after losing a CO, a complex incorporating  $P_4$  as a dihapto ligand was isolated.



**Scheme 1.14.** Synthesis of  $[\text{Cp}^*\text{Co}(\eta^2\text{-P}_4)(\text{CO})]$  by thermolysis.

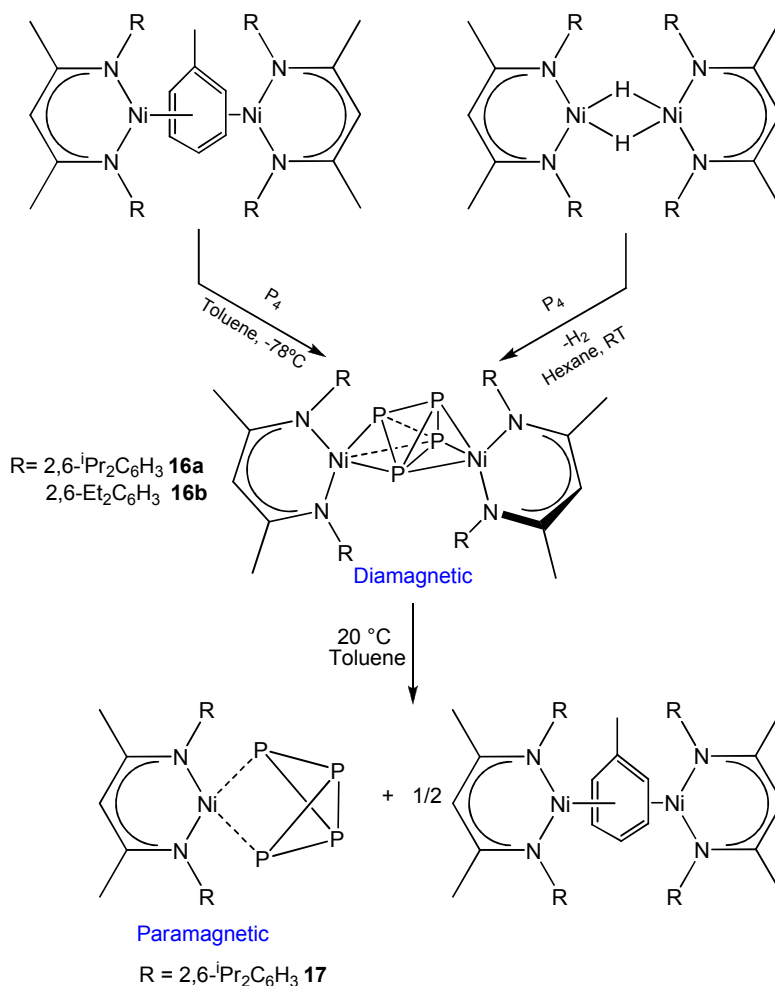
Reaction of the highly reactive complex  $[\text{Ir}(\text{dppm})_2]\text{OTf}$  ( $\text{OTf} = \text{CF}_3\text{SO}_3$ ,  $\text{dppm} = \text{Ph}_2\text{CH}_2\text{PPh}_2$ ) with white phosphorus at room temperature resulted in the nucleophilic attack of one terminal  $\text{Ph}_2\text{P}$  end of the  $\text{dppm}$  to the  $P_4$  molecule, leading to  $[\text{Ir}(\text{dppm})(\text{Ph}_2\text{PCH}_2\text{PPh}_2\text{PPPP})]\text{OTf}$  (**13**) which contains a new unexpected ligand constituted by a chain of five phosphorus atoms,  $\text{Ph}_2\text{PCH}_2\text{PPh}_2\text{PPPP}$ , coordinated to iridium. **13** exhibits a pseudo-octahedral coordination around the metal, see **Scheme 1.15.** A possible resonance structure of this ligand containing a dihapto  $\text{P}=\text{P}$  bond is also shown. On the other hand, the same reaction carried out at  $-40^\circ\text{C}$  allowed us to isolate the iridium complex  $[\text{Ir}(\text{dppm})_2(\eta^2\text{-P}_4)]\text{OTf}$  (**14**) where white phosphorus behaves as a dihapto ligand, assuming a butterfly geometry.<sup>41</sup> Reaction of **13** with water in the presence of an

amine allowed the functionalization of the polyphosphorus ligand  $\text{Ph}_2\text{PCH}_2\text{PPh}_2\text{PPPP}$  and gave  $[\text{Ir}(\kappa^2\text{-dppm})(\kappa^1\text{-dppm})\{\eta^3\text{-P}_3\text{P}(\text{O})\text{H}\}]^{\text{15}}$  that displays a rare  $\eta^3\text{-P}_3\text{P}(\text{O})\text{H}$  puckered tetraphosphabutadienylyde ring.<sup>42</sup>



**Scheme 1.15.** Synthesis of the complexes **14** and **15**.

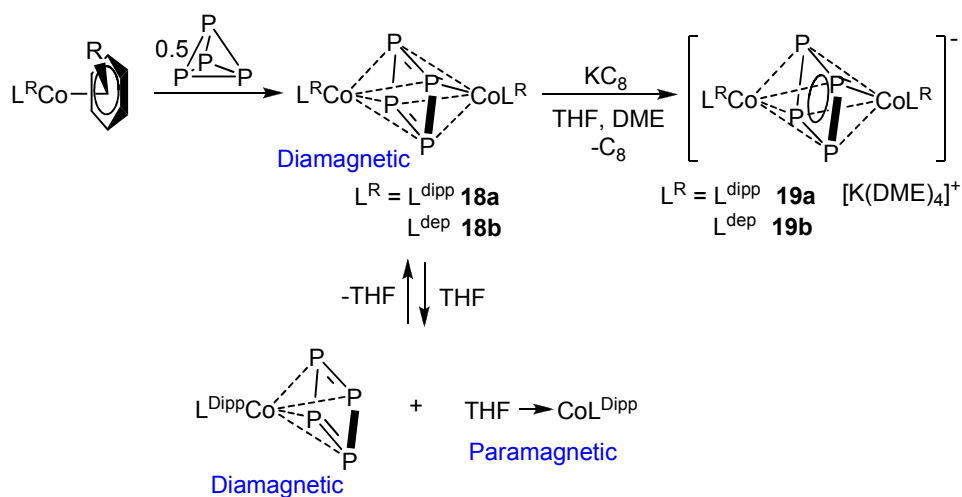
While  $\eta^1\text{-}$  and  $\eta^2\text{-P}_4$  species were well known since the first studies dealing with the coordination chemistry of  $\text{P}_4$ , the first example of  $\eta^3\text{-P}_4$  coordination topology was reported in 2010 by Driess *et al.*<sup>43</sup> As shown in **Scheme 1.16.**, white phosphorus was reacted with dinuclear  $\beta$ -diketiminato nickel(I) complexes affording dinuclear derivatives  $[(\text{LNi}^{\text{I}})_2\text{P}_4]$  (L:  $\text{L}^{\text{iPr}} = \text{CH}[\text{CMeN}(2,6\text{-iPr}_2\text{C}_6\text{H}_3)]_2$  **16a**,  $\text{L}^{\text{Et}} = \text{CH}[\text{CMeN}(2,6\text{-Et}_2\text{C}_6\text{H}_3)]_2$  **16b**) bearing a double  $\eta^3\text{-P}_4$  moiety, where three phosphorus atoms are coordinated to each metal center without reduction of  $\text{P}_4$ . These complexes are diamagnetic in the solid state but **16a** can reversibly dissociate in solution into a paramagnetic  $\eta^2\text{-P}_4$  Ni<sup>I</sup> complex **17** and  $[(\text{L}^{\text{iPr}}\text{Ni})_2 \cdot (\text{toluene})]$ .



**Scheme 1.16.** Activation of  $\text{P}_4$  mediated by  $\beta$ -diketiminato nickel(I) complexes.

Driess *et al.*<sup>44</sup> studied also the reactivity of white phosphorus with  $\beta$ -diketiminato cobalt(I) complexes and isolated successfully the first complexes bearing the neutral tetraphosphacyclobutadiene ligand  $[(\text{LCo})_2(\mu_2:\eta^4,\eta^4\text{-P}_4)]$  (L:  $\text{L}^{\text{Dipp}} = \text{CH}[\text{CHN}(2,6\text{-}^i\text{Pr}_2\text{C}_6\text{H}_3)]_2$  **18a**,  $\text{L}^{\text{Dep}} = \text{CH}[\text{CMeN}(2,6\text{-Et}_2\text{C}_6\text{H}_3)]_2$  **18b**), (Scheme 1.17.), whose molecular structure contains a  $[\text{Co}_2(\mu^2:\eta^4,\eta^4\text{-P}_4)]$  octahedral core, coordinated by

two slightly puckered  $\beta$ -diketiminato ligands. The  $P_4$  unit featured by complexes **18** is planar with two long and two short P-P bonds which form a rectangular arrangement of P-atoms. These complexes are diamagnetic in the solid state but their dissociation in solution led to paramagnetic species, as described above for Ni(I) complex **16a**. Mixed-valent monoanionic complexes  $[(LCo^{II/III})_2(\mu_2:\eta^4,\eta^4-P_4)][K(DME)_4]$  ( $L = L^{Dipp}$  **19a**,  $L^{Dep}$  **19b**; DME = dimethoxyethane), containing an almost square planar cyclo- $P_4^{2-}$  unit, with  $\pi$ -electron delocalization within the  $P_4$  ring, were isolated after reduction of **18** with an equimolar amount of  $KC_8$  (see **Scheme 1.17**).

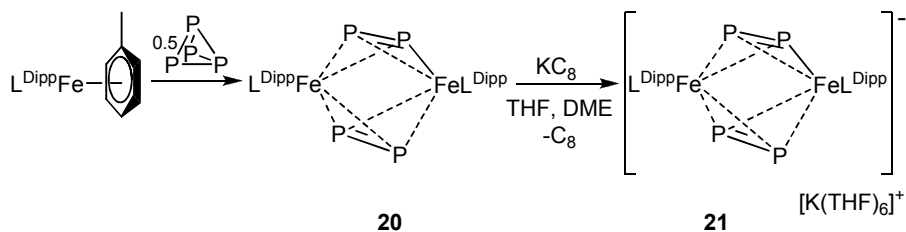


**Scheme 1.17.** Activation of  $P_4$  mediated by  $\beta$ -diketiminato Co(I) complexes.

Treatment of  $[(L^{Dipp}Fe^I)_2\text{toluene}]$  with  $P_4$  gave the dinuclear complex  $[(L^{Dipp}Fe^{III})_2(\mu_2:\eta^2,\eta^2-P_2)_2]$  (**20**) with two dianionic  $P_2$  units, see **Scheme 1.18**. Further reduction with  $KC_8$  afforded the mixed-valent complex  $[(L^{Dipp}Fe^{II/III})_2(\mu_2:\eta^2,\eta^2-P_2)_2][K(THF)_6]$  (**21**), with geometrical parameters of the ligands almost identical to those observed for the precursor; only a

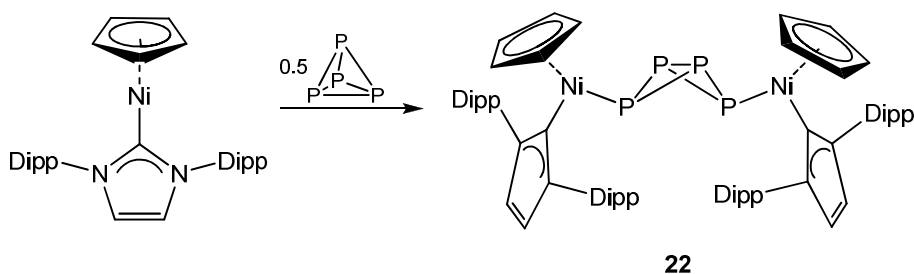


slight variation on the P-P distances was observed. All these complexes are paramagnetic in solution and in the solid state.<sup>45</sup> (**Scheme 1.18.**)



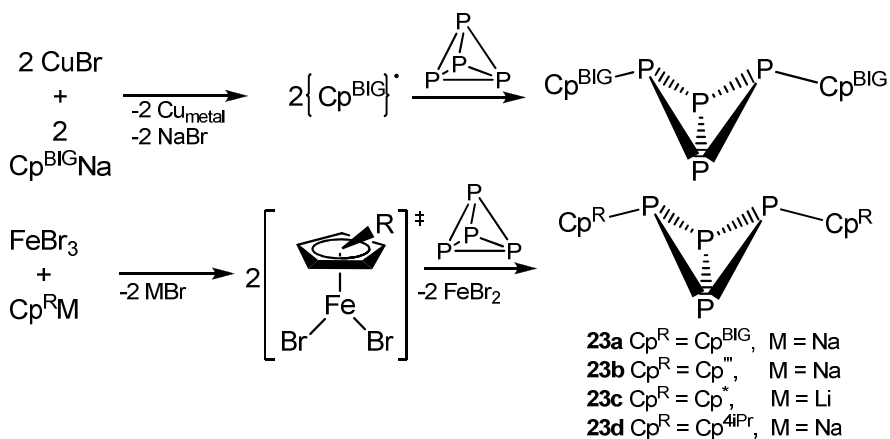
**Scheme 1.18.** Synthesis of  $\beta$ -diketiminato trivalent and mixed-valent Fe complexes.

Recently, it was shown that the metal-mediated activation of white phosphorus can proceed as well by a radical mechanism. A contribution by Cummins' group showed that trialkyl, triaryl, trisilyl and tristannyl phosphines can be prepared directly from  $P_4$  through a radical reaction mediated by a titanium complex, in stoichiometric amount respect to  $P_4$ .<sup>46</sup> Wolf *et al.*<sup>47</sup> performed the reaction of the  $17e^-$  nickel(I) radical  $[CpNi(L^{Dipp})]$  with  $P_4$  which resulted in the nickel tetraphosphide  $[[CpNi(L^{Dipp})]_2(\mu-\eta^1:\eta^1-P_4)]$  (**22**), as shown in **Scheme 1.19.**, with a butterfly- $P_4^{2-}$  ligand bridging the two metal centers.



**Scheme 1.19.** Synthesis of the novel  $[[CpNi(L^{Dipp})]_2(\mu-\eta^1:\eta^1P_4)]$ .

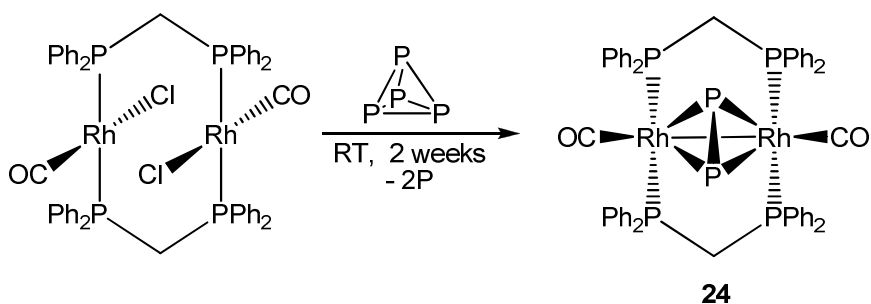
Activation of white phosphorus mediated by hindered  $\text{Cp}^{\text{R}}$  radicals was studied by Scheer *et al.*<sup>48</sup> Starting from a copper or iron salt in the presence of substituted cyclopentadienes, see **Scheme 1.20.**, a radical  $\{\text{Cp}^{\text{R}}\}^{\cdot}$  is formed that easily reacts with  $\text{P}_4$  through a selective cleavage of one P-P bond and led to the formation of a new family of butterfly organophosphorus compounds  $\text{Cp}^{\text{R}}_2\text{P}_4$  ( $\text{Cp}^{\text{R}}$ :  $\text{Cp}^{\text{BIG}} = \text{C}_5(4\text{-}^n\text{BuC}_6\text{H}_4)_5$  **23a**,  $\text{Cp}''' = \text{C}_5\text{H}_2\text{tBu}_3$  **23b**,  $\text{Cp}^* = \text{C}_5\text{Me}_5$  **23c**,  $\text{Cp}^{4i\text{Pr}} = \text{C}_5\text{H}_4\text{iPr}$  **23d**). While the “copper route” works only for  $\text{Cp}^{\text{BIG}}$ , the “iron route” has the advantage to be extended to other  $\text{Cp}^{\text{R}}$ , as shown in **Scheme 1.20.** This provides a practical and safe pathway to activate selectively white phosphorus through a stoichiometric process mediated by a transition metal.



**Scheme 1.20.** Activation of white phosphorus by hindered organic radicals.

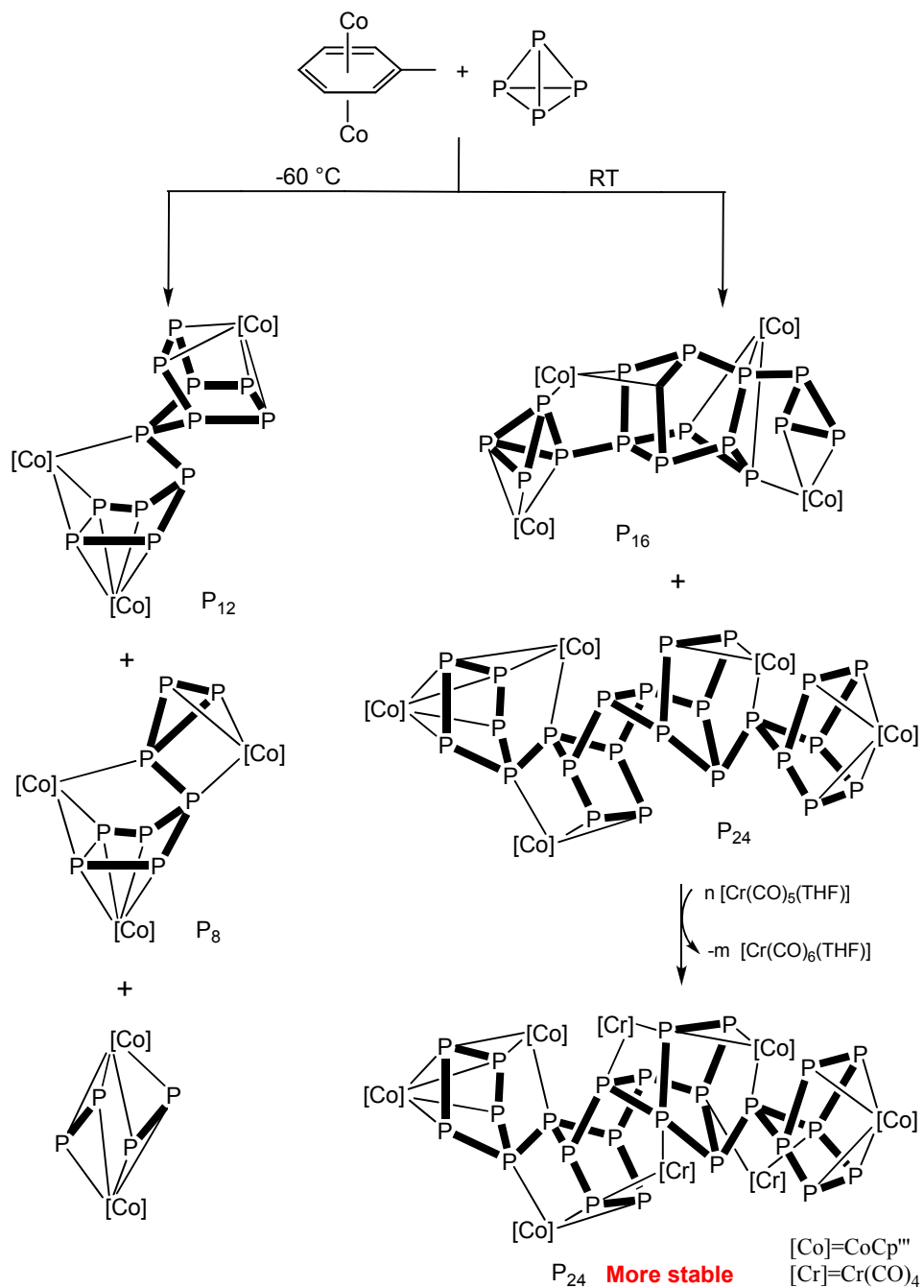
Beyond the coordination topologies of  $\text{P}_4$  towards a metal shown in **Scheme 1.11.**, fragmentation of white phosphorus into  $\text{P}_3$ ,  $\text{P}_2$  or  $\text{P}$  units or re-aggregation to form  $\text{P}_n$  cluster, where  $n > 4$ , were observed. A recent example of fragmentation<sup>49</sup> was observed in the reaction of oxidative

addition of  $P_4$  to the dimer  $trans$ - $[Rh^I Cl(CO)(dppm)]_2$ . As shown in **Scheme 1.21.**, the first  $Rh^{II}$  carbonyl dimer  $[Rh^{II}_2(CO)_2(\mu-dppm)_2(\mu,\eta^2-P_2)]$  **24** containing a diphosphenyl  $\mu,\eta^2-P_2$  ( $\mu-\kappa^2:\kappa^2-P_2$ ) ligand was isolated and characterized by X-ray structure analysis.



**Scheme 1.21.** Activation of  $P_4$  mediated by a rhodium A-frame dimer.

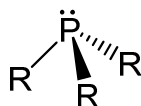
Scheer and co-workers<sup>50</sup> studied the reactivity of white phosphorus towards the cobalt dimer  $\{[Cp''Co]_2(\text{toluene})\}$  where  $Cp'' = \eta^5-1,2,4\text{-}t\text{Bu}_3\text{C}_5\text{H}_2$  which easily decomposes in solution to give electronically unsaturated 14-valence-electron  $[Cp''Co]$  moiety. The latter reacts with  $P_4$  under mild conditions and shows the ability to stabilize large  $P_n$  units. Using an excess of  $P_4$ , or changing the reaction conditions, such as temperature and reaction time, the formation cobalt-coordinated phosphorus cages of different size, such as  $P_8$ ,  $P_{12}$ ,  $P_{16}$  and  $P_{24}$ , was accomplished (see **Scheme 1.22.**)



**Scheme 1.22.** Preparation of  $P_8$ ,  $P_{12}$ ,  $P_{16}$  and  $P_{24}$  cobalt clusters from white phosphorus and  $[Co_2(\mu^2, \eta^6, \eta^6-C_7H_8)]$  depending on the reaction conditions.

## 1.4 Phosphines and related compounds

Phosphines are a class of organophosphorus compounds with oxidation state of phosphorus -3. Phosphine,  $\text{PH}_3$ , is the most simple phosphine. It is a colourless, flammable, toxic gas. Industrially, its production is accomplished by boiling white phosphorus with a strong basic solution in atmosphere of coal gas or hydrogen.<sup>51</sup>



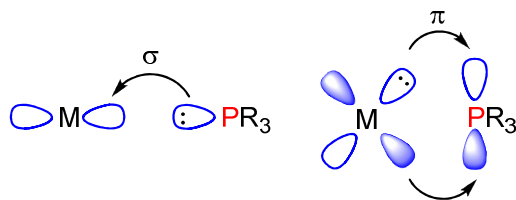
R = H, alkyl, aryl

Substitution of hydrogen atoms of  $\text{PH}_3$  by alkyl or aryl groups gives primary ( $\text{RPH}_2$ ), secondary ( $\text{R}_2\text{PH}$ ) and tertiary phosphines ( $\text{R}_3\text{P}$ ). Like amines, phosphines have pyramidal geometry with an electron lone pair on the central P-atom that can be donated to electrophilic centers.

Phosphines are widely used as ligands for transition metals because of their extreme versatility in term of both steric hindrance and electronic properties. The analysis of the structure-activity relationship is a keyword on the design of new ligands.<sup>52</sup> For instance, chiral phosphine ligands are used as ligands in asymmetric catalysis.<sup>53</sup> Different factors, such as electronic contributions, steric bulk or bite angle size, influence the bonding of phosphorus donor ligands to transition metals and afterwards the resulting catalytic activity of the coordination complexes is affected.

### 1.4.1 Electronic and steric properties

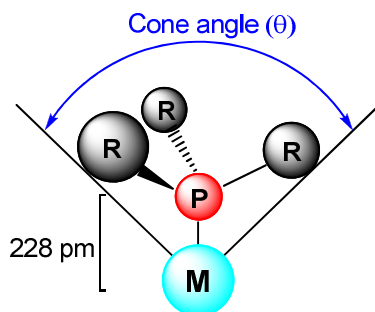
Phosphines possess an amphoteric electronic character, since metal-phosphine bonding can be explained by  $\sigma$ -donation, effective dative electron donation of the phosphorus lone pair towards empty metal orbitals and  $\pi$ -acidity, referring to the acceptance (back donation) of electron density from filled metal orbitals to empty ligand orbitals ( $\sigma^*$ P-R). (**Scheme 1.21.**) Phosphine ligands can be strong  $\pi$ -acceptors, if R is an electron withdrawing substituent, favoring the  $\pi$ -acceptor backbonding, or weak  $\pi$ -acceptors if R is an electron-donating one.<sup>54</sup> For example, phosphines, like  $\text{PMe}_3$ ,  $\text{PEt}_3$  or  $\text{PMe}_2\text{Ph}$  are strong  $\sigma$ -donors and poor  $\pi$ -acceptors. On the other hand, phosphites, like  $\text{P}(\text{OMe})_3$ ,  $\text{P}(\text{OPh})_3$ , are weak  $\sigma$ -donors with a strong  $\pi$ -acidity character. The effect of the  $\sigma$ -donation and  $\pi$ -back-donation in transition metal complexes can be seen as a result of the symmetry of the orbitals involved in the metal phosphorus bonding.



**Scheme 1.21.**  $\text{P} \rightarrow \text{M}$   $\sigma$ -donation,  $\text{M} \rightarrow \text{P}$   $\pi$ - backbonding.

Steric parameters are closely related with electronic effects. For monodentate phosphine ligands, metal-ligand bondings are affected by both the electronic and steric properties of the ligand. Tolman<sup>55</sup> introduced the “cone angle  $\theta$ ” concept to quantify the size of the ligand,

*i.e.* the steric bulk, see **Scheme 1.22**. This parameter controls the reactivity of transition-metal complexes in terms of ligand dissociation rates, insertion barriers, *cis-trans* isomerization, and so on. Allen and co-workers<sup>56</sup> developed a computational method to determine the exact cone angle applicable to any ligand tied to a metal center.

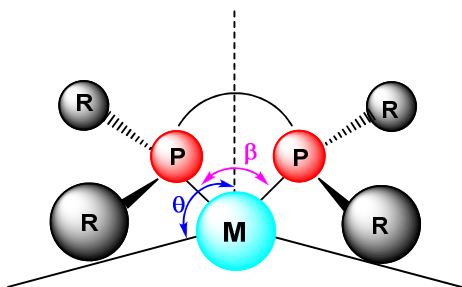


**Scheme 1.22.** Tolman's cone angle ( $\theta$ ) of a phosphine bound to a metal.

A geometric parameter associated to any chelating ligand, but mainly to diphosphines, is the "bite angle effect" ( $\beta$ ), see **Scheme 1.23**. Diphosphines are a kind of chelating ligand, consisting of 2 phosphine groups bridged by a backbone. They have the capacity to increase the stability and, in some cases, the regio- and the stereoselectivity of the catalytic system. Two different effects are related to the bite angle of diphosphines affecting the properties of the metal complexes. On the one hand, the *steric bite angle effect* which is related to the steric interactions (ligand–ligand or ligand–substrate) around the metal complex generated when the backbone is modified and keeping the substituents at the phosphorus donor atoms constant. The resulting steric interactions can change the activity or selectivity of the catalytic system. On the other hand, the *electronic bite angle effect* is referred to electronic modifications at the catalytic metal centre when the bite angle of the

## Chapter 1

bidentate ligand is changed. The bite angle determines metal hybridisation and, as a consequence, metal orbital energies and reactivity, thus, it could be described as an orbital effect. Both effects, different in nature but with the same origin, affect in different way and are connected when diphosphines with variable bite angles are used.<sup>57</sup>



**Scheme 1.23.** Measurement of the bite angle  $\beta$  and the cone angle  $\theta$  in bidentate phosphines.

### 1.4.2 Halophosphines

Halophosphines,  $PX_3$  ( $X = \text{halogen}$ ) are a special kind of organophosphorus compounds whose formal oxidation number is +3. Especially, chlorophosphines have great interest in organic and inorganic chemistry and play an important role for the manufacturing of organophosphorus compounds.<sup>58</sup> Fluorophosphines are a class of ligand barely studied, in spite of their strong  $\pi$ -accepting properties, similar to carbon monoxide, with high ability to stabilize transition metal fragments. Historically, different methods for the synthesis of fluorophosphines have been described using a variety of mild or strong fluorinating agents according to the different precursors. Coordination of the highly toxic  $PF_3$  gas under harsh conditions directly to the metal fragment,<sup>59,60,61</sup> chlorine-



## Chapter 1

fluorine exchange in chlorophosphines, using fluoride salts,<sup>62,63,64</sup> or conversion of phosphorus oxyacids using  $\alpha$ -fluoroenamines or cyanuric fluoride<sup>65</sup> are just a few examples of the many synthetic methodologies followed for the preparation of fluorophosphines. Due to their instability towards redox disproportionation,<sup>66</sup> only few applications of fluorophosphines in catalysis have been described. In spite of the high conversion on the olefin-hydrogenation reaction in the presence of  $[\text{RhH}(\text{PF}_3)(\text{PPh}_3)_3]$ .<sup>67</sup> Nixon *et al.*<sup>68</sup> studied the catalytic activity of different Ru(II) complexes bearing fluorophosphines of general formula  $[\text{RuH}(\text{PRF}_2)_x(\text{PPh}_3)_{4-x}]$  ( $\text{R} = \text{NMe}_2, \text{F}; x = 1, 2$ ) whose activity was slight or non-existent in 1-octene hydrogenation. Pringle<sup>69</sup> prepared fluorophosphines ligands having a phosphatrioxa-adamantane and phosphabicyclic backbone. They resulted to be thermally stable and, once coordinated to rhodium or nickel, their catalytic activity was studied. The new complexes showed to perform as well as, or better than commercial rhodium complexes in the hydroformylation of 1-heptene and commercial nickel complexes in the hydrocyanation of 3-pentenitrile.

### 1.5. Metal Phosphides

Transition metal phosphides, whose general formula is  $\text{M}_x\text{P}_y$ , are well known for their capability to form a great variety of binary phases with compositions spanning from metal-rich to phosphorus-rich (*i.e.*  $\text{Cu}_3\text{P}$  to  $\text{MnP}_4$ ). They are endowed with peculiar electronic properties that open to a broad number of applications.<sup>70</sup> Phosphorus-rich  $\text{MP}_x$  phases have been described as promising material for Li-ion battery electrodes,<sup>71</sup> on this regard, the first study appeared in 2002 describing the Li-uptake by a

## Chapter 1

Co<sub>2</sub>P electrode.<sup>72</sup> One of the most interesting applications is their catalytic activity, since the 1990s metal phosphide nanoparticles have been applied in hydrotreating reactions.<sup>73</sup> Some studies on electronic applications, such as the use of semiconducting Zn<sub>3</sub>P<sub>2</sub> nanowires as metal–insulator–semiconductor field-effect transistors<sup>74</sup> was reported. Further applications as initiators on nanostructures growth, as well as optical and magnetic uses have been described.<sup>70</sup>

The synthesis of metal phosphide nanoparticles requires a strict control of the process because several characteristics as composition, shape, size and crystallinity are strongly dependent on the reaction conditions: stoichiometry of the reagents, temperature, metal and phosphorus precursor, reducing agent, reaction time and medium.<sup>75</sup> Generally, metal phosphide nanoparticles can be obtained by thermal treatment of M<sup>n+</sup> or M<sup>0</sup> organometallic precursors or directly from preformed metallic M(0) nanoparticles. Different ‘P’ sources can be used for these purposes. Phosphine PH<sub>3</sub>, generated *in situ* from sodium hypophosphite (NaH<sub>2</sub>PO<sub>2</sub>) in basic hydrothermal conditions has been the P-source in the synthesis of nickel phosphide nanoparticles,<sup>76</sup> also PH<sub>3</sub> produced by addition of HCl on Zn<sub>3</sub>P<sub>2</sub> or Ca<sub>3</sub>P<sub>2</sub>, *in situ* or as secondary reaction, respectively, was used for the synthesis of indium phosphide nanoparticles.<sup>70</sup> Due to the high toxicity of PH<sub>3</sub>, the preparation of metal phosphides using phosphines as safer alternative ‘P’ sources was preferred. *Tris-n-octylphosphine* (TOP) has been used not only as capping agent to stabilize metal nanoparticles, but also as ‘P’ source.<sup>77</sup> Actually, it is the most often P-source used in the formation of metal phosphide nanoparticles due to its low toxicity. Generally, formation of metal phosphide nanoparticles using TOP is produced from preformed metal nanoparticles or metal (0) precursors by

thermal decomposition, requiring temperatures of *ca.* 300 °C. The use of other phosphines, such as PEt<sub>3</sub> or PPh<sub>3</sub> or even, highly reactive phosphines, such as P(SiMe<sub>3</sub>)<sub>3</sub> or P(GeMe<sub>3</sub>)<sub>3</sub>, have also been studied. Phosphorus as elemental form can be also used as ‘P’ source.<sup>78</sup> Its use has some advantages, such as a better control of the M/P ratio, no by-products formation and does not require harsh reaction conditions, as high temperature.

## **1.6 Aims of the thesis**

As previously reported, phosphorus chemistry is a very broad field with a great range of applications. The objectives of this PhD thesis are related to different aspects of low-valent phosphorus chemistry: going from the synthesis of fluorophosphine ligands through a “green” and innovative pathway, to the activation and functionalization of elemental white phosphorus in the presence of late transition metals, and, finally, to the not yet explored synthesis of ruthenium phosphide nanoparticles starting from white phosphorus.

The research described in Chapter 2 aims at the synthesis of fluorophosphine ligands starting from phosphorus oxyacids and using a mild, commercially available, deoxofluorinating reagent, thus circumventing the use of toxic reagents, commonly used in this reaction.

On chapter 3, the activation of white phosphorus mediated by unsaturated ruthenium complexes bearing a bulky phosphine (i.e.PCy<sub>3</sub>) and different halogen ligands is described. Moreover and more interestingly the functionalization of coordinated P<sub>4</sub> has been accomplished by subsequent

## *Chapter 1*

reaction with organic reagents. This project is part of a collaboration with the group of Prof. H. Grützmacher at ETHZ, Zürich, Switzerland.

Chapter 4 deals with the preparation of ruthenium phosphide nanoparticles using white phosphorus as P-source. Catalytic tests of hydrogenation of unsaturated organic substrates in the presence of ruthenium phosphide nanoparticles are in progress. This work is part of a collaboration with the group of Dr. N. Mézailles at CNRS, Toulouse, France.

Both collaborations, with ETHZ and CNRS are in the frame of SusPhos, an European Training Network on Sustainable Phosphorus Chemistry (02/2013-01/2017 Marie Curie ITN SusPhos, Grant Agreement No. 317404). <http://www.susphos.eu>

## References

---

- <sup>1</sup> M. Butusov, A. Jernelov, “*Phosphorus An element that could have been called Lucifer*”, **2013**, Springer.
- <sup>2</sup> D. L. Childers, J. Corman, M. Edwards, J. J. Elser, *BioScience* **2011**, *61*, 2, 117-124.
- <sup>3</sup> A. D. F. Toy, “*The chemistry of phosphorus: Pergamon Texts in Inorganic Chemistry, Volumen 3*”, **2013**, Elsevier.
- <sup>4</sup> John Wiley & Sons, “*Ullmann's Encyclopedia of Industrial Chemistry, Volumen 40*” **2003**, Wiley-VCH.
- <sup>5</sup> H. Okudera, R. E. Dinnebier A. Simon, *Z. Kristallogr.* **2005**, *220*, 259-264.
- <sup>6</sup> “*e-Study Guide for: General Chemistry: The Essential Concepts: Chemistry, 2013*” Cram101 Textbook Reviews.
- <sup>7</sup> Msds N°. M7588 “*White Phosphorus*” **2008**, Glenn Spring Holdings Inc.
- <sup>8</sup> R. E. Marx, *J. Oral Maxillofac. Surg.* **2008**, *66*, 11, 2356-2363.
- <sup>9</sup> L. Pauling, “*General Chemistry*” **2014** Courier Corporation, 213.
- <sup>10</sup> K.L. Kosanke, B. J. Kosanke, Barry T. Sturman, R. M. Minokur, *Encyclopedic Dictionary of Pyrotechnics (and Related Subjects) Journal of Pyrotechnics*, **2012**, 839-840.
- <sup>11</sup> E. Wiberg, N. Wiberg, *Inorganic Chemistry* **2001**, Academic Press, 683.
- <sup>12</sup> P. W. Bridgman, *J. Am. Chem. Soc.* **1914**, *36*, 1344-1363.
- <sup>13</sup> H. Krebs, H. Weitz, K. H. Worms, *Z. Anorg. Allg. Chem.* **1955**, *280*, 119-133.
- <sup>14</sup> Y. Maruyama, S. Suzuki, K. Kobayashi, S. Tanuma, *Phys. B C* **1981**, *105*, 99-102.
- <sup>15</sup> S. Lange, P. Schmidt, T. Nilges, *Inorg. Chem.* **2007**, *46*, 4028-4035.
- <sup>16</sup> T. Nilges, M. Kersting, T. Pfeifer, *J. Solid State Chem.* **2008**, *181*, 1707-1711.
- <sup>17</sup> I. Shirovani, *Molecular Crystals and Liquid Crystals* **1982**, *86*, 1, 203-211.
- <sup>18</sup> M. Baba, Y. Takeda, K. Shibata, T. Ikeda, A. Morita *Jpn. J. Appl. Phys.* **1989**, *28*, 11, L2104-L2106.
- <sup>19</sup> H. Liu, Y. Du, Y. Deng, P. D. Ye, **2014**, arXiv:1411.0056
- <sup>20</sup> D. Hanlon, C. Backes, E. Doherty, C. S. Cucinotta, N. C. Berner, C. Boland, K. Lee, P. Lynch, Z. Gholamvand, A. Harvey, S. Zhang, K. Wang, G. Moynihan, A. Pokle, Q. M. Ramasse, N. McEvoy, W. J. Blau, J. Wang, S. Sanvito, D. D. O'Regan, G. S. Duesberg, V. Nicolosi, J. N. Coleman, **2015**, arXiv:1501.01881 [cond-mat.mes-hall]
- <sup>21</sup> D. J. Late, M. B. Erande, S. R. Suryawanshi, M. A. More, *Eur. J. Inorg. Chem.* **2015**, 3102–3107.
- <sup>22</sup> R. D. Jones, D. J. J. Holl, *Chem. Phys.* **1990**, *92*, 6710.
- <sup>23</sup> E. Fluck, C. M. E. Pavlidou, R. Janoschek, *Phosphorus Sulfur* **1979**, *6*, 469.

- <sup>24</sup> J.-L. Abboud, M. Herreros, R. Notario, M. Essefar, O. Mó, M. J. Yañez, *J. Am. Chem. Soc.* **1996**, *118*, 1126.
- <sup>25</sup> M. Arrowsmith, M. S. Hill, A. L. Johnson, G. Kociok-Köhn, M. F. Mahon, *Angew. Chem. Int. Ed.* **2015**, *54*, 7882-7885.
- <sup>26</sup> J. D. Masuda, W. W. Schoeller, B. Donnadiou, G. Bertrand, *J. Am. Chem. Soc.* **2007**, *129*, 14180-14181.
- <sup>27</sup> C.L. Dorsey, B. R. Squires, T. W. Hudnall, *Angew. Chem. Int. Ed.* **2013**, *52*, 4462-4465.
- <sup>28</sup> C. D. Martin, C. M. Weinstein, C. E. Moore, A. L. Rheingold, G. Bertrand, *Chem. Commun.* **2013**, *49*, 4486-4488.
- <sup>29</sup> J. D. Masuda, W. W. Schoeller, B. Donnadiou, G. Bertrand, *Angew. Chem. Int. Ed.* **2007**, *46*, 1-5.
- <sup>30</sup> M. Peruzzini, L. Gonsalvi, A. Romerosa, *Chem. Soc. Rev.* **2005**, *34*, 1038–1047.
- <sup>31</sup> K. M. Armstrong, P. Kilian, *Eur. J. Inorg. Chem.* **2011**, 2138-2147.
- <sup>32</sup> B. M. Cossairt, C. C. Cummins, *Angew. Chem. Int. Ed.* **2008**, *47*, 8863-8866.
- <sup>33</sup> W. Huang, P.L. Diaconescu, *Chem. Commun.* **2012**, *48*, 2216-2218.
- <sup>34</sup> A. P. Ginsberg, W. E. Lindsell, *J. Am. Chem. Soc.* **1971**, *93*, 8, 2082-2084.
- <sup>35</sup> P. Dapporto, S. Midollini, L. Sacconi, *Angew. Chem.* **1979**, *91*, 6, 510.
- <sup>36</sup> I. De los Rios, J. R. Hamon, P. Hamon, C. Lapinte, L. Toupet, A. Romerosa, M. Peruzzini, *Angew. Chem. Int. Ed.* **2001**, *40*, 3910-3911.
- <sup>37</sup> M. Di Vaira, M. Peruzzini, S. Seniori Costantini, P. Stoppioni, *J. Organomet. Chem.* **2006**, *691*, 3931.
- <sup>38</sup> M. Caporali, M. Di Vaira, M. Peruzzini, S. Seniori Costantini, P. Stoppioni, F. Zanobini, *Eur. J. Inorg. Chem.* **2010**, 152–158.
- <sup>39</sup> M. Di Vaira, P. Frediani, S. Seniori Costantini, M. Peruzzini, P. Stoppioni, *Dalton Trans.* **2005**, 2234.
- <sup>40</sup> O. J. Scherer, M. Swarowsky, G. Wolmershäuser, *Organometallics* **1989**, *8*, 841-842.
- <sup>41</sup> D. Yakhvarov, P. Barbaro, L. Gonsalvi, S. Mañas Carpio, S. Midollini, A. Orlandini, M. Peruzzini, O. Sinyashin, F. Zanobini, *Angew. Chem. Int. Ed.* **2006**, *45*, 4182–4185.
- <sup>42</sup> V. Mirabello, M. Caporali, L. Gonsalvi, G. Manca, A. Ienco, M. Peruzzini, *Chem. Asian J.* **2013**, *8*, 3177-3184.
- <sup>43</sup> S. Yao, Y. Xiong, C. Milsman, E. Bill, S. Pfirmann, C. Limberg, M. Driess, *Chem. Eur. J.* **2010**, *16*, 436-439.

- 
- <sup>44</sup> S. Yao, N. Lindenmaier, Y. Xiong, S. Inoue, T. Szilvási, M. Adelhardt, J. Sutter, K. Meyer, M. Driess, *Angew. Chem.* **2015**, *127*, 1266-1270.
- <sup>45</sup> S. Yao, T. Szilvási, N. Lindenmaier, Y. Xiong, S. Inoue, M. Adelhardt, J. Sutter, K. Meyer, M. Driess, *Chem. Commun.* **2015**, *51*, 6153-6156.
- <sup>46</sup> B. Cossairt, C. C. Cummins, *New J. Chem.* **2010**, *34*, 1533-1536.
- <sup>47</sup> S. Pelties, D. Herrmann, B. Bruin, F. Hartl, R. Wolf, *Chem. Commun.* **2014**, *50*, 7014-7016.
- <sup>48</sup> S. Heintl, S. Reisinger, C. Schwarzmaier, M. Bodensteiner, M. Scheer, *Angew. Chem. Int. Ed.* **2014**, *53*, 1-5.
- <sup>49</sup> M. Caporali, L. Gonsalvi, V. Mirabello, A. Ienco, G. Manca, F. Zanobini, M. Peruzzini, *Eur. J. Inorg. Chem.* **2014**, 1652-1659.
- <sup>50</sup> F. Dielmann, M. Sierka, A. V. Virovets, M. Scheer, *Angew. Chem. Int. Ed.* **2010**, *49*, 6860-6864.
- <sup>51</sup> A. K. De, "A Text Book of Inorganic Chemistry" **2007** New Age International, 437.
- <sup>52</sup> P. C. J. Kamer, P. W.N.M. van Leeuwen, "Phosphorus(III) ligands in homogeneous catalysis: design and synthesis" **2012** John Wiley & Sons, Ltd.
- <sup>53</sup> Y. Xiao, Z. Sun, H. Guo, O. Kwon, *J. Org. Chem.* **2014**, *10*, 2089-2121.
- <sup>54</sup> N. Praingam, PhD thesis, *The effect of phosphine on silicon-hydrogen bond activation reaction with platinum complexes* **2008**, ProQuest, 43-48.
- <sup>55</sup> C. A. Tolman, *Chemical Reviews* **1977**, *77*, 3, 313-348.
- <sup>56</sup> J. A. Bilbrey, A. H. Kazez, J. Locklin, W. D. Allen, *J. Comput. Chem.* **2013**, *34*, 1189-1197.
- <sup>57</sup> Z. Freixa, P. W. N. M. van Leeuwen, *Dalton Trans.* **2003**, 1890-1901.
- <sup>58</sup> D. E. C. Corbridge, *Phosphorus 2000. Chemistry, Biochemistry and Technology* **2000**, Elsevier, Amsterdam, NL.
- <sup>59</sup> J. Chatt, *Nature* **1950**, *165*, 637.
- <sup>60</sup> G. Wilkinson, *J. Am. Chem. Soc.* **1951**, *73*, 5501-5502.
- <sup>61</sup> J. F. Nixon, R. Swain, *Plat. Met. Rev.* **1975**, *19*, 22-29.
- <sup>62</sup> D. W. Allen, B. J. Walker, *Organophosphorus Chemistry* **1997**, 23.
- <sup>63</sup> R. J. Clark, H. Belefant, S. M. Williamson, *Inorg. Synth.* **1990**, *28*, 310.
- <sup>64</sup> O. Stelzer, R. Schmutzler, *Inorg. Synth.* **1978**, *18*, 173-179.
- <sup>65</sup> a) R. Wärme, L. Juhlin, L. Trogen, *Phosphorus, Sulfur, and Silicon* **2008**, *183*, 483-486; b) R. Wärme, L. Juhlin, *Phosphorus, Sulfur, and Silicon* **2010**, *185*, 2402-2408.
- <sup>66</sup> a) O. Stelzer, *Chem. Ber.* **1974**, *107*, 2329-2340; b) M. Pabel, A.C. Willis, S.B. Wild, *Inorg. Chem.* **1996**, *35*, 1244-1249; c) L. Riesel, J. Haenel, *J.*

*Fluorine Chem.* **1988**, 38, 335-340; d) R. Schmutzler, O. Stelzer, J. F. Liebman, *J. Fluorine Chem.* **1984**, 25, 289-299.

<sup>67</sup> J. F. Nixon, J. R. Swain, *J. Organomet. Chem.* **1974**, 72, C15-C17.

<sup>68</sup> R. A. Head, J. F. Nixon, *J.C.S. Dalton* **1978**, 913-915.

<sup>69</sup> N. Fey, M. Garland, J. P. Hopewell, C. L. McMullin, S. Mastroianni, A. Guy Orpen, P. G. Pringle, *Angew. Chem. Int. Ed.* **2012**, 51, 118-122.

<sup>70</sup> S. Carencio, D. Portehault, C. Boissière, N. Mézailles, C. Sanchez, *Chem. Rev.*, **2013**, 113, 10, 7981-8065.

<sup>71</sup> F. Gillot, L. Boganov, M. Dupont, M. Morcrette, L. Monconduit, J.-M. Tarascon, *Chem. Mater.* **2005**, 17, 6327.

<sup>72</sup> V. Pralong, D. C. S. Souza, K. T. Leung, L. F. Nazar, *Electrochem. Commun.* **2002**, 4, 516.

<sup>73</sup> a) R. Prins, M. E. Bussell *Catal. Lett.* **2012**, 142, 1413-1436; b) Y. Kanda, Y. Uemichi, *J. Jpn. Petrol. Inst.* **2015**, 58, 1, 20-32.

<sup>74</sup> C. Liu, L. Dai, L. P. You, W. J. Xu, R. M. Ma, W. Q. Yang, Y. F. Zhang, G. G. Qin, *J. Mater. Chem.* **2008**, 18, 3912.

<sup>75</sup> S. Carencio, D. Portehault, C. Boissière, N. Mézailles, C. Sanchez, *Adv. Mater.* **2014**, 26, 371-390.

<sup>76</sup> a) Y. Ni, A. Tao, G. Hu, X. Cao, X. Wei, Z. Yang, *Nanotechnology* **2006**, 17, 5013. b) L. Song, S. Zhang, *Powder Technol.* **2011**, 208, 713.

<sup>77</sup> A. E. Henkes, R. E. Schaak, *Chem. Mater.* **2007**, 19, 17, 4234-4242.

<sup>78</sup> a) S. Carencio, M. Demange, J. Shi, C. Boissière, C. Sanchez, P. LeFloch, N. Mézailles, *Chem. Commun.* **2010**, 46, 5578-5580; b) S. Carencio, Y. Hu, I. Florea, O. Ersen, C. Boissière, N. Mézailles, C. Sanchez, *Chem. Mater.* **2012**, 24, 4134-4145; c) S. Carencio, Y. Hu, I. Florea, O. Ersen, C. Boissière, C. Sanchez, N. Mézailles, *Dalton Trans.* **2013**, 42, 12667.



## **XtalFluor-E, the key to ruthenium-coordinated fluorophosphines from phosphorous oxyacids**

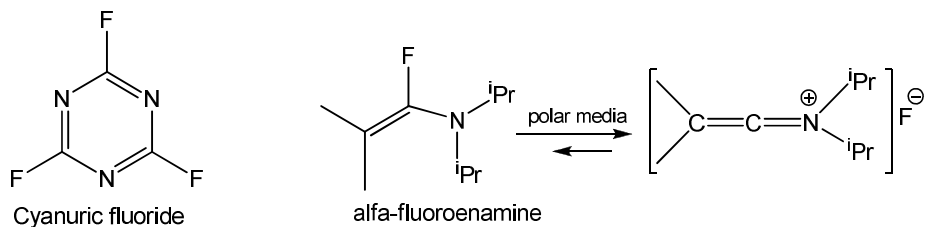
### **2.1. Overview**

This chapter describes the study of the transformation of phosphorous oxyacids, such as PhPO(OH)H, H<sub>3</sub>PO<sub>3</sub>, H<sub>3</sub>PO<sub>2</sub>, into the corresponding fluorophosphines mediated by [CpRu(PPh<sub>3</sub>)<sub>2</sub>Cl] under mild reaction conditions using a soft deoxyfluorinating agent. The reaction is selective, proceeds with high yields and can be extended to a wide range of phosphorous oxyacids once coordinated to the ruthenium fragment {CpRu(PPh<sub>3</sub>)<sub>2</sub>}<sup>+</sup> as their hydroxyphosphine tautomer. Deoxyfluorination of phenylphosphinic acid was also mediated by [Cp<sup>R</sup>Ru(CH<sub>3</sub>CN)<sub>3</sub>]PF<sub>6</sub>, where Cp<sup>R</sup>: Cp = C<sub>5</sub>H<sub>5</sub>, Cp\* = C<sub>5</sub>Me<sub>5</sub>, and {η<sup>6</sup>-(*p*-cymene)Ru(μ-Cl)Cl}<sub>2</sub>.

## *Chapter 2*

## 2.2 Introduction

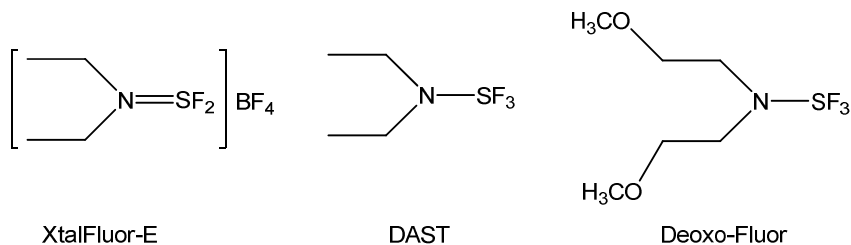
Phosphorus halides, especially chlorides, are of great interest in many genres of organic and inorganic chemistry, and represent the key-materials for the manufacturing of several organophosphorus compounds.<sup>1</sup> Among P-halides, fluorophosphines,  $\text{PR}_x\text{F}_y$  ( $\text{R}$  = organyl group;  $x+y = 3$ ) have been less considered as ligands towards transition-metals in spite their dual function being good  $\sigma$ -donating and strong  $\pi$ -accepting ligands at the same time thus showing great ability to stabilize transition metals in several oxidation states, including the lowest ones.<sup>2</sup> Up to now, the development of new methods and reagents for the synthesis of fluorophosphines is scarcely explored.<sup>3</sup> Due to their instability with respect to the redox disproportionation,<sup>4</sup> a very few applications in catalysis, such as hydroformylation,<sup>5</sup> have been described. Tri-fluorophosphine complexes of different metals (Pt, Ni) were prepared more than sixty years ago by Chatt<sup>6</sup> and Wilkinson,<sup>7</sup> respectively and, afterwards, analogous complexes of different platinum group metals by Nixon,<sup>8</sup> starting from the suitable metal precursor in the presence of high temperature and high pressure of gaseous  $\text{PF}_3$ . Trying to avoid the use of highly toxic  $\text{PF}_3$ , fluorophosphines have been prepared starting from different chlorophosphines by chlorine-fluorine exchange, using a fluorinating agent, such as  $\text{NEt}_3\cdot\text{HF}$ ,<sup>9</sup>  $\text{SbF}_3$ ,<sup>10</sup>  $\text{NaF}$ <sup>11</sup> or triorganotin(IV) fluorides.<sup>12</sup> Conversion of phosphorous oxyacids to the corresponding fluorinated phosphines using  $\alpha$ -fluoroenamines or cyanuric fluoride as reagents,<sup>13</sup> as shown in **Scheme 2.1.**, is a very efficient and almost quantitative method, but these liquid reagents are corrosive, toxic and very sensitive to hydrolysis.



**Scheme 2.1.** Fluorinating agents used for delivering fluoride to phosphorous oxyacids.

Facing the feasibility to form hydroxyphosphine ruthenium complexes of the general formula,  $[\text{CpRu}(\text{PPh}_3)_2\{\text{PH}_x(\text{HO})_y\}]^+$  ( $x+y = 3$ ;  $x = 0, 1, 2$ ), by coordination of hydroxyphosphines, such as  $\text{P}(\text{OH})_3$ ,  $\text{PH}(\text{OH})_2$  and  $\text{PH}_2(\text{OH})$  to  $\{\text{CpRu}(\text{PPh}_3)_2\}^+$ , via ruthenium-promoted tautomerization of the corresponding phosphorous oxyacids ( $\text{H}_3\text{PO}_3$ ,  $\text{H}_3\text{PO}_2$  and  $\text{H}_3\text{PO}$ ),<sup>14,15</sup> a great interest on the preparation of fluorophosphines by selective fluorination of the P-OH functional group was originated. To the best of our knowledge, the deoxyfluorination reaction has been traditionally used to convert organic substrates such as alcohols, ketones or carboxylic acids into their fluorinated derivatives. Fuming liquid alternatives to the highly toxic gas,  $\text{SF}_4$ , were synthesized, such as DAST,<sup>16</sup> and Deoxo-Fluor, (bis(2-methoxyethyl)aminosulfur trifluoride),<sup>17</sup> see **Scheme 2.2**. These compounds are commonly used as deoxyfluorinating agents for organic substrates, even if they are difficult to handle in humid environments and violently reactive in contact with water, that easily convert alcohol into alkyl fluorides, ketones into *gem*-difluorides and carboxylic acids to acid fluorides. Markovskii *et al.*<sup>18</sup> synthesized safer and more cost-efficient dialkylaminodifluorosulfonium tetrafluoroborate salts  $[(\text{R}_2\text{NSF}_2)\text{BF}_4]$  ( $\text{R} =$  ethyl or morpholine), commercialized as XtalFluor-E and XtalFluor-M, respectively by reaction of DAST with  $\text{BF}_3 \cdot \text{Et}_2\text{O}$ . These salts are stable

solids, and easily manageable which led to their successful application for the deoxofluorination of oxo-substrates.<sup>19</sup>

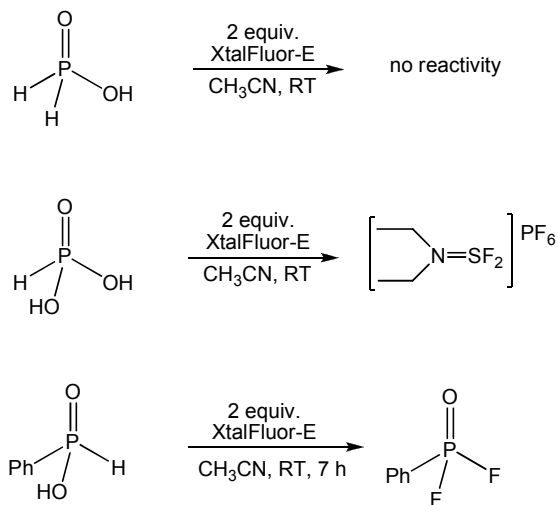


**Scheme 2.2.** Deoxofluorinating agents.

### 2.3 Direct deoxofluorination of P-oxyacids

XtalFluor-E, DAST and Deoxo-Fluor reagents, shown in **Scheme 2.2.** have been used for deoxofluorinating organic substrates, as alcohols, carboxylic acids, ketones or acyl chlorides. We envisaged to extend this reaction to phosphorus oxyacids aiming to obtain by a one pot procedure the corresponding fluorophosphines.

In a first attempt we tried the deoxofluorination of three different phosphorous oxyacids,  $\text{H}_3\text{PO}_2$ ,  $\text{H}_3\text{PO}_3$  and  $\text{PhP(O)(OH)(H)}$ , using one or two equivalents of XtalFluor-E in acetonitrile at room temperature. As a result, no reaction was observed with  $\text{H}_3\text{PO}_2$ , whereas  $\text{H}_3\text{PO}_3$  gave unexpectedly the anion  $\text{PF}_6^-$  ( $^{31}\text{P}$  NMR septuplet at -146.2 ppm,  $^1J_{\text{PF}} = 706$  Hz) as the only phosphorus containing species. However when phenyl phosphinic acid was reacted with XtalFluor-E the corresponding difluorophosphine oxide was obtained in quantitative yield (**Scheme 2.3.**), and its identity confirmed by NMR and ESI-MS.<sup>20</sup>



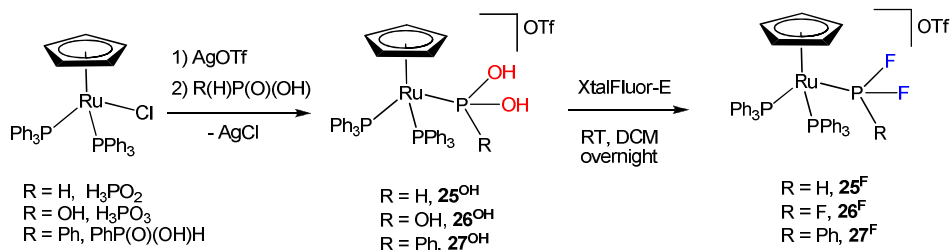
Scheme 2.3.

Attempts to reduce the difluorophosphine oxide to the corresponding phosphine, by DIBAL (DIBAL = di-isobutyl-aluminium hydride) or by the more basic  $n\text{Bu}_3\text{P}$  led to decomposition of the fluorophosphine oxide, which was not further studied.

## 2.4. Synthesis and characterization of $[\text{CpRu}(\text{PPh}_3)_2(\text{PF}_2\text{R})]\text{X}$

The capability of the organometallic fragment  $[\text{CpRu}(\text{PPh}_3)_2]^+$  to stabilize phosphorous oxyacids in the form of their corresponding hydroxyphosphine tautomers is known from literature.<sup>15</sup> We coordinated the oxyacids reported in **Scheme 2.4** to  $[\text{CpRu}(\text{PPh}_3)_2]^+$  obtaining the following derivatives  $[\text{CpRu}(\text{PPh}_3)_2\{\text{HP}(\text{OH})_2\}]\text{OTf}$  (**25<sup>OH</sup>**),  $[\text{CpRu}(\text{PPh}_3)_2\{\text{P}(\text{OH})_3\}]\text{OTf}$  (**26<sup>OH</sup>**),  $[\text{CpRu}(\text{PPh}_3)_2\{\text{P}(\text{OH})_3\}]\text{PF}_6$  (**26<sup>OH+</sup>**) and  $[\text{CpRu}(\text{PPh}_3)_2\{\text{PhP}(\text{OH})_2\}]\text{OTf}$  (**27<sup>OH</sup>**) where  $\text{OTf} = \text{OSO}_2\text{CF}_3$

(Scheme 2.4.).  $25^{\text{OH}}$  and  $26^{\text{OH}}$  are known compounds,<sup>17a</sup> while  $27^{\text{OH}}$  was prepared following the same synthetic procedure as reported for the former complexes.



**Scheme 2.4.** Synthesis of the Ru-coordinated fluorophosphines.

The molecular structure of  $27^{\text{OH}}$  was confirmed by a single crystal X-ray structure analysis, showing the  $[\text{CpRu}(\text{PPh}_3)_2\{\text{PhP}(\text{OH})_2\}]^+$  cation and one triflate anion in the asymmetric unit. The ORTEP-diagram of  $27^{\text{OH}}$  as shown in **Figure 2.1.**, exhibits hydrogen bond interactions between both OH units of the coordinated hydroxyphosphine and two of the triflate oxygen atoms.

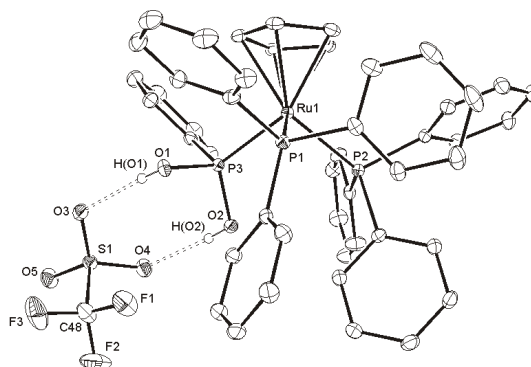


**Figure 2.1.** ORTEP-diagram of  $27^{\text{OH}}$  with 30% probability ellipsoids. Hydrogen atoms, except for O(1) and O(2) are omitted for clarity. Selected bond length ( $\text{\AA}$ ) and angles ( $^\circ$ ): Ru(1)-P(1), 2.3670(7); Ru(1)-P(2), 2.3408(7); Ru(1)-P(3),

## Chapter 2

2.2745(7); Ru-centroid(Cp), 1.8959; O(3)-H(O1), 2.0401; O(4)-H(O2), 2.0177; P(1)-Ru(1)-P(2), 98.20(2); P(1)-Ru(1)-P(3), 97.74(2); P(2)-Ru(1)-P(3), 96.37(2).

Compound **26<sup>OH</sup>** having PF<sub>6</sub> as counteranion, was quantitatively deoxofluorinated upon reaction with an equimolar amount of XtalFluor-E, and the corresponding fluorophosphine complex [CpRu(PPh<sub>3</sub>)<sub>2</sub>{PF<sub>3</sub>}]PF<sub>6</sub> (**26<sup>F</sup>**) was isolated. On the other hand, the deoxofluorination of **26<sup>OH</sup>** having CF<sub>3</sub>SO<sub>3</sub> as counteranion needs a three times excess of XtalFluor-E to be completed. In the absence of further experimental evidences for the counter anion effect on the deoxyfluorination we speculate that hydrogen bond interactions in solution between the triflate anion and the hydroxyl groups of the coordinated P(OH)<sub>3</sub>, as observed for **27<sup>OH</sup>** in the solid state, may hamper the accessibility of hydroxyl groups by the fluoride.

The deoxyfluorination of P(OH)<sub>3</sub> to PF<sub>3</sub>, once coordinated to the metal, represents an easy and safe method to prepare ruthenium complexes with PF<sub>3</sub> ligand, circumventing the usage of PF<sub>3</sub> which is a very toxic and hazardous gas. For comparison, it is worth noticing that the generation of PF<sub>3</sub> on laboratory scale usually involves the reaction of PCl<sub>3</sub> with HF gas,<sup>21</sup> SbF<sub>3</sub>,<sup>22</sup> AsF<sub>3</sub>,<sup>23</sup> or ZnF<sub>2</sub>.<sup>24</sup> Alternatively, it can be synthesized by the dropwise addition of PBr<sub>3</sub> to excess powdered SbF<sub>3</sub>.<sup>25</sup>

The fluoro derivatives were isolated and fully characterized in solution by multinuclear NMR, see **Table 2.1.** below for <sup>31</sup>P and <sup>19</sup>F.



Complex		$\delta(^{19}\text{F})$	$\delta(^{31}\text{P})$	$^1\text{J}(\text{PF})$ Hz	$^2\text{J}(\text{PP})$ Hz	$^3\text{J}(\text{PF})$ Hz
$[\text{CpRu}(\text{PPh}_3)_2(\text{HPF}_2)]^+$	<b>1<sup>F</sup></b>	4.6	225.1	1088	57	8
$[\text{CpRu}(\text{PPh}_3)_2(\text{PF}_3)]^+$	<b>2<sup>F</sup></b>	4.5	144.8	1302	72	-
$[\text{CpRu}(\text{PPh}_3)_2(\text{PhPF}_2)]^+$	<b>3<sup>F</sup></b>	-34.2	227.4	1087	56	7

**Table 2.1.**  $^{19}\text{F}$  and  $^{31}\text{P}$  chemical shifts and relative coupling constants in  $\text{CD}_2\text{Cl}_2$  solution at  $25^\circ\text{C}$  of the fluorophosphine complexes.

Particularly diagnostic it is the direct coupling constant  $^1J_{\text{PF}}$  where we observe a large variation in the values, going from 1087 Hz to 1300 Hz, and agrees well with the values already known in literature for similar ruthenium complexes<sup>25,26</sup> bearing difluorophosphine and trifluorophosphine ligands. The variation of  $^1J(^{31}\text{P}-^{19}\text{F})$  with the number of fluorine atoms on P is indeed remarkable:  $^1J_{\text{PF}}$  is 1302 Hz in **2<sup>F</sup>** bearing  $\text{PF}_3$  ligand, while there is a progressive lowering of the value going down to 1087 Hz in **3<sup>F</sup>**, bearing a difluorophosphine. Considering that  $^1J(^{31}\text{P}-^{19}\text{F})$  is, as absolute value, 1403 Hz in the free gaseous  $\text{PF}_3$ , the decrease of the coupling constant observed in our complexes may account for a reduction of the phosphorus-fluorine bond order. In detail, the  $\sigma$ - and  $\pi$ -components for the dative bond of  $\text{PF}_3$  toward a transition metal, operate in the same synergic way observed for carbon monoxide, therefore the  $\pi$ -component is expected to be favoured in trifluorophosphine complexes, in comparison to complexes bearing the ligands  $\text{PhPF}_2$ ,  $\text{HPF}_2$ , because of the presence of three highly electronegative fluorine atoms.<sup>25</sup> Examining the Ru-P distance in the crystal structure of Ru- $\text{PF}_3$  complexes,<sup>25</sup> it is interesting to see that this distance is very much shorter (2.184 Å) than the Ru- $\text{PPh}_3$  distance (average 2.34 Å), which is consistent with the stronger  $\pi$ -bonding ability of  $\text{PF}_3$  in comparison to triphenylphosphine. Likewise, the variation in

chemical shifts in  $^{31}\text{P}$  and  $^{19}\text{F}$  NMR is relatively big going from  $\text{PF}_3$  to  $\text{PhPF}_2$  ligand there is a variation of ca. 80 and 63 ppm, respectively as shown in **Table 2.1**.

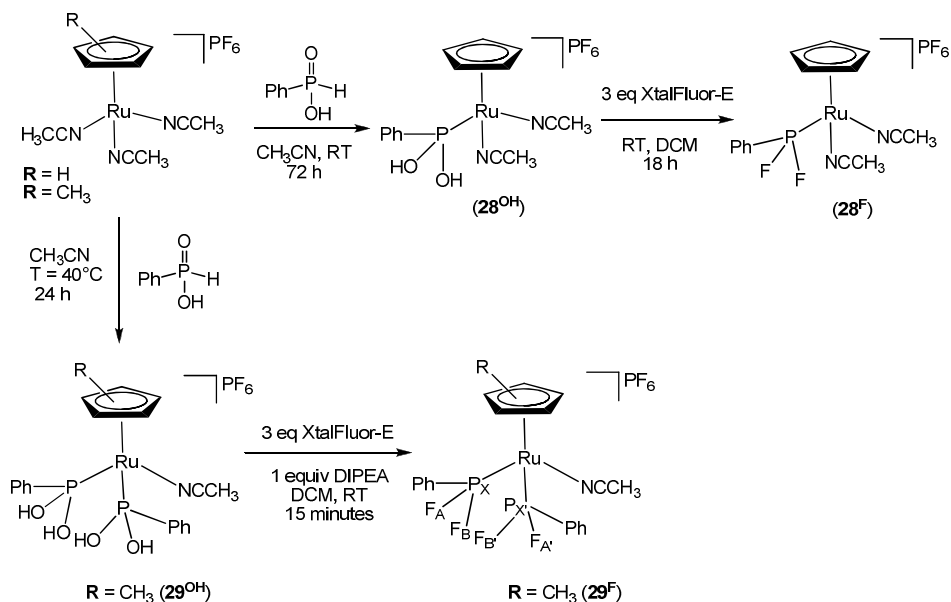
Any attempt to de-coordinate the fluorophosphine ligand from the ruthenium centre by reaction of **27<sup>F</sup>** with a more basic phosphine such as PTA (1,3,5-triaza-7-phosphaadamantane) or CO pressure, failed. This experimental result is in agreement with theoretical<sup>27,1b</sup> and experimental studies based on photoelectron spectroscopy,<sup>28</sup> and  $^{13}\text{C}$  NMR spectroscopy carried out on a series of  $\text{LNi}(\text{CO})_3$  complexes<sup>29</sup> (L = trihalophosphine ligands), which showed the  $\pi$ -acceptor properties of  $\text{PF}_3$  to be similar to CO and its basicity ( $\sigma$  donor) resembles that of  $\text{PET}_3$ .

## 2.5. Synthesis and characterization of $[\text{Cp}^{\text{R}}\text{Ru}(\text{CH}_3\text{CN})_{3-x}(\text{PhPF}_2)_x]\text{PF}_6$

We tried mono-cationic ruthenium precursors of the general formula  $[\text{Cp}^{\text{R}}\text{Ru}(\text{CH}_3\text{CN})_3]\text{PF}_6$  where (R = H,  $\text{CH}_3$ ).<sup>30,31</sup> These species are characterized by three coordinating acetonitrile molecules, which can be easily replaced by a stronger coordinating ligand. Attempts to coordinate  $\text{H}_3\text{PO}_2$  and  $\text{H}_3\text{PO}_3$  to the ruthenium center failed, even after a prolonged heating and only the starting material was recovered. Unlike  $\text{H}_3\text{PO}_2$  and  $\text{H}_3\text{PO}_3$ , phenylphosphinic acid displaced coordinated acetonitrile and after optimization of the reaction conditions two new, analytically pure complexes of the formula  $[\text{CpRu}(\text{CH}_3\text{CN})_2\{\text{PhP}(\text{OH})_2\}]\text{PF}_6$  (**28<sup>OH</sup>**) and  $[(\text{C}_5\text{Me}_5)\text{Ru}(\text{CH}_3\text{CN})\{\text{PhP}(\text{OH})_2\}_2]\text{PF}_6$  (**29<sup>OH</sup>**) were isolated. (**Scheme 2.5.**)

## Chapter 2

Interestingly, in the case of  $[\text{Cp}^{\text{R}}\text{Ru}(\text{CH}_3\text{CN})_3]\text{PF}_6$  only one phenylphosphinic acid coordinates to ruthenium, while substituting Cp with  $\text{C}_5\text{Me}_5$  it is formed exclusively the derivative bearing two molecules of phenylphosphinic acid as ligands. The reason for this latter different reactivity might be due to electronic effects.



**Scheme 2.5.** Coordination of phenylphosphinic acid to  $[\text{Cp}^{\text{R}}\text{Ru}(\text{CH}_3\text{CN})_3]\text{PF}_6$  and subsequent deoxofluorination.

The reaction of  $28^{\text{OH}}$  and  $29^{\text{OH}}$  with a three-fold excess of fluorinating reagent gave the corresponding complexes  $28^{\text{F}}$  and  $29^{\text{F}}$ , respectively, bearing the fluorinated phosphine (**Scheme 2.5**). The deoxofluorination of  $28^{\text{OH}}$  and  $29^{\text{OH}}$  occurred with completely different kinetics, since the former compound  $28^{\text{OH}}$  underwent a very sluggish reaction (*i.e.* reaction time of 18 h for complete conversion), while  $29^{\text{OH}}$  reacted rapidly (15 min) in the presence of di-isopropylamine (DIPEA).

## Chapter 2

The diphosphine complex **29<sup>F</sup>** displays symmetrical second order <sup>31</sup>P and <sup>19</sup>F spectra, see **Figures 2.2.** and **2.3.**, respectively. The two fluorine atoms at each phosphorus atom in **29<sup>F</sup>** are diastereotopic, forming together with the two phosphorus atoms a AA'BB'XX' (A, B: <sup>19</sup>F, X: <sup>31</sup>P) spin system. In fact in the <sup>19</sup>F NMR spectrum we observed two distinct multiplets at  $\delta = -53.9$  and  $\delta = -49.3$  ppm.

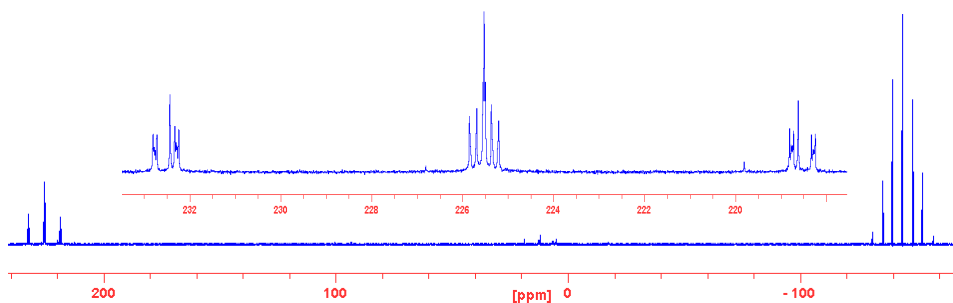


**Figure 2.2.** <sup>31</sup>P{<sup>1</sup>H} NMR of **29<sup>F</sup>** in MeOD with inset enlarging the signal at 224.8 ppm.

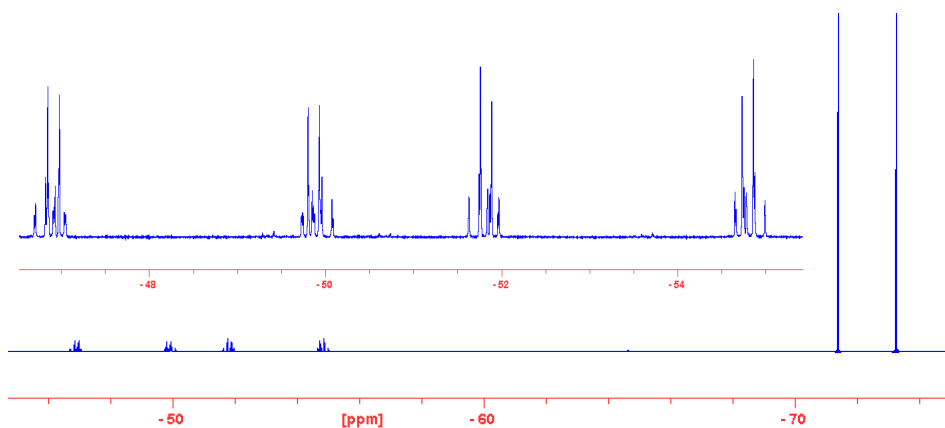


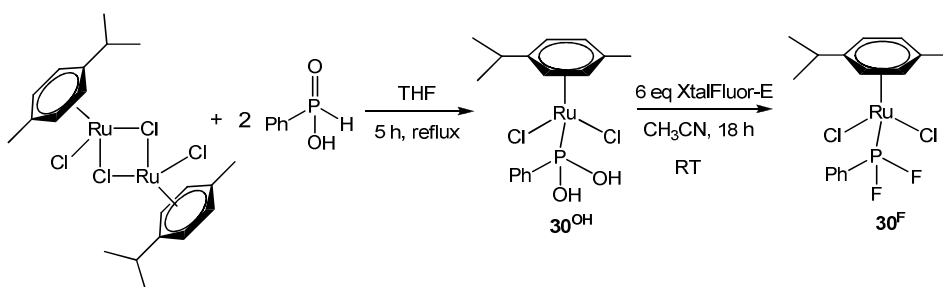
**Figure 2.3.** <sup>19</sup>F{<sup>1</sup>H} NMR of **29<sup>F</sup>** with inset enlarging the low field multiplets.

Actually, we found out that this in-equivalence is common for transition metal complexes bearing two fluorophosphines,<sup>32</sup> which show two

isochronous phosphorus nuclei at ambient temperature as in our case. On this regard, Heuer *et al.*<sup>33</sup> described these symmetrical higher order spin systems, invoking a virtual coupling between  $^{31}\text{P}$  and  $^{19}\text{F}$  nuclei, and reported the absolute value of the direct coupling constant  $J(\text{PF})$  as the sum of two coupling constants  $|^1J_{\text{PF}} + ^3J_{\text{PF}}|$ .

## 2.6 Synthesis and characterization of $[\eta^6\text{-}(p\text{-cymene})\text{RuCl}_2(\text{PhPF}_2)]$

The dimer  $\{\eta^6\text{-}(p\text{-cymene})\text{Ru}(\mu\text{-Cl})\text{Cl}\}_2$  is known to form mononuclear complexes by cleavage of the chloride bridges in the presence of a two-electron donor ligand. For instance, trihalophosphine ligands such as  $\text{PF}_3$  were successfully coordinated to the moiety  $\{\eta^6\text{-}(p\text{-cymene})\text{RuCl}_2\}$ .<sup>27</sup> We observed that upon reaction of the former dimer<sup>34</sup>  $\{\eta^6\text{-}(p\text{-cymene})\text{Ru}(\mu\text{-Cl})\text{Cl}\}_2$  with phenylphosphinic acid, the desired mononuclear species  $[\eta^6\text{-}(p\text{-cymene})\text{RuCl}_2\{\text{PhP}(\text{OH})_2\}]$  ( $\mathbf{30}^{\text{OH}}$ ) was isolated (**Scheme 2.6**). The coordination of phenylphosphinic acid to ruthenium in the form of the corresponding tautomer,  $\text{PhP}(\text{OH})_2$  was proved by a single crystal X-ray structure analysis, an ORTEP-plot of which is shown in **Figure 2.6**.



**Scheme 2.6.** Preparation of complexes  $\mathbf{30}^{\text{OH}}$  and  $\mathbf{30}^{\text{F}}$ .

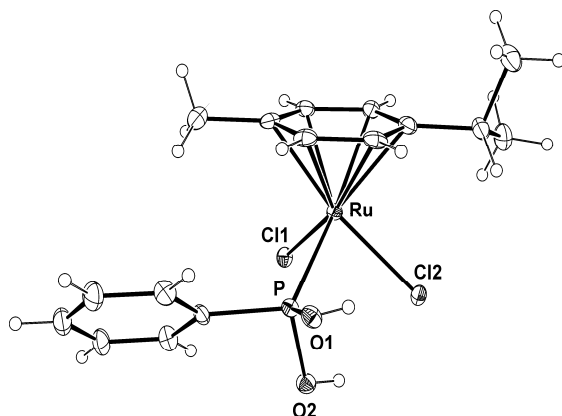


**Figure 2.6.** ORTEP-diagram of  $\mathbf{30}^{\text{OH}}$  with 30% probability ellipsoids. Hydrogen atoms, except for O(1) and O(2), are omitted for clarity. Selected bond length (Å) and angles ( $^{\circ}$ ): Ru(1)-P(1), 2.2969(9); Ru(1)-Cl(1), 2.4245(8); Ru(1)-Cl(2), 2.4275(9); Ru(1)-centroid(Cp), 1.7045; P(1)-Ru(1)-Cl(1), 87.27(3); P(1)-Ru(1)-Cl(2), 82.78(3).

$\text{H}_3\text{PO}_2$  and  $\text{H}_3\text{PO}_3$  did not react with  $\{\eta^6\text{-}(p\text{-cymene})\text{Ru}(\mu\text{-Cl})\text{Cl}\}_2$  even after a prolonged reaction time of 48 hours, which is the consequence of the electron poor metal center not capable of stabilizing. In fact, within the Ru-precursors employed, only  $[\text{CpRu}(\text{PPh}_3)_2]\text{OTf}$  was suitable to coordinate and stabilize the tautomers of hypophosphorous and phosphorous acid.<sup>15</sup> The deoxofluorination of  $\mathbf{30}^{\text{OH}}$  was carried out first in dichloromethane with six times excess of fluorinating agent (*i.e.* XtalFluor-E) under reflux for several hours. With these experimental conditions, a mixture of fluorinated Ru-species was obtained, according to  $^{31}\text{P}$  NMR monitoring. By changing the reaction medium to acetonitrile and using a six-fold excess of fluorinating reagent, the desired derivative  $[\eta^6\text{-}(p\text{-cymene})\text{RuCl}_2\{\text{PhPF}_2\}]$  ( $\mathbf{30}^{\text{F}}$ ) was obtained after 18 hours at room

temperature, as the only phosphorus containing species in high yield. (Scheme 2.6.)

## 2.7 Conclusions

In this chapter, a new way to synthesize a fluorophosphine ligand, using the commercial salt XtalFluor-E<sup>®</sup> as the fluorine source was studied, thus avoiding the use of highly toxic and unstable fluorinating agents. Phosphorous oxyacids as phosphinic, phenyl phosphinic and phosphonic acids, are the starting materials of choice and the procedure of deoxofluorination here applied for the first time to phosphorous oxyacids, represents an efficient and mild methodology for their transformation into the corresponding fluorophosphines, once coordinated to ruthenium as their tautomer counterpart, i.e. hydroxyphosphanes.

A series of half-sandwich Ru(II) complexes bearing the desired fluorophosphine ligands were prepared and fully characterized by multinuclear NMR. Their synthesis was not trivial, since the working conditions, as solvent, amount of XtalFluor-E<sup>®</sup>, reaction time and temperature, had to be tuned each time to get complete selectivity in the desired product. A dramatic change in  $^1J(\text{P-F})$  has been observed either changing the ancillary ligand or substituting one atom of fluorine by an hydrogen or a phenyl ring, suggesting that subtle electronic and steric effects are operating.

## 2.8 Experimental Section

### 2.8.1 Chemicals

All reactions and manipulations were carried out under nitrogen using standard Schlenk glassware and techniques. Dichloromethane was purified by distillation over CaH<sub>2</sub>. THF was purified by distillation over sodium wire and benzophenone. Diethyl ether and *n*-pentane were purified by passing them over two columns filled with molecular sieves (4Å) (LabMaster MBRAUN MD SPS). *n*-Hexane, H<sub>3</sub>PO<sub>3</sub>, H<sub>3</sub>PO<sub>2</sub> in water solution 50% w/w, PhP(O)(OH)H and diethylaminodifluorosulfonium tetrafluoroborate salt (commercial name XtalFluor-E) were used as purchased from Aldrich. Dichloromethane-d<sub>2</sub> (Aldrich) was pre-treated with three freeze-thaw pump cycles before use and kept under an inert atmosphere. Literature methods were used for the preparation of the following compounds: [CpRu(PPh<sub>3</sub>)<sub>2</sub>{HP(OH)<sub>2</sub>}]CF<sub>3</sub>SO<sub>3</sub> (**25<sup>OH</sup>**) [CpRu(PPh<sub>3</sub>)<sub>2</sub>{P(OH)<sub>3</sub>}]CF<sub>3</sub>SO<sub>3</sub> (**26<sup>OH</sup>**), [CpRu(PPh<sub>3</sub>)<sub>2</sub>{P(OH)<sub>3</sub>}]PF<sub>6</sub> (**26<sup>OH'</sup>**),<sup>15a</sup> [CpRu(CH<sub>3</sub>CN)<sub>3</sub>]PF<sub>6</sub>,<sup>30</sup> [Cp<sup>\*</sup>Ru(CH<sub>3</sub>CN)<sub>3</sub>]PF<sub>6</sub>,<sup>31</sup> and [{η<sup>6</sup>-(*p*-cymene)Ru(μ-Cl)Cl<sub>2</sub>}]<sub>2</sub>.<sup>34a</sup>

### 2.8.2 Characterization methods

#### Nuclear Magnetic Resonance spectroscopy (NMR)

Solution multinuclear NMR spectra were recorded on a Bruker Avance 300 and 400 MHz spectrometer. <sup>1</sup>H chemical shifts are referenced to tetramethylsilane (TMS), <sup>31</sup>P chemical shifts are referenced to 85% H<sub>3</sub>PO<sub>4</sub>, <sup>13</sup>C chemical shifts are referenced to tetramethylsilane, <sup>19</sup>F chemical shifts are referenced to CFCl<sub>3</sub> (376.5 MHz).



### **ElectroSpray Ionization-Mass spectrometry (ESI-MS)**

ESI-MS spectrum were recorded by direct introduction of the samples at 5  $\mu\text{l}/\text{min}$  flow rate in an LTQ-Orbitrap high-resolution mass spectrometer (Thermo, San Jose, CA, USA), equipped with a conventional ESI source. The working conditions comprised the following: spray voltage 4 kV, capillary voltage 3 V, capillary temperature 220  $^{\circ}\text{C}$ , tube lens 120 V. The sheath and auxiliary gases were set, respectively, at 10 (arbitrary units) and 3 (arbitrary units). For acquisition, Xcalibur 2.0. software (Thermo) and IT analyser were used.

### **InfraRed spectroscopy (IR)**

IR spectra were recorded with a Perkin Elmer spectrometer in KBr disks.

### **X-ray diffraction**

Diffraction data were collected with an Oxford Diffraction CCD diffractometer, using Mo- $K\alpha$  radiation ( $\lambda = 0.71069 \text{ \AA}$ ) and corrected for Lorentz and polarization effects. Absorption corrections were performed using the XABS2 program.<sup>35a</sup> All the structures were solved by direct methods using SHELXS-97<sup>39b</sup> and refined by full-matrix least-squared methods against  $F^2$  using the WINGX<sup>39c</sup> software package. All non-hydrogen atoms were refined anisotropically, whereas hydrogen atoms were added at calculated positions and refined applying a riding model with isotropic  $U$  values depending on the  $U_{eq}$  of the adjacent carbon atom.

### 2.8.3 Procedures

#### Synthesis of $\{[\text{CpRu}(\text{PPh}_3)_2\{\text{PhP}(\text{OH})_2\}]\text{CF}_3\text{SO}_3\}$ ( $27^{\text{OH}}$ )

To a suspension of  $[\text{CpRu}(\text{PPh}_3)_2\text{Cl}]$  (250.0 mg, 0.344 mmol) and  $\text{AgCF}_3\text{SO}_3$  (90.1 mg, 0.350 mmol) in a mixture of  $\text{CH}_2\text{Cl}_2$  (15 ml) and THF (7 ml) was added phenylphosphinic acid (49.0 mg, 0.344 mmol). The resulting slurry was stirred at room temperature for 2 hours. The precipitated  $\text{AgCl}$  was filtered off and yellow microcrystals of  $[\text{CpRu}(\text{PPh}_3)_2\{\text{PhP}(\text{OH})_2\}]\text{CF}_3\text{SO}_3$  were obtained by adding 20 ml of  $\text{Et}_2\text{O}$  and bubbling nitrogen gas for *ca* 30 minutes to evaporate the solvent. Yield: 84%. Crystals suitable for X-ray analysis were obtained by layering Petroleum Ether (30 ml) over the  $\text{CH}_2\text{Cl}_2/\text{THF}$  solution.  $^1\text{H}$ NMR (400 MHz,  $\text{CD}_2\text{Cl}_2$ , 298 K):  $\delta = 8.3$  (br. s, 2H,  $\text{PhP}(\text{OH})_2$ ) = 7.7-6.6 (m, 35H, Ph), 4.3 (m, 5H,  $\text{C}_5\text{H}_5$ ) ppm.  $^{31}\text{P}\{^1\text{H}\}$  NMR (162 MHz,  $\text{CD}_2\text{Cl}_2$ , 295 K):  $\delta = 147.6$  (t,  $^2J_{\text{PAPB}} = 56$  Hz, 1P,  $\text{P}_\text{A}$ ), 42.2 (d,  $^2J_{\text{PAPB}} = 56$  Hz, 2P,  $\text{P}_\text{B}$ ) ppm.  $^{13}\text{C}\{^1\text{H}\}$  NMR (100.6 MHz,  $\text{CD}_2\text{Cl}_2$ , 295 K):  $\delta = 133.9$  (s,  $\text{CH}_\text{ar}$ ), 130.1 (s,  $\text{CH}_\text{ar}$ ), 129.9 (s,  $\text{CH}_\text{ar}$ ), 129.0 (d,  $^1J_{\text{CP}} = 12$  Hz,  $\text{C}_\text{q}$ ), 127.9 (m,  $\text{C}_\text{q}$ ), 87.3 (s,  $\text{C}_5\text{H}_5$ ) ppm. IR (KBr,  $\text{cm}^{-1}$ ):  $\nu = 3058$  (broad, OH), 1223 (s,  $\text{CF}_3\text{SO}_3$ ) 887, 847 (s, P-OH).

#### Synthesis of $\{[\text{CpRu}(\text{PPh}_3)_2(\text{HPF}_2)]\text{CF}_3\text{SO}_3\}$ ( $25^{\text{F}}$ )

$[\text{CpRu}(\text{PPh}_3)_2\{\text{HP}(\text{OH})_2\}]\text{CF}_3\text{SO}_3$  (250.0 mg, 0.276 mmol) and  $[\text{Et}_2\text{NSF}_2]\text{BF}_4$  (126.2 mg, 0.552 mmol, 2 eq) were charged in a schlenk tube and dissolved in  $\text{CH}_2\text{Cl}_2$  (15 ml). The resulting suspension was stirred at room temperature overnight and finally cooled down (*ca*  $-78^\circ\text{C}$ ). A white crystalline compound precipitated out from the solution and the yellow supernatant was cannulated into a 50 ml schlenk flask and  $\{[\text{CpRu}(\text{PPh}_3)_2(\text{HPF}_2)]\text{CF}_3\text{SO}_3\}$  was obtained as a yellow microcrystalline

## Chapter 2

solid by cooling the solution down (*ca.* 0°C) and adding 50 ml of Et<sub>2</sub>O. Yield: 86%. ESI-MS: 761.1 [M]<sup>+</sup>. <sup>1</sup>H NMR (400.13 MHz, CD<sub>2</sub>Cl<sub>2</sub>, 298 K):  $\delta$  = 8.7 (dt, <sup>1</sup>J<sub>H-PA</sub> = 465 Hz, <sup>2</sup>J<sub>H-F</sub> = 63 Hz, 1H, HPF<sub>2</sub>), 7.6-6.7 (m, 30H, CH<sub>ar</sub>), 4.9 (s, 5H, C<sub>5</sub>H<sub>5</sub>) ppm. <sup>31</sup>P{<sup>1</sup>H} NMR (161.9 MHz, CD<sub>2</sub>Cl<sub>2</sub>, 295 K):  $\delta$  = 225.1 (tt, <sup>1</sup>J<sub>PAF</sub> = 1088 Hz, <sup>2</sup>J<sub>PAPB</sub> = 57 Hz, 1P, P<sub>A</sub>), 40.2 (dt, <sup>2</sup>J<sub>PAPB</sub> = 57 Hz, <sup>3</sup>J<sub>PF</sub> = 8 Hz, 2P, P<sub>B</sub>) ppm. <sup>31</sup>P NMR (161.9 MHz, CD<sub>2</sub>Cl<sub>2</sub>, 295 K):  $\delta$  = 225.1 (tt, <sup>1</sup>J<sub>H-PA</sub> = 465 Hz, 1P, P<sub>A</sub>) 40.2 (dt, <sup>2</sup>J<sub>PAPB</sub> = 57 Hz, <sup>3</sup>J<sub>PF</sub> = 8 Hz, 2P, P<sub>B</sub>) ppm. <sup>19</sup>F NMR (376.5 MHz, CD<sub>2</sub>Cl<sub>2</sub>, 295 K):  $\delta$  = 4.6 (d, <sup>1</sup>J<sub>PAF</sub> = 1088 Hz, PF<sub>2</sub>), -78.9 (s, CF<sub>3</sub>SO<sub>3</sub><sup>-</sup>) ppm. <sup>13</sup>C{<sup>1</sup>H} NMR (100.6 MHz, CD<sub>2</sub>Cl<sub>2</sub>, 295 K):  $\delta$  = 133.1 (t, <sup>2</sup>J<sub>CP</sub> = 5 Hz, CH<sub>ar</sub>), 131.2 (m, C<sub>q</sub>), 128.8 (s, CH<sub>ar</sub>), 128.9 (t, <sup>3</sup>J<sub>CP</sub> = 5 Hz, CH<sub>ar</sub>), 89.3 (s, C<sub>5</sub>H<sub>5</sub>) ppm. IR (KBr, cm<sup>-1</sup>):  $\nu$  = 2464 (w, P-H), 1275 (s, CF<sub>3</sub>SO<sub>3</sub>), 819 (s, P-F).

### Synthesis of {[CpRu(PPh<sub>3</sub>)<sub>2</sub>(PF<sub>3</sub>)]CF<sub>3</sub>SO<sub>3</sub>} (26<sup>F</sup>)

[CpRu(PPh<sub>3</sub>)<sub>2</sub>{P(OH)<sub>3</sub>}]CF<sub>3</sub>SO<sub>3</sub> (250.0 mg, 0.271 mmol) and [Et<sub>2</sub>N=SF<sub>2</sub>]BF<sub>4</sub> (497.0 mg, 2.168 mmol, 8 eq) were charged in a schlenk tube (100 ml) and dissolved in CH<sub>2</sub>Cl<sub>2</sub> (15 ml). The resulting suspension was stirred at room temperature overnight and finally cooled down (*ca.* -78°C). A white crystalline compound precipitated out of the solution, presumably a salt by-product of the reaction. The yellow supernatant was cannulated into a 50 ml schlenk flask and {[CpRu(PPh<sub>3</sub>)<sub>2</sub>(PF<sub>3</sub>)]CF<sub>3</sub>SO<sub>3</sub>} was obtained as yellow microcrystals by adding 20 ml of Et<sub>2</sub>O and bubbling nitrogen gas for *ca.* 30 minutes. [CpRu(PPh<sub>3</sub>)<sub>2</sub>(PF<sub>3</sub>)]CF<sub>3</sub>SO<sub>3</sub> is air stable in solution for a long time. Yield: 94 %. ESI-MS: 779.1 [M]<sup>+</sup>. <sup>1</sup>H NMR (400.0 MHz, CD<sub>2</sub>Cl<sub>2</sub>, 298 K):  $\delta$  = 7.6-6.8 (m, 30H, CH<sub>ar</sub>), 4.9 (m, 5H, C<sub>5</sub>H<sub>5</sub>) ppm. <sup>31</sup>P{<sup>1</sup>H} NMR (161.9 MHz, CD<sub>2</sub>Cl<sub>2</sub>, 295 K):  $\delta$  = 144.8 (qt, <sup>1</sup>J<sub>PAF</sub> = 1302 Hz, <sup>2</sup>J<sub>PAPB</sub> = 72 Hz, 1P, P<sub>A</sub>), 37.3 (d, <sup>2</sup>J<sub>PAPB</sub> = 72 Hz, 2P<sub>B</sub>)

## Chapter 2

ppm.  $^{19}\text{F}$  NMR (376.5 MHz,  $\text{CD}_2\text{Cl}_2$ , 295 K):  $\delta = 4.5$  (d,  $^1J_{\text{PF}} = 1302$  Hz,  $\text{PF}_3$ ),  $-78.7$  (s,  $\text{CF}_3\text{SO}_3^-$ ) ppm.  $^{13}\text{C}\{^1\text{H}\}$  NMR (100.6 MHz,  $\text{CD}_2\text{Cl}_2$ , 295 K):  $\delta = 134.3$  (m,  $\text{C}_q$ ),  $133.1$  (t,  $^2J_{\text{CP}} = 5$  Hz,  $\text{CH}_{\text{ar}}$ ),  $131.3$  (m,  $\text{CH}_{\text{ar}}$ ),  $128.9$  (t,  $^3J_{\text{CP}} = 5$  Hz,  $\text{CH}_{\text{ar}}$ ),  $89.4$  (s,  $\text{C}_5\text{H}_5$ ) ppm. IR (KBr,  $\text{cm}^{-1}$ ):  $\nu = 1263$  (s,  $\text{CF}_3\text{SO}_3$ ),  $864$  (s, P-F).

### Synthesis of $\{[\text{CpRu}(\text{PPh}_3)_2(\text{PF}_3)]\text{PF}_6\}$ ( $26^{\text{F}'}$ )

$[\text{CpRu}(\text{PPh}_3)_2\{\text{P}(\text{OH})_3\}]\text{PF}_6$  (250.0 mg, 0.272 mmol) and  $[\text{Et}_2\text{N}=\text{SF}_2]\text{BF}_4$  (187.2 mg, 0.817 mmol, 3 eq) were charged in a schlenk tube and dissolved in  $\text{CH}_2\text{Cl}_2$  (15 ml). The resulting suspension was stirred at room temperature overnight and finally cooled down (*ca*  $-78^\circ\text{C}$ ). A white crystalline compound precipitated out of the solution, presumably a salt by-product of the reaction. The yellow supernatant was cannulated into a 50 ml schlenk flask and  $\{[\text{CpRu}(\text{PPh}_3)_2(\text{PF}_3)]\text{PF}_6\}$  was obtained as yellow microcrystals by adding 20 ml of  $\text{Et}_2\text{O}$  and bubbling nitrogen gas for *ca* 30 minutes.  $[\text{CpRu}(\text{PPh}_3)_2(\text{PF}_3)]\text{PF}_6$  is air stable in solution for a long time. Yield: 93%

### Synthesis of $\{[\text{CpRu}(\text{PPh}_3)_2(\text{PhPF}_2)]\text{CF}_3\text{SO}_3\}$ ( $27^{\text{F}}$ )

$[\text{CpRu}(\text{PPh}_3)_2\{\text{PhP}(\text{OH})_2\}]\text{CF}_3\text{SO}_3$  (250.0 mg, 0.255 mmol) and  $[\text{Et}_2\text{NSF}_2]\text{BF}_4$  (233.6 mg, 1.02 mmol, 4 eq) were charged in a schlenk tube (100 ml) and dissolved in  $\text{CH}_2\text{Cl}_2$  (20 ml). The resulting suspension was stirred at room temperature for overnight and finally cooled down (*ca*  $-78^\circ\text{C}$ ) for 2 hours. A white crystalline compound precipitated and the yellow solution was cannulated into a 50 ml schlenk flask. The solution was concentrated to 10 ml by evaporating the solvent under reduced pressure.  $\{[\text{CpRu}(\text{PPh}_3)_2(\text{PhPF}_2)]\text{CF}_3\text{SO}_3\}$  was obtained as yellow

## Chapter 2

microcrystalline solid by adding 50 ml Et<sub>2</sub>O. Yield: 90%. ESI-MS: 837.1 [M]<sup>+</sup>. <sup>1</sup>H NMR (400.13 MHz, CD<sub>2</sub>Cl<sub>2</sub>, 298 K): δ = 7.7-6.5 (m, 45H, Ph), 4.9 (s, 5H, C<sub>5</sub>H<sub>5</sub>) ppm. <sup>31</sup>P{<sup>1</sup>H} NMR (161.97 MHz, CD<sub>2</sub>Cl<sub>2</sub>, 295 K): δ = 220.8 (tt, <sup>1</sup>J<sub>PAF</sub> = 1087 Hz, <sup>2</sup>J<sub>PAPB</sub> = 56 Hz, 1P, P<sub>A</sub>, PF<sub>2</sub>), 38.6 (dt, <sup>2</sup>J<sub>PAPB</sub> = 56 Hz, <sup>3</sup>J<sub>PF</sub> = 7 Hz, 2P, P<sub>B</sub>) ppm. <sup>19</sup>F NMR (376.5 MHz, CD<sub>2</sub>Cl<sub>2</sub>, 295 K): δ = -34.2 (d, <sup>1</sup>J<sub>PAF</sub> = 1087 Hz, PF<sub>2</sub>), -79.0 (s, CF<sub>3</sub>SO<sub>3</sub><sup>-</sup>) ppm. <sup>13</sup>C{<sup>1</sup>H} NMR (100.6 MHz, CD<sub>2</sub>Cl<sub>2</sub>, 295 K): δ = 133.8 (t, <sup>2</sup>J<sub>CP</sub> = 5 Hz, CH<sub>ar</sub>), 131.5 (s, CH<sub>ar</sub>), 129.1 (t, <sup>3</sup>J<sub>CP</sub> = 5 Hz, CH<sub>ar</sub>), 127.7 (dt, <sup>1</sup>J<sub>CP</sub> = 14 Hz, <sup>2</sup>J<sub>CF</sub> = 3 Hz, C<sub>q</sub>), 89.7 (s, C<sub>5</sub>H<sub>5</sub>) ppm. IR (KBr, cm<sup>-1</sup>): ν = 1263 (s, CF<sub>3</sub>SO<sub>3</sub>), 801 (s, P-F).

### Synthesis of {[Cp\**Ru*(CH<sub>3</sub>CN)<sub>3</sub>]PF<sub>6</sub>}

The compound was prepared by a modification of the published procedure.<sup>3</sup>

To a solution of [Cp\**Ru*Cl<sub>2</sub>]<sub>2</sub> (350.0 mg, 1.139 mmol) in acetonitrile (10 ml) was added zinc dust (149.0 mg, 2.279 mmol). After stirring 1 hour at room temperature, dry KPF<sub>6</sub> (318.0 mg, 1.608 mmol) was added. The mixture was stirred for 16 hours at room temperature, afterwards the solvent was evaporated to dryness. To the solid residue was added CH<sub>2</sub>Cl<sub>2</sub> (20 ml) and the supernatant was cannulated into a schlenk tube and evaporated to dryness affording a brown-yellow solid. Yield: 78 %. <sup>1</sup>H NMR (400.0 MHz, CD<sub>2</sub>Cl<sub>2</sub>, 298 K): δ = 2.4 (br. s, 9H, CH<sub>3</sub>CN), 2.3 (s, 15H, Cp\*) ppm. <sup>31</sup>P{<sup>1</sup>H} NMR (161.9 MHz, CD<sub>2</sub>Cl<sub>2</sub>, 298 K): δ = -144.8 (sept, 1P, PF<sub>6</sub>, <sup>1</sup>J<sub>PF</sub> = 702 Hz) ppm.

**Synthesis of  $\{[\text{CpRu}(\text{CH}_3\text{CN})_2\{\text{PhP}(\text{OH})_2\}]\text{PF}_6\}$  ( $28^{\text{OH}}$ )**

$[\text{CpRu}(\text{CH}_3\text{CN})_3]\text{PF}_6$  (300.1 mg, 0.691 mmol) and  $\text{PhP}(\text{O})(\text{H})(\text{OH})$  (98.1 mg, 0.691 mmol) were charged in a schlenk tube (100 ml) and dissolved in  $\text{CH}_3\text{CN}$  (60 ml). The resulting yellow solution was stirred at room temperature for three days. The solution was concentrated to dryness under reduced pressure and the solid residue was washed three times, each with 15 mL of pentane. A mustard solid was obtained and dried under vacuum. Yield: 74%. ESI-MS (acetonitrile):  $m/z = 390.9$   $[\text{M}]^+$ .  $^1\text{H}$  NMR (400.1 MHz,  $\text{CD}_2\text{Cl}_2$ , 298 K):  $\delta = 7.8$ - $7.5$  (m, 5H, Ph), 4.6 (s, 5H,  $\text{C}_p$ ), 2.3 (s, 6H,  $\text{CH}_3\text{CN}$ ).  $^{31}\text{P}\{^1\text{H}\}$  NMR (161.9 MHz,  $\text{CD}_2\text{Cl}_2$ , 298 K):  $\delta = 151.3$  (s, 1P), -143.7 (sept,  $\text{PF}_6$ ,  $^1J_{\text{PF}} = 702$  Hz).  $^{13}\text{C}\{^1\text{H}\}$  NMR (100.6 MHz,  $\text{CD}_2\text{Cl}_2$ , 295 K):  $\delta = 142.1$  (d,  $^1J_{\text{PC}} = 64$  Hz,  $\text{C}_q$ ), 130.9 (d,  $^2J_{\text{CP}} = 2$  Hz,  $\text{CH}_{\text{ar}}$ ), 129.2 (d,  $^2J_{\text{CP}} = 13$  Hz,  $\text{CH}_{\text{ar}}$ ), 128.7 (d,  $^3J_{\text{CP}} = 10$  Hz,  $\text{CH}_{\text{ar}}$ ), 127.3 (s,  $\text{CH}_3\text{CN}$ ), 77.6 (d,  $^2J_{\text{CP}} = 3$  Hz,  $\text{C}_5\text{H}_5$ ), 4.1 (s,  $\text{CH}_3\text{CN}$ ). IR (KBr,  $\text{cm}^{-1}$ ):  $\nu = 2263$  (w, CN), 1113, (broad,  $\text{P}(\text{OH})_2$ ), 836 (s, P-F,  $\text{PF}_6$ ).

**Synthesis of  $\{[\text{Cp}^*\text{Ru}(\text{CH}_3\text{CN})\{\text{PhP}(\text{OH})_2\}_2]\text{PF}_6\}$  ( $29^{\text{OH}}$ )**

$[\text{Cp}^*\text{Ru}(\text{CH}_3\text{CN})_3]\text{PF}_6$  (100.0 mg, 0.198 mmol, 1 eq) and  $\text{PhP}(\text{O})(\text{H})(\text{OH})$  (28.1 mg, 0.198 mmol, 1 eq) were charged in a schlenk tube (50 ml) and dissolved in  $\text{CH}_3\text{CN}$  (20 ml). The resulting solution was stirred at  $40^\circ\text{C}$  for 24 hours. The solution was concentrated to a small volume and were added in the order, 1 ml of toluene and 50 ml of pentane to precipitate the final product.  $[\text{Cp}^*\text{Ru}(\text{CH}_3\text{CN})\{\text{PhP}(\text{OH})_2\}_2]\text{PF}_6$  was obtained as yellow-brown solid after filtration under nitrogen and was dried in vacuum. Yield: 52%. ESI-MS (acetonitrile):  $m/z = 562.1$   $[\text{M}]^+$ ;  $[\text{M}]^+ - [\text{PhP}(\text{OH})_2]$ : 419.8.  $^1\text{H}$ NMR (300.1 MHz,  $\text{CD}_3\text{OD}$ ), 295 K):  $\delta = 7.8$  (m, 4H,  $\text{H}_{\text{ar}}$ ), 7.5 (m, 6H,  $\text{H}_{\text{ar}}$ ), 2.5 (s, 3H,  $\text{CH}_3\text{CN}$ ), 1.4 (s, 15H,  $\text{C}_5\text{Me}_5$ ) ppm.  $^{31}\text{P}\{^1\text{H}\}$  NMR (121.5

## Chapter 2

MHz, CD<sub>3</sub>OD, 295 K):  $\delta$  = 153.5 (s, 1P), -144.5 (sept,  $^1J_{PF}$  = 708 Hz, PF<sub>6</sub>) ppm. <sup>13</sup>C{<sup>1</sup>H} NMR (75.5 MHz, CD<sub>3</sub>OD, 295 K):  $\delta$  = 142.8 (t,  $^1J_{CP}$  = 30 Hz, C<sub>q</sub>), 131.4 (s, CH<sub>ar</sub>), 130.8 (t,  $^2J_{CP}$  = 6 Hz, CH<sub>ar</sub>), 129.0 (t,  $^3J_{CP}$  = 5 Hz, CH<sub>ar</sub>), 127.0 (s, CH<sub>3</sub>CN), 94.4 (s, C<sub>5</sub>Me<sub>5</sub>), 9.5 (s, C<sub>5</sub>Me<sub>5</sub>) 3.6 (s, CH<sub>3</sub>CN) ppm. IR (KBr, cm<sup>-1</sup>):  $\nu$  = 2962 (s, OH), 2267 (w, CN), 836 (s, P-F, PF<sub>6</sub>).

The reaction was repeated using a ratio complex/ligand 1:2 as follows: [Cp\**Ru*(CH<sub>3</sub>CN)<sub>3</sub>]PF<sub>6</sub> (350.0 mg, 0.6925 mmol, 1 eq) and PhP(O)(H)(OH) (196.8 mg, 1.385 mmol, 2 eq) were charged in a schlenk tube and dissolved in CH<sub>3</sub>CN (30 ml). The resulting solution was stirred at 40°C for 24 hours. The solution was concentrated to dryness, the solid residue was rinsed with pentane, than dichloromethane and diethyl ether (ratio 2:1) were added to precipitate the pure product. [Cp\**Ru*(CH<sub>3</sub>CN){PhP(OH)<sub>2</sub>]<sub>2</sub>]PF<sub>6</sub> was obtained as yellow solid after filtration under nitrogen and was dried in vacuum. Yield: 71%.

The NMR data are the same as above.

### Synthesis of {[CpRu(CH<sub>3</sub>CN)<sub>2</sub>(PhPF<sub>2</sub>)]PF<sub>6</sub>} (28<sup>F</sup>)

[CpRu(CH<sub>3</sub>CN)<sub>2</sub>{PhP(OH)<sub>2</sub>}]PF<sub>6</sub> (100.0 mg, 0.187 mmol) and XtalFluor-E (128.3 mg, 0.560 mmol, 3 eq) were charged in a schlenk tube and dissolved in CH<sub>2</sub>Cl<sub>2</sub> (30 ml). The resulting solution was stirred at room temperature for 18 hours and afterwards the reaction mixture was kept in the freezer at -30°C overnight. A white crystalline compound precipitated out and the yellow solution was cannulated into a schlenk flask. The solution was concentrated to a small volume and 50 ml of diethyl ether were added. The desired complex precipitated out of the solution as brown-yellow solid. Yield: 68 %. ESI-MS (acetonitrile):  $m/z$  = 394.7 [M]<sup>+</sup>. <sup>1</sup>H NMR (300.1 MHz, CD<sub>2</sub>Cl<sub>2</sub>, 298 K):  $\delta$  = 7.8-7.6 (m, 5H, Ph), 4.9 (s, 5H,

## Chapter 2

$C_5H_5$ ), 2.3 (s, 6H,  $CH_3CN$ ) ppm.  $^{31}P\{^1H\}$  NMR (121.5 MHz,  $CD_2Cl_2$ , 295 K):  $\delta = 224.9$  (t,  $^1J_{PF} = 1148$  Hz,  $PF_2$ ),  $-144.4$  (sept,  $^1J_{PF} = 711$  Hz,  $PF_6$ ) ppm.  $^{19}F$  NMR (376.5 MHz,  $CD_2Cl_2$ , 295 K):  $\delta = -52.1$  (d,  $^1J_{FP} = 1147$  Hz,  $PhPF_2$ ),  $-72.6$  (d,  $^1J_{FP} = 711$  Hz,  $PF_6$ ) ppm.  $^{13}C\{^1H\}$  NMR (75.5 MHz,  $CD_2Cl_2$ , 295 K):  $\delta = 134.0$  (d,  $^2J_{CP} = 2$  Hz,  $CH_{ar}$ ),  $129.8$  (dt,  $^1J_{CP} = 18$  Hz,  $^2J_{CF} = 4$  Hz,  $C_q$ ),  $129.5$  (s,  $CH_{ar}$ ),  $129.3$  (s,  $CH_{ar}$ ),  $128.7$  (s,  $CH_3CN$ ),  $79.9$  (d,  $^2J_{CP} = 2$  Hz,  $C_5H_5$ ),  $4.3$  (s,  $CH_3CN$ ) ppm. IR (KBr,  $cm^{-1}$ ):  $\nu = 2228$  (w, CN),  $839$  (br. s, P-F,  $PF_2$ ,  $PF_6$ ).

### Synthesis of $\{[Cp^*Ru(CH_3CN)(PhPF_2)_2]PF_6\}$ (**29<sup>F</sup>**)

$[Cp^*Ru(CH_3CN)\{PhP(OH)_2\}_2]PF_6$  (190.0 mg, 0.2689 mmol) and XtalFluor-E (184.8 mg, 0.868 mmol, 3 eq) were charged in a schlenk tube (50 ml). In another schlenk and dissolved in  $CH_2Cl_2$  (14 ml). The resulting solution was stirred at room temperature for 15 min. The solution was dried by evaporating the solvent under reduced pressure. Afterwards the reaction mixture was kept at  $-78^\circ C$  for 2 hours. A white crystalline compound precipitated out and the brownish solution was cannulated into a schlenk flask. The solution was dried and the remaining oil was washed with diethyl ether and pentane several times until a brownish solid was obtained. Yield: 63%. ESI-MS (acetonitrile):  $m/z = 390.9$   $[M]^+$ .  $^1H$  NMR (300.1 MHz,  $CD_3OD$ , 298 K):  $\delta = 7.9-7.5$  (m, 10H,  $Ph$ ),  $2.4$  (s, 3H,  $CH_3CN$ ),  $1.3$  (s, 15H,  $CH_3$ ) ppm.  $^{31}P\{^1H\}$  NMR (121.5 MHz,  $CD_3OD$ , 295 K):  $\delta = 225.9$  (second order multiplet,  $|^1J_{PF} + ^3J_{PF}| = 1184$  Hz, 2P),  $-141.4$  (spt,  $^1J_{PF} = 708$  Hz, 1P,  $PF_6$ ) ppm.  $^{19}F$  NMR (376.5 MHz,  $CD_3OD$ , 295 K):  $\delta = -49.3$  (dm,  $|^1J_{PF} + ^3J_{PF}| = 1185$  Hz,  $PhPFA$ ),  $-53.9$  (dm,  $|^1J_{PF} + ^3J_{PF}| = 1184$  Hz,  $PhPFB$ ),  $-73.9$  (d,  $^1J_{FP} = 708$  Hz,  $PF_6$ ) ppm.  $^{13}C\{^1H\}$  NMR (75.5 MHz,  $CD_3OD$ , 295 K):  $\delta = 135.1$  (s,  $CH_3CN$ ),  $133.5$  (d,  $^4J_{CP} = 3$  Hz,  $CH_{ar}$ ),  $132.4$  (d,  $^3J_{CP} = 10$  Hz,



## Chapter 2

CH<sub>ar</sub>), 130.4 (d, <sup>2</sup>J<sub>CP</sub> = 11 Hz, CH<sub>ar</sub>), 129.6 (d, <sup>1</sup>J<sub>CP</sub> = 15 Hz, C<sub>q</sub>), 128.9 (s, CH<sub>3</sub>CN), 100.3 (s, C<sub>5</sub>Me<sub>5</sub>), 9.8 (s, C<sub>5</sub>Me<sub>5</sub>), 3.5 (s, CH<sub>3</sub>CN) ppm.

<sup>1</sup>H NMR (400.1 MHz, (CD<sub>3</sub>)<sub>2</sub>CO, 298 K): δ = 7.8-7.7 (m, 10H, Ph), 2.5 (s, 3H, CH<sub>3</sub>CN), 1.8 (s, 15H, CH<sub>3</sub>) ppm. <sup>31</sup>P{<sup>1</sup>H} NMR (161.9 MHz, (CD<sub>3</sub>)<sub>2</sub>CO, 295 K): δ = 227.5 (second order multiplet, |<sup>1</sup>J<sub>PF</sub> + <sup>3</sup>J<sub>PF</sub>| = 1184 Hz, 2P), -144.4 (spt, <sup>1</sup>J<sub>PF</sub> = 707 Hz, 1P, PF<sub>6</sub>) ppm. <sup>19</sup>F NMR (376.5 MHz, (CD<sub>3</sub>)<sub>2</sub>CO, 295 K): δ = -48.3 (dm, |<sup>1</sup>J<sub>PF</sub> + <sup>3</sup>J<sub>PF</sub>| = 1184 Hz, PhPFA), -53.4 (dm, |<sup>1</sup>J<sub>PF</sub> + <sup>3</sup>J<sub>PF</sub>| = 1184 Hz, PhPFB), -72.4 (<sup>1</sup>J<sub>FP</sub> = 708 Hz, PF<sub>6</sub>) ppm. <sup>13</sup>C{<sup>1</sup>H} NMR (100.6 MHz, (CD<sub>3</sub>)<sub>2</sub>CO, 253 K): δ = 135.5 (dt, <sup>1</sup>J<sub>CP</sub> = 50 Hz, <sup>2</sup>J<sub>CF</sub> = 14 Hz, C<sub>q</sub>), 135.0 (s, CH<sub>ar</sub>), 131.1 (s, CH<sub>ar</sub>), 130.1 (s, CH<sub>ar</sub>), 129.6 (s, CH<sub>3</sub>CN), 99.5 (s, C<sub>5</sub>Me<sub>5</sub>), 9.6 (s, C<sub>5</sub>Me<sub>5</sub>) 4.2 (s, CH<sub>3</sub>CN) ppm. IR (KBr, cm<sup>-1</sup>): ν = 2229 (w, CN), 814 (s, P-F, PF<sub>2</sub>), 843 (s, P-F, PF<sub>6</sub>).

### Synthesis of [(η<sup>6</sup>-*p*-cymene)RuCl<sub>2</sub>{PhP(OH)<sub>2</sub>}] (30<sup>OH</sup>)

To a suspension of [(η<sup>6</sup>-*p*-cymene)RuCl<sub>2</sub>]<sub>2</sub> (250.0 mg, 0.816 mmol) in THF (50 ml) was added phenylphosphinic acid (232.0 mg, 1.6326 mmol) as a solid. The solution was refluxed for 5 hours, afterwards the reaction mixture was cooled down to room temperature and concentrated to small volume by evaporating the solvent under reduced pressure. [(η<sup>6</sup>-*p*-cymene)RuCl<sub>2</sub>{PhP(OH)<sub>2</sub>}] was obtained as an orange solid by adding 50 ml of pentane. Yield: 78%. Crystals suitable for X-ray analysis were obtained by cooling down to 4°C a solution of the complex in dichloromethane and allowing a slow diffusion of pentane. <sup>1</sup>H NMR (300.0 MHz, CD<sub>2</sub>Cl<sub>2</sub>, 295 K): δ = 7.9 (m, 1H, CH<sub>ar</sub>), 7.7 (m, 4H, CH<sub>ar</sub>), 5.2 (s, 4H, CH<sub>ar</sub>, *p*-cymene), 2.6 (sept, <sup>3</sup>J<sub>HH</sub> = 7 Hz, 1H, CH(CH<sub>3</sub>)<sub>2</sub>), 2.0 (s, 3H, CH<sub>3</sub>), 1.1 (d, <sup>3</sup>J<sub>HH</sub> = 7 Hz, 6H, CH(CH<sub>3</sub>)<sub>2</sub>) ppm. <sup>31</sup>P{<sup>1</sup>H} NMR (121.5 MHz, CD<sub>2</sub>Cl<sub>2</sub>, 295 K): δ = 147.6 (s) ppm. <sup>13</sup>C{<sup>1</sup>H} NMR (75.5 MHz, CD<sub>2</sub>Cl<sub>2</sub>,

## Chapter 2

295 K):  $\delta = 136.9$  (d,  $^1J_{CP} = 88$  Hz,  $C_q$ ), 132.1 (s,  $CH_{ar}$ ), 130.3 (d,  $^2J_{CP} = 12$  Hz,  $CH_{ar}$ ), 128.8 (d,  $^3J_{CP} = 12$  Hz,  $CH_{ar}$ ), 105.6 (s,  $C_q$ ), 98.1 (s,  $C_q$ ), 90.0 (d,  $^2J_{CP} = 6$  Hz,  $CH_{p-cym}$ ), 88.2 (d,  $^2J_{CP} = 6$  Hz,  $CH_{p-cym}$ ), 30.3 (s,  $CH(CH_3)_2$ ), 21.5 (s,  $CH(CH_3)_2$ ), 18.3 (s,  $CH_3$ -ring) ppm. IR (KBr,  $cm^{-1}$ ):  $\nu = 3065$  (broad, OH), 858 (s, P-OH).

### Synthesis of $[(\eta^6\text{-}p\text{-cymene})RuCl_2(PhPF_2)]$ (**30<sup>F</sup>**)

$[(\eta^6\text{-}p\text{-cymene})RuCl_2\{PhP(OH)_2\}]$  (100.0 mg, 0.223 mmol) and  $[Et_2NSF_2]BF_4$  (467.2 mg, 1.338 mmol, 6 eq) were charged in a schlenk tube and dissolved in  $CH_3CN$  (40ml). The solution was stirred at room temperature for 18 hours. The solution was dried by evaporating the solvent under reduced pressure. The solid residue was re-dissolved in dichloromethane and cooled down (ca  $-78^\circ C$ ) to allow the precipitation of excess of fluorinating agent. After filtration under nitrogen, pentane was added to the filtrate and the desired product precipitated out from the solution. The brown solid was recovered by filtration under inert atmosphere. Yield: 80%. ESI-MS:  $m/z = 457.83$  [ $M^+ - Cl + CH_3CN$ ]; 417.08 [ $M^+ - CH_3CN$ ].  $^1H$ NMR (300.0 MHz,  $CD_2Cl_2$ , 295 K):  $\delta = 7.9 - 7.7$  (m, 5H,  $CH_{ar}$ ), 5.6 (d,  $^3J_{HH} = 6$  Hz, 2H,  $CH_{ar}$ ,  $p$ -cymene), 5.5 (d,  $^3J_{HH} = 6$  Hz, 2H,  $CH_{ar}$ ,  $p$ -cymene), 3.8 (sept,  $^3J_{HH} = 6$  Hz, 1H,  $CH(CH_3)_2$ ), 2.5 (s, 3H,  $CH_3$ ), 1.3 (d,  $^3J_{HH} = 6$  Hz, 6H,  $CH(CH_3)_2$ ) ppm.  $^{31}P\{^1H\}$  NMR (121.5 MHz,  $CD_2Cl_2$ , 295 K):  $\delta = 215.1$  (t,  $^1J_{PF} = 1156$  Hz,  $PF_2$ ) ppm.  $^{19}F$  NMR (376.5 MHz,  $CD_2Cl_2$ , 295 K):  $\delta = -58.6$  ( $^1J_{FP} = 1159$  Hz,  $PhPF_2$ ) ppm.  $^{13}C\{^1H\}$  NMR (75.5 MHz,  $CD_2Cl_2$ , 295 K):  $\delta = 135.2$  (br.s,  $CH_{ar}$ ), 130.0 (d,  $^2J_{CP} = 12$  Hz,  $CH_{ar}$ ), 129.4 (dt,  $^1J_{CP} = 16$  Hz,  $^2J_{CF} = 4$  Hz,  $C_q$ ), 127.1 (d,  $^3J_{CP} = 12$  Hz,  $CH_{ar}$ ), 102.2 (s,  $C_q$ ), 97.6 (s,  $C_q$ ), 79.3 (s,  $CH_{p-cym}$ ), 78.4 (s,

*Chapter 2*

$\text{CH}_{\text{p-cym}}$ , 31.8 (s,  $\text{CH}(\text{CH}_3)_2$ ), 22.2 (s,  $\text{CH}(\text{CH}_3)_2$ ), 20.8 (s,  $\text{CH}_3$ -ring) ppm.

IR (KBr,  $\text{cm}^{-1}$ ):  $\nu = 801$  (s, P-F).

## References

---

- <sup>1</sup> D. E. C. Corbridge, *Phosphorus 2000. Chemistry, Biochemistry and Technology*, Elsevier, Amsterdam, NL, 2000.
- <sup>2</sup> For a review describing the first examples of PF<sub>3</sub> metal complexes, see: T. Kruck, *Angew. Chem. Int. Engl. Ed.* **1967**, *6*, 53-67.
- <sup>3</sup> a) M. Nivsarkar, A. K. Gupta, M. P. Kaushik, *Tetrahedron Lett.* **2004**, *45*, 6863; b) B. Nawrot, M. Sobczak, S. Antoszczyk, *Org. Lett.* **2002**, *4*, 1799.
- <sup>4</sup> a) O. Stelzer, *Chem. Ber.* **1974**, *107*, 2329-2340; b) M. Pabel, A.C. Willis, S.B. Wild, *Inorg. Chem.* **1996**, *35*, 1244-1249; c) L. Riesel, J. Haenel, *J. Fluorine Chem.* **1988**, *38*, 335-340.
- <sup>5</sup> N. Fey, M. Garland, J. P. Hopewell, C. L. McMullin, S. Mastroianni, A. Guy Orpen, P. G. Pringle, *Angew. Chem. Int. Ed.* **2012**, *51*, 118-122.
- <sup>6</sup> J. Chatt, *Nature* **1950**, *165*, 637.
- <sup>7</sup> G. Wilkinson, *J. Am. Chem. Soc.* **1951**, *73*, 5501-5502.
- <sup>8</sup> J. F. Nixon, R. Swain, *Plat. Met. Rev.* **1975**, *19*, 22-29.
- <sup>9</sup> D. W. Allen, B. J. Walker, *Organophosphorus Chemistry* **1997**, 23.
- <sup>10</sup> R. J. Clark, H. Belefant, S. M. Williamson, *Inorg. Synth.* **1990**, *28*, 310.
- <sup>11</sup> O. Stelzer, R. Schmutzler, *Inorg. Synth.* **1978**, *18*, 173-179.
- <sup>12</sup> P. Svec, P. Novak, M. Nadvornik, Z. Padelkova, I. Cisarova, L. Kolarova, A. Ruzicka, J. Holecek, *J. Fluorine Chem.* **2007**, *128*, 1390-1395.
- <sup>13</sup> a) R. Wärme, L. Juhlin, L. Trogen, *Phosphorus, Sulfur, and Silicon*, **2008**, *183*, 483-486; b) R. Wärme, L. Juhlin, *Phosphorus, Sulfur, and Silicon*, **2010**, *185*, 2402-2408.
- <sup>14</sup> For reviews on the coordination chemistry of phosphinous acids and related compounds, see: (a) D. M. Roundhill, R. P. Sperline, W. B. Beaulieu, *Coord. Chem. Rev.* **1978**, *26*, 263-279. (b) B. Walther, *Coord. Chem. Rev.* **1984**, *60*, 67-105. (c) T. Appleby, J. D. Woollins, *Coord. Chem. Rev.* **2002**, *235*, 121-140.
- <sup>15</sup> a) D. N. Akbayeva, M. Di Vaira; S. S. Costantini, M. Peruzzini, P. Stoppioni, *Dalton Trans.*, **2006**, 389-395. b) D. Yakhvarov, M. Caporali, L. Gonsalvi, S. Latypov, V. Mirabello, I. Rizvanov, W. Schipper, O. Sinyashin, P. Stoppioni, M. Peruzzini *Angew. Chem. Int. Ed.* **2011**, *50*, 5370-5373. *Ibid.* **2012**, *51*, 2533. c) G. Manca, M. Caporali, A. Ienco, M. Peruzzini, C. Mealli, *J. Organomet. Chem.* **2014**, *760*, 177-185.
- <sup>16</sup> W. J. Middleton, *J. Org. Chem.* **1975**, *40*, 574.
- <sup>17</sup> a) G. S. Lal, G.P. Pez, R. J. Pesaresi, F. M. Prozonc, H. Cheng, *J. Org. Chem.* **1999**, *71*, 7048; b) G. S. Lal *Chem. Commun.* **1999**, 215.
- <sup>18</sup> L. N. Markovskii, V. E. Pashinnik, E. P. Saenko, *Zh. Org. Khim.* **1977**, *13*, 1116.

- 
- <sup>19</sup> a) F. Beaulieu, L.-P. Beauregard, G. Courchesne, M. Couturier, F. LaFlamme, A. L'Hereux, *Org. Lett.* **2009**, *11*, 5050-5053; b) A. L'Hereux, F. Beaulieu, C. Bennet, D. R. Bill, S. Clayton, F. LaFlamme, M. Mirmehrabi, S. Tadayon, D. Tovell, M. Couturier, *J. Org. Chem.* **2010**, *75*, 3401-3411; c) M. Couturier, A. L'Hereux, US 2012/0108801 A1.
- <sup>20</sup> O. Farooq, *J. Chem. Soc. Perkin Trans. 1*, **1998**, 839-840.
- <sup>21</sup> G. Brauer, *Handbook of Preparative Inorganic Chemistry*, 2<sup>nd</sup> Ed.; Academic Press: New York, **1963**; Vol. 1, pp 189-190.
- <sup>22</sup> H. S. Booth, A. R. Bozarth, *J. Am. Chem. Soc.* **1939**, *61*, 2927-2934.
- <sup>23</sup> C. J. Hoffman, *Inorg. Synth.* **1953**, *4*, 149-150.
- <sup>24</sup> A. A. Williams, *Inorg. Synth.* **1957**, *5*, 95-97.
- <sup>25</sup> A. M. A. Boshala, S. J. Simpson, J. Autschbach, S. Zheng, *Inorg. Chem.* **2008**, *47*, 9279-9292.
- <sup>26</sup> J. F. Nixon, R. Schmutzler, *Spectrochim. Acta*, **1964**, *20*, 1835-1842.
- <sup>27</sup> a) M. P. Mitoraj, A. Michalak, *Inorg. Chem.* **2010**, *49*, 578-582; b) T. Leyssens, D. Peeters, A. Guy Orpen, J. N. Harvey, *Organometallics* **2007**, *26*, 2637-2645.
- <sup>28</sup> L. W. Yarbrough, M. B. Hall, *Inorg. Chem.* **1978**, *17*, 2269-2275.
- <sup>29</sup> M. G. Bodner, M. P. May, L. E. McKinney, *Inorg. Chem.* **1980**, *19*, 1951-1958.
- <sup>30</sup> E. P. Kundig, F.-R. Monnier, *Adv. Synth. Catal.* **2004**, *346*, 901-904.
- <sup>31</sup> B. Steinmetz, W.A. Schenk, *Organometallics* **1999**, *18*, 943-946.
- <sup>32</sup> J. D. Warren, R.J. Clark, *Inorg. Chem.* **1970**, *9*, 373-379.
- <sup>33</sup> L. Heuer, M. Shell, R. Schmutzler, *Polyhedron*, **1987**, *6*, 6, 1295-1307.
- <sup>34</sup> a) M. A. Bennet, T. N. Huang, T. W. Matheson, A. K. Smith, *Inorg. Synth.* **1981**, *21*, 74-75; b) V. Cadierno, P. Crochet, S. E. García-Garrido, J. Gimeno, *Dalton Trans.* **2004**, 3635-3641.
- <sup>35</sup> a) S. Parkin, B. Moezzi, H. Hope, *J. Appl. Crystallogr.* **1995**, *28*, 53-56; b) G. M. Sheldrick, *SHELX-97*, University of Göttingen, Germany, 1997; c) L. J. Farrugia, *J. Appl. Crystallogr.* **1999**, *32*, 837-838.



## **Activation of P<sub>4</sub> mediated by ruthenium(II) complexes**

### **3.1 Overview**

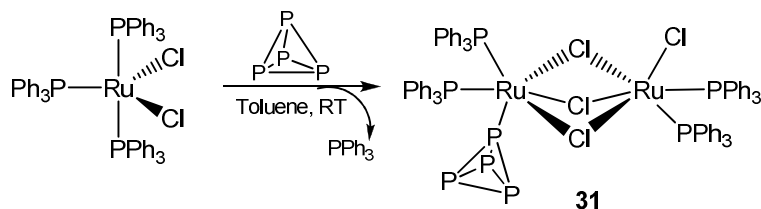
This chapter describes the coordination chemistry of white phosphorus towards a 16 electron ruthenium(II) organometallic complex [Cp\**Ru*PCy<sub>3</sub>X], where Cp\* = C<sub>5</sub>Me<sub>5</sub>, X = Cl, Br, I. The different electronegativity and ionic radius in the series of halogens changes the reactivity with white phosphorus. Migration of the halogen from ruthenium to the P<sub>4</sub> moiety was observed, in the case of chloride and bromide, obtaining bimetallic complexes bearing the unexpected and unprecedented P<sub>4</sub>X<sub>2</sub> (X = Cl, Br) moiety as bridging ligand. In the case of iodide, a completely different structure is proposed, containing the not yet previously reported P<sub>4</sub>I ligand as a bridging moiety between two Ru(II) centers.

## *Chapter 3*



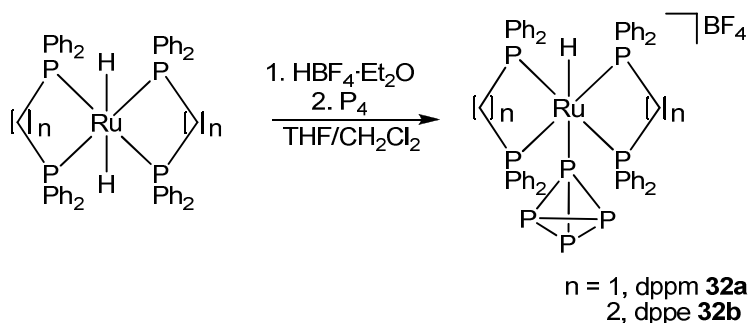
### 3.2 Activation of P<sub>4</sub> by ruthenium(II) complexes: State-of-the-art

In view of the continuous search for new sustainable routes to activate white phosphorus avoiding the traditional pathway in which chlorine is involved, the study on the coordination chemistry of the P<sub>4</sub> molecule towards a great variety of metal fragments has been achieved. Despite the first transition metal complex bearing white phosphorus as ligand was prepared long ago, in 2000 the first ruthenium complex  $[\{(PPh_3)_2ClRu\}(\mu-Cl_3)\{Ru(PPh_3)_2(\eta^1-P_4)\}]$  (**31**) was isolated.<sup>1</sup> It was prepared by reacting  $[Ru(PPh_3)_3Cl_2]$  with white phosphorus in toluene at room temperature. In complex **31** an intact P<sub>4</sub> molecule was coordinated to the metal center causing the displacement of one triphenylphosphine, as shown in **Scheme 3.1**. The resulting unstable and neutral binuclear complex exhibits the octahedral geometry for each of the two metal atoms while the  $\eta^1-P_4$  ligand is coordinated to one ruthenium atom.



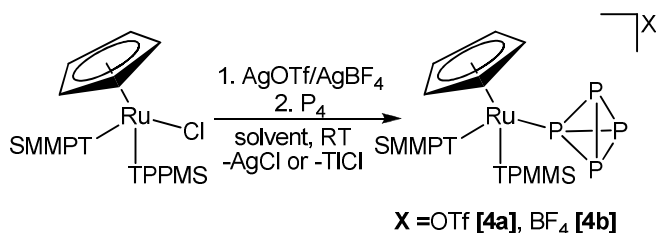
**Scheme 3.1.** Synthesis of  $[\{(PPh_3)_2ClRu\}(\mu-Cl_3)\{Ru(PPh_3)_2(\eta^1-P_4)\}]$

Since then, a short list of ruthenium complexes bearing white phosphorus were studied. Peruzzini and coworkers<sup>2</sup> reported the preparation of the mononuclear ruthenium complexes  $[HRuL_2(\eta^1-P_4)]$  ( $L = dpmm$  **32a**,  $dppe$  **32b**) obtained by treatment of a mixture 1:1 of  $[RuH_2L_2]$  ( $L = dpmm$ ,  $dppe$ ) and  $HBF_4 \cdot Et_2O$  in  $CH_2Cl_2$  with P<sub>4</sub> in THF, see **Scheme 3.2**.



**Scheme 3.2.** Synthetic route for the preparation of **32**.

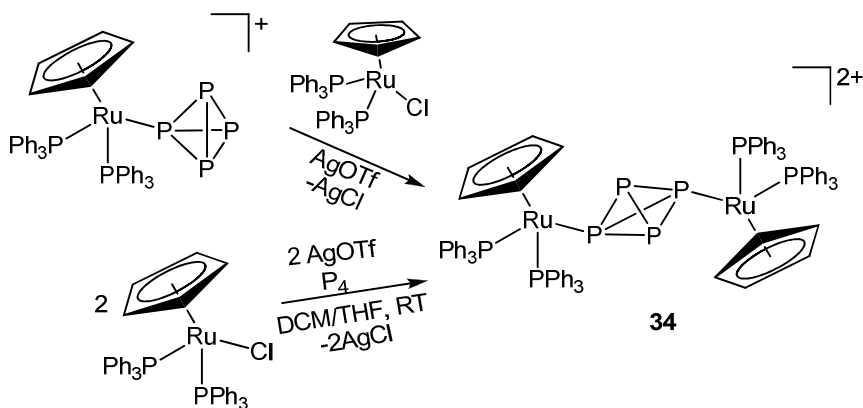
As reported in **Scheme 1.13**, in the first chapter, reaction of white phosphorus with mononuclear ruthenium complexes containing cyclopentadienyl<sup>2</sup> or pentamethylcyclopentadienyl<sup>3</sup> ligands and phosphanes led to the coordination of the intact *tetrahedro*- $\eta^1$ -P<sub>4</sub> molecule. Another example of this class of compounds is represented by the water-soluble complexes [CpRu(TPPMS)<sub>2</sub>( $\eta^1$ -P<sub>4</sub>)]X (X = BF<sub>4</sub> **33a**, PF<sub>6</sub> **33b**) by treatment of [CpRu(TPPMS)<sub>2</sub>Cl] [TPPMS = PPh<sub>2</sub>(*m*-SO<sub>3</sub>C<sub>6</sub>H<sub>4</sub><sup>+</sup>Na<sup>-</sup>)] with P<sub>4</sub>, in the presence of a chloride scavenger such as silver triflate, see **Scheme 3.3**.<sup>4</sup>



**Scheme 3.3.** Synthetic pathway for the formation of [CpRu(TPPMS)<sub>2</sub>( $\eta^1$ -P<sub>4</sub>)]X.

Bimetallic ruthenium complexes containing P<sub>4</sub> as ligand were also prepared. Thus, treatment of [CpRu(PPh<sub>3</sub>)<sub>2</sub>( $\eta^1$ -P<sub>4</sub>)]<sup>+</sup> (**11a**<sup>+</sup>) with 1 equivalent of [CpRu(PPh<sub>3</sub>)<sub>2</sub>]<sup>+</sup> fragment or, as alternative pathway, the

direct reaction of  $[\text{CpRu}(\text{PPh}_3)_2\text{Cl}]$  with half equivalent of  $\text{P}_4$  in the presence of  $\text{AgOTf}$  afforded the homobimetallic complex  $[\{\text{CpRu}(\text{PPh}_3)_2\}_2(\mu,\eta^{1:1}\text{-P}_4)](\text{OTf})_2$  (**34**)<sup>5</sup> as shown in **Scheme 3.4**.



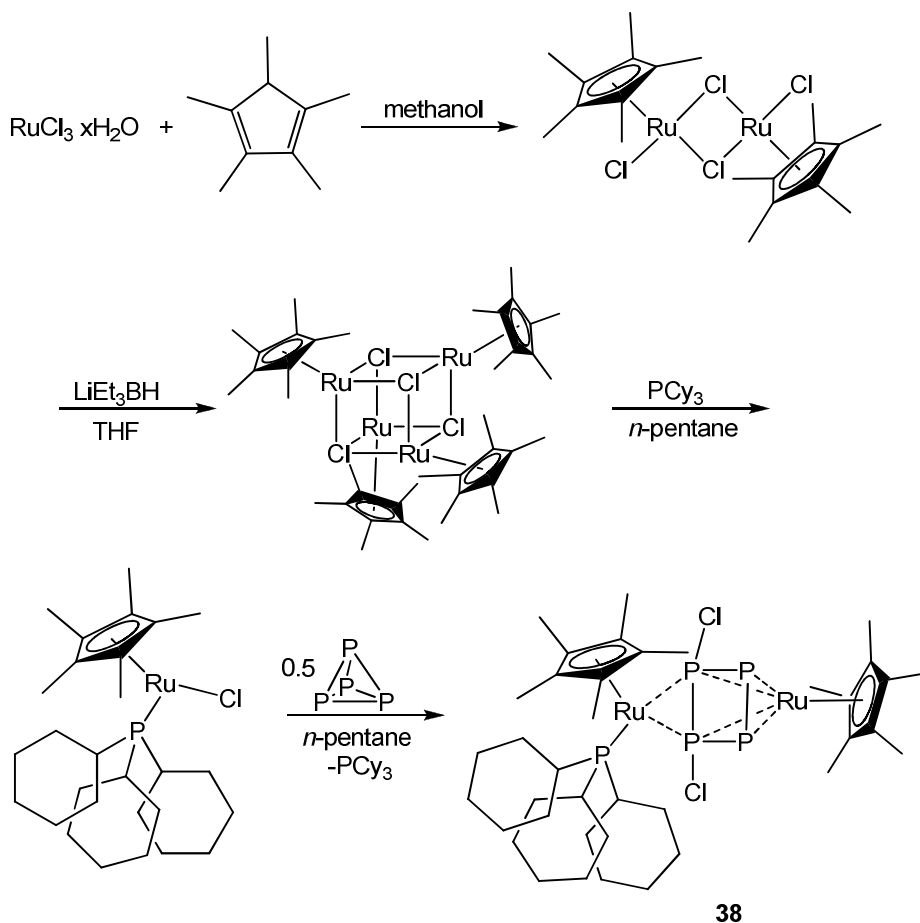
**Scheme 3.4.** The two synthetic routes for the synthesis of  $[\{\text{CpRu}(\text{PPh}_3)_2\}_2(\mu,\eta^{1:1}\text{-P}_4)](\text{OTf})_2$ .

An intriguing point is the reactivity toward water of cyclopentadienyl complexes once  $\text{P}_4$  is coordinated to the metal fragment, in comparison to the high stability of free white phosphorus in water. Hydrolysis of mononuclear ruthenium complexes leads to the formation of complexes bearing, not only phosphine ligand  $[\text{CpRuL}_2(\text{PH}_3)]^+$  ( $\text{L} = \text{PPh}_3$  **35a**<sup>+</sup>,  $\frac{1}{2}$  dppe **35b**<sup>+</sup>, TPPMS **35c**<sup>+</sup>), but also hydroxy phosphine ligands,  $[\text{CpRuL}_2\{\text{P}(\text{OH})_2\}]^+$  ( $\text{L} = \text{PPh}_3$  **36a**<sup>+</sup>,  $\frac{1}{2}$  dppe **36b**<sup>+</sup>, TPPMS **36c**<sup>+</sup>) and  $[\text{CpRuL}_2\{\text{P}(\text{OH})_3\}]^+$  ( $\text{L} = \text{PPh}_3$  **37a**<sup>+</sup>,  $\frac{1}{2}$  dppe **37b**<sup>+</sup>, TPPMS **37c**<sup>+</sup>) and free phosphorus oxyacids as by-products.<sup>2,6,7</sup> Also studies of the reactivity of the bimetallic complex **34** with an excess of water in different ratio were reported.<sup>8,9,10</sup>

### 3.3 Activation and functionalization of white phosphorus by $[\text{Cp}^*\text{Ru}(\text{PCy}_3)\text{X}]$ ( $\text{X} = \text{Cl}, \text{Br}, \text{I}$ )

#### 3.3.1 Synthesis and characterization of $[\{\text{Cp}^*\text{Ru}(\text{PCy}_3)\}(\mu_2, \eta^{2:4}\text{P}_4\text{Cl}_2)\{\text{RuCp}^*\}]$

Being white phosphorus a mild nucleophile, not such a strong  $\sigma$ -donor ligand as alkyl or aryl-phosphine,<sup>11</sup> a highly reactive 16-electron complex as  $[\text{Cp}^*\text{Ru}(\text{PCy}_3)\text{Cl}]$ <sup>12</sup> was chosen to explore its activation. The bulky ligand  $\text{PCy}_3$ , was intentionally chosen since it allows a certain stability to the complex, which is coordinatively unsaturated. The deep blue coloured 16-electron complex  $[\text{Cp}^*\text{Ru}(\text{PCy}_3)\text{Cl}]$ , may indeed easily prepared *in situ* by reaction of  $\text{PCy}_3$  with the cubane-like tetramer  $[\text{Cp}^*\text{RuCl}]_4$ . This latter was generated in THF solution by reduction of the dimer  $[\text{Cp}^*\text{RuCl}(\mu\text{-Cl})]_2$  with lithium triethyl borohydride. *In situ* reaction of the ruthenium  $[\text{Cp}^*\text{Ru}(\text{PCy}_3)\text{Cl}]$  complex with white phosphorus gave afforded a new unexpected product. (see **Scheme 3.5.**) In principle, the formation of a mononuclear ruthenium complex bearing  $\text{P}_4$  coordinated eta-1 to the metal, *i.e.*  $[\text{Cp}^*\text{Ru}(\text{PCy}_3)\text{Cl}(\eta^1\text{-P}_4)]$  would be expected. In spite the electronic deficiency at ruthenium should also favour the formation of an  $\eta^2$ -coordinated isomer, *i.e.*  $[\text{Cp}^*\text{Ru}(\text{PCy}_3)\text{Cl}(\eta^2\text{-P}_4)]$  resulting from the formal oxidative addition of one P-P bond to the unsaturated Ru(II) metal. Actually, <sup>31</sup>P NMR inspection of the reaction mixture showed no traces of such compounds, whose NMR pattern is easily predictable on the basis of literature data of already existing for  $\eta^1\text{-P}_4$  or  $\eta^2\text{-P}_4$  ruthenium complexes.<sup>2,3,4</sup>



**Scheme 3.5.** Full synthesis of  $[\{\text{Cp}^*\text{Ru}(\text{PCy}_3)\}(\mu_2, \eta^{2,4}\text{P}_4\text{Cl}_2)\{\text{RuCp}^*\}]$

This reaction was briefly reported by Akbayeva<sup>13</sup> and incorrectly characterized, based only on NMR studies, suggesting a mononuclear complex containing a  $\eta^2$ -coordinated  $\text{P}_4$ ,  $[\text{Cp}^*\text{RuPCy}_3(\eta^2\text{-P}_4)]$ . A definitive evidence of the unusual structure of complex **38** was provided by single crystal X-ray diffraction, whose crystals were grown by Ph.D. student Mark Bispinghoff at ETHZ (Zurich, Switzerland) in the frame of a bilateral collaboration sponsored by the ITN–Marie Curie network SusPhos. Red crystals of **38** were obtained from a saturated solution in

DME at low temperature (-30 °C). The crystallographic analysis showed the presence of an unexpected bimetallic complex  $[\{\text{Cp}^*\text{Ru}(\text{PCy}_3)\}(\mu_2, \eta^{2:4}\text{P}_4\text{Cl}_2)\{\text{RuCp}^*\}]$  (**38**) featuring an unprecedented bridging  $\text{P}_4\text{Cl}_2$  ligand. Halogen migration from the metal to the activated  $\text{P}_4$  moiety had taken place forming two symmetrical P-Cl bonds. This ligand may be considered as a  $\text{P}_4\text{Cl}_2^{2-}$  butadienyl-like moiety, whose bond lengths are in equilibria due to the delocalization of the  $\pi$ -electrons on the structure. P-P bond lengths are in the range 2.16 - 2.17 Å, except for (Cl)P1-P4(Cl) whose value is larger (2.52 Å), as shown in **Figure 3.1.**, causing a sort of trapezoidal distortion of the ligand structure owing to the charge repulsive effect of the lone electron pairs. The complex is highly symmetric, with a mirror plane passing through the two metal centers, the phosphorus corresponding to the unique tricyclohexylphosphine and the  $\text{P}_4\text{Cl}_2$  plane.

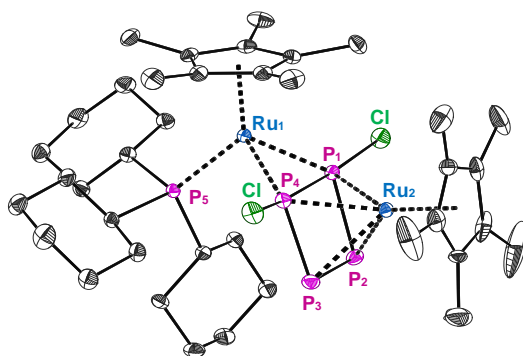


**Figure 3.1.** X-ray crystal structure of  $[\{\text{Cp}^*\text{Ru}(\text{PCy}_3)\}(\mu_2, \eta^{2:4}\text{P}_4\text{Cl}_2)\{\text{RuCp}^*\}]$

Selected bond length (Å) and angles (°): Ru(1)-P(1), 2.2930(5); Ru(1)-P(4), 2.2876(5); Ru(1)-P(5), 2.3919(5); Ru(1)-centroid(Cp), 1.926; Ru(2)-P(1), 2.3508(5); Ru(2)-P(2), 2.4261(5); Ru(2)-P(3), 2.4498(5); Ru(2)-P(4), 2.3289(5); Ru(2)-centroid(Cp), 1.872; P(1)-Cl(1), 2.1186(7); P(4)-Cl(2), 2.1113(7); P(1)-P(2), 2.1635(7); P(1)-P(4), 2.5165(7); P(2)-P(3), 2.1563(8); P(3)-P(4),

### Chapter 3

2.1707(8); P(1)-Ru(1)-P(5), 98.404(18); P(4)-Ru(1)-P(5), 99.641(17); Ru(1)-P(1)-Cl(1), 122.31(3); Ru(1)-P(4)-Cl(2), 123.00(3).

$^{31}\text{P}\{^1\text{H}\}$  NMR of **38** in THF- $d_8$  is shown in **Figure 3.2**. The complex exhibits a dynamic behaviour at room temperature, featuring two group of signals of identical intensity. The broad doublet centered at 251 ppm ( $w_{1/2} = 325$  Hz,  $^1J = 400$  Hz), highly deshielded in comparison to the known  $^{31}\text{P}$ -NMR resonances of  $\text{P}_4$  moiety bound to ruthenium<sup>14</sup> is assigned to the chlorine-substituted phosphorus atoms (P1 and P4) while the very broad signal around -70 ppm ( $w_{1/2} = 3000$  Hz) is attributed to the remaining P2 and P3 atoms. Finally the narrower triplet centered at 43 ppm ( $^2J = 37$  Hz) is ascribed to the residual  $\text{PCy}_3$  coordinated to the ruthenium center bounded to the chlorinated edge of the 1,4-dichlorobutadienyde unit.

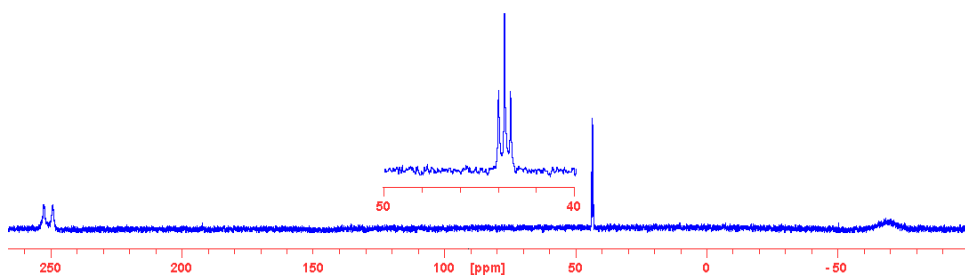


**Figure 3.2.**  $^{31}\text{P}\{^1\text{H}\}$  NMR spectrum of **38** measured at room temperature in THF- $d_8$ ; 203 MHz.

To investigate and understand the fluxional behaviour of the molecule, variable temperature  $^{31}\text{P}\{^1\text{H}\}$  NMR studies were performed within the temperature window of THF- $d_8$ , see **Figure 3.3**.

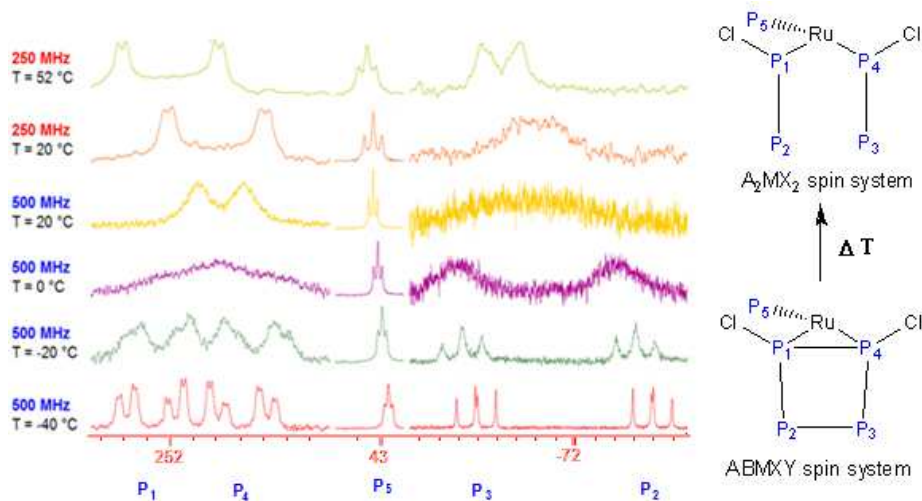


**Figure 3.3.** Variable temperature  $^{31}\text{P}\{^1\text{H}\}$  NMR spectrum of  $[\{\text{Cp}^*\text{Ru}(\text{PCy}_3)\}(\mu_2, \eta^{2:4}\text{P}_4\text{Cl}_2)\{\text{RuCp}^*\}]$  in  $\text{THF-}d_8$ .

The low-limiting spectrum is easily obtained at  $-40\text{ }^\circ\text{C}$  when five chemically inequivalent phosphorus atoms corresponding to a ABMXY ( $\text{M} = \text{PCy}_3$ ) spin system are observed. The high field resonances (P1 and P4) may be described as a slightly perturbed second order AB multiplet featuring a sixteen line pattern consisting of two doublets of doublets of doublets. In contrast, the low field multiplets (P2 and P3) appears as a pair of doublets of doublets being negligible the  $^3J$  coupling to the  $\text{PCy}_3$  ligand. The latter maintains its triplet structure along all the investigated temperature thus pointing out that no dissociation of the ancillary phosphine takes place in solution. Increasing the temperature, P1 and P4 go through coalescence at about  $0\text{ }^\circ\text{C}$ , while the collapse of the P2 and P3 low-field multiplet occurs at about  $20\text{ }^\circ\text{C}$ . At higher temperature both multiplets simplify and at  $52\text{ }^\circ\text{C}$ , the highest investigated temperature, the spectrum consists of a doublet of doublets for P1 and P4 and a broad doublet for P2 and P3. This behaviour suggests both phosphorus atoms



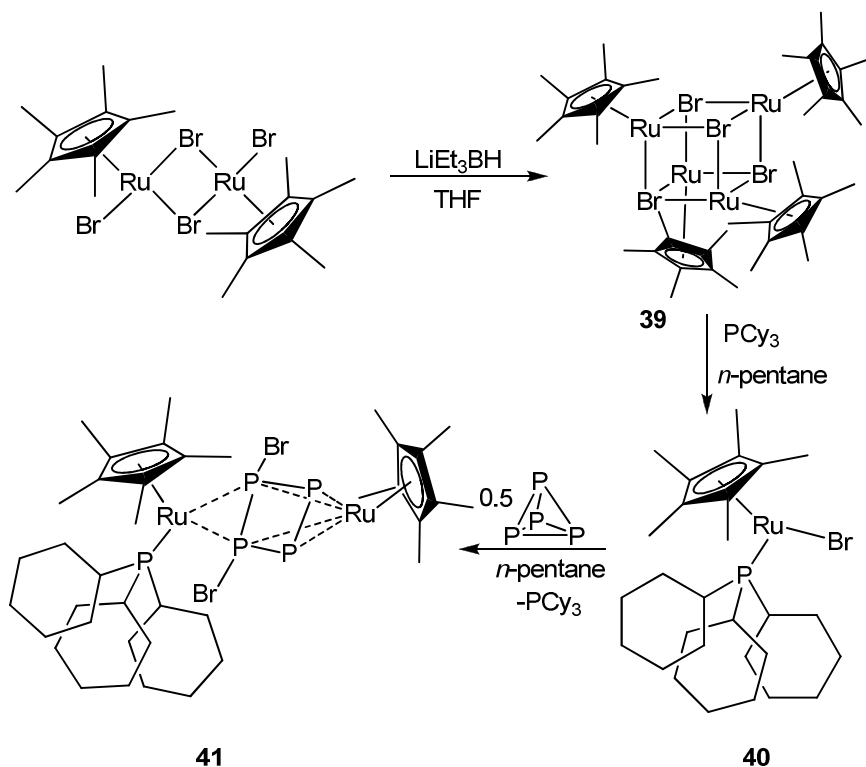
pairs become equivalents, thus featuring the NMR appearance proper of an  $A_2MX_2$  spin system. Attempts to achieve the fast-exchange spectrum at higher temperature brought to extensive decomposition.

Although the potentially highly reactive complex **38** was not yet targeted for studying its reactivity in a systematic way, we did perform only a few hydrolysis experiments with excess of water leading only to extensive decomposition and giving an intractable material as the final product.

### 3.3.2 Synthesis and characterization of $[\{Cp^*Ru(PCy_3)\}(\mu_2, \eta^{2:4}P_4Br_2)\{RuCp^*\}]$

Intrigued by the results obtained with the reaction of white phosphorus with  $[Cp^*Ru(PCy_3)Cl]$ , we decided to investigate the analogue ruthenium complexes, having as halogen ligand either bromide or iodide instead of chloride.

Reduction of the dimer  $[Cp^*RuBr(\mu-Br)]_2$  with  $LiEt_3BH$  gave the tetramer  $[Cp^*RuBr]_4$  (**39**) using the same procedure as for the preparation of  $[Cp^*RuCl]_4$ .<sup>15</sup> Addition of  $PCy_3$  ( $PCy_3:Ru = 1:1$ ) gave a deep blue suspension of  $[Cp^*RuPCy_3Br]$  (**40**) from which the corresponding bromide complex  $[\{Cp^*Ru(PCy_3)\}(\mu_2, \eta^{2:4}P_4Br_2)\{RuCp^*\}]$  (**41**) could be easily obtained after addition of half equivalent of white phosphorus and work-up as for the chloride analogue **38**. The reaction leading to **41** is shown in **Scheme 3.6**.



**Scheme 3.6.** Synthesis of the bromide derivative  
 $[\{\text{Cp}^*\text{Ru}(\text{PCy}_3)\}(\mu_2, \eta^{2:4}\text{P}_4\text{Br}_2)\{\text{RuCp}^*\}]$ .

The assignment to **41** of the same solution structure of the cognate chloride species is a consequence of the strict similarity between the  $^{31}\text{P}\{^1\text{H}\}$  NMR spectra of the two compounds, which also share an identical fluxionality with the temperature. The sharp singlet at 10 ppm is due to free  $\text{PCy}_3$  meaning that one of the two organometallic fragments lost the phosphine ligand and, therefore, it coordinates the  $\text{P}_4$  moiety in tetra-hapto fashion. Also, the bromide derivative shows dynamic behaviour at room temperature, showing a broad doublet around 261 ppm ( $w_{1/2} = 255$  Hz,  $^1J = 387$  Hz), attributed to the two bromine-substituted phosphorus atoms and a very broad singlet around -58 ppm ( $w_{1/2} = 1300$

### Chapter 3

Hz) whose resonance concurs with the other two phosphorus atoms. Besides, a triplet at 40 ppm ( $^2J = 37$  Hz) corresponds to  $\text{PCy}_3$ .

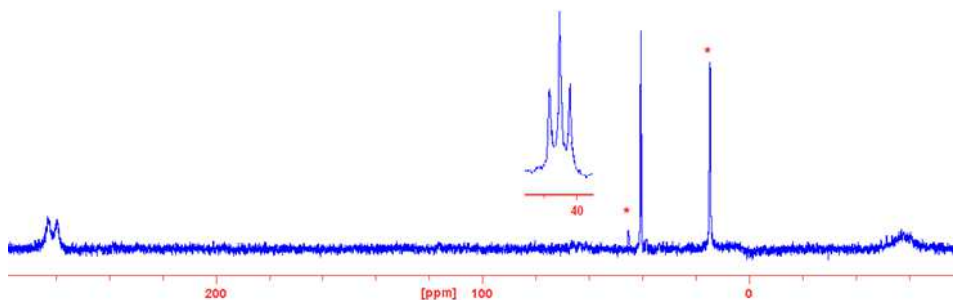


**Figure 3.5.**  $^{31}\text{P}\{^1\text{H}\}$  NMR spectrum of  $[\{\text{Cp}^*\text{Ru}(\text{PCy}_3)\}(\mu_2, \eta^{2:4}\text{P}_4\text{Br}_2)\{\text{RuCp}^*\}]$  measured at room temperature in  $\text{THF-}d_8$ , 121 MHz. Impurities are marked with \*.

The dynamic behaviour of **41** was also examined by variable temperature  $^{31}\text{P}\{^1\text{H}\}$  NMR spectroscopy in in  $\text{THF-}d_8$ , see **Figure 3.6**.

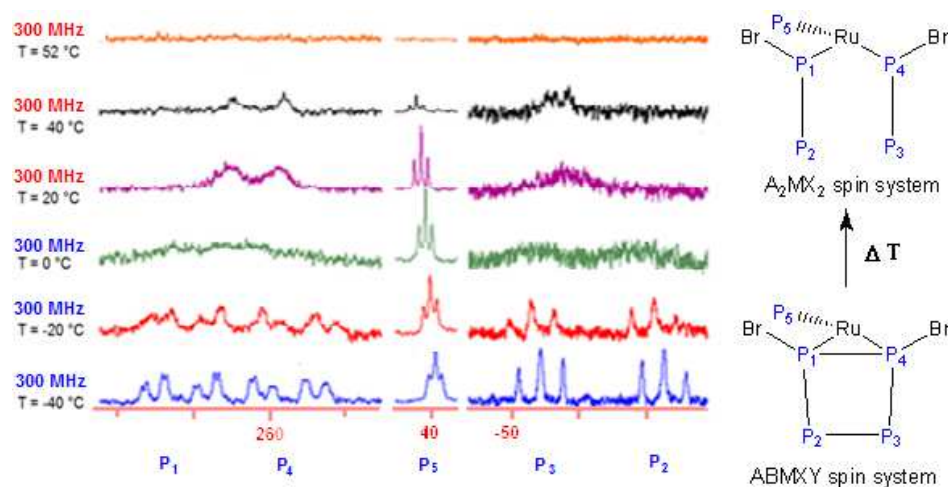


**Figure 3.6.** Variable temperature  $^{31}\text{P}\{^1\text{H}\}$  NMR spectra of  $[\{\text{Cp}^*\text{Ru}(\text{PCy}_3)\}(\mu_2, \eta^{2:4}\text{P}_4\text{Br}_2)\{\text{RuCp}^*\}]$  in  $\text{THF-}d_8$ , 121 MHz.

### Chapter 3

Complex **41** shows an identical behaviour as for the  $P_4Cl_2$  complex **38** at -40 °C compatible with a ABMXY spin system. At 0 °C P1 and P4 go through coalescence, whereas P2 and P3 coalesce into a broad bump at about 20°C. Unfortunately, but similarly to **38**, both signals disappear at higher temperature, showing only an uninformative singlet at 32 ppm, indicating the decomposition of the complex.

It should be noticed that the compound **41** is more air and moisture sensitive than **38** and its synthesis and manipulation requests strictly anhydrous and oxygen-free conditions. Thus, its synthesis was carried out in drybox. In keeping with the extremely high instability of the bromide derivative, the reaction does not tolerate Schlenck-type synthetic procedure. Under such circumstances, when less strict anaerobic and dry conditions were used, **41** is not produced, rather a mixture of two different complexes was obtained, in 3:2 (A:B) ratio, as it was shown by inspection of the solution by  $^{31}P$  NMR spectroscopy (see **Figure 3.7.**). Several efforts to separate and isolate either of the two complexes from the reaction solution were carried out without success.

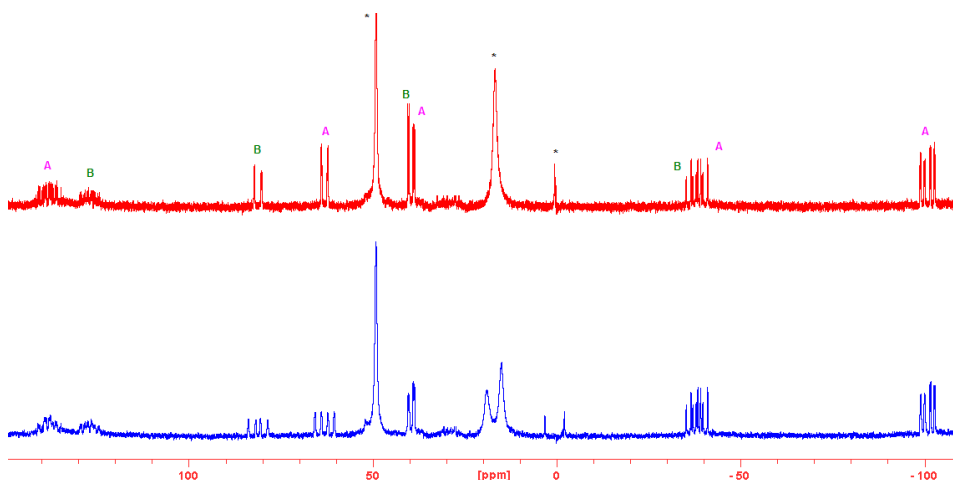


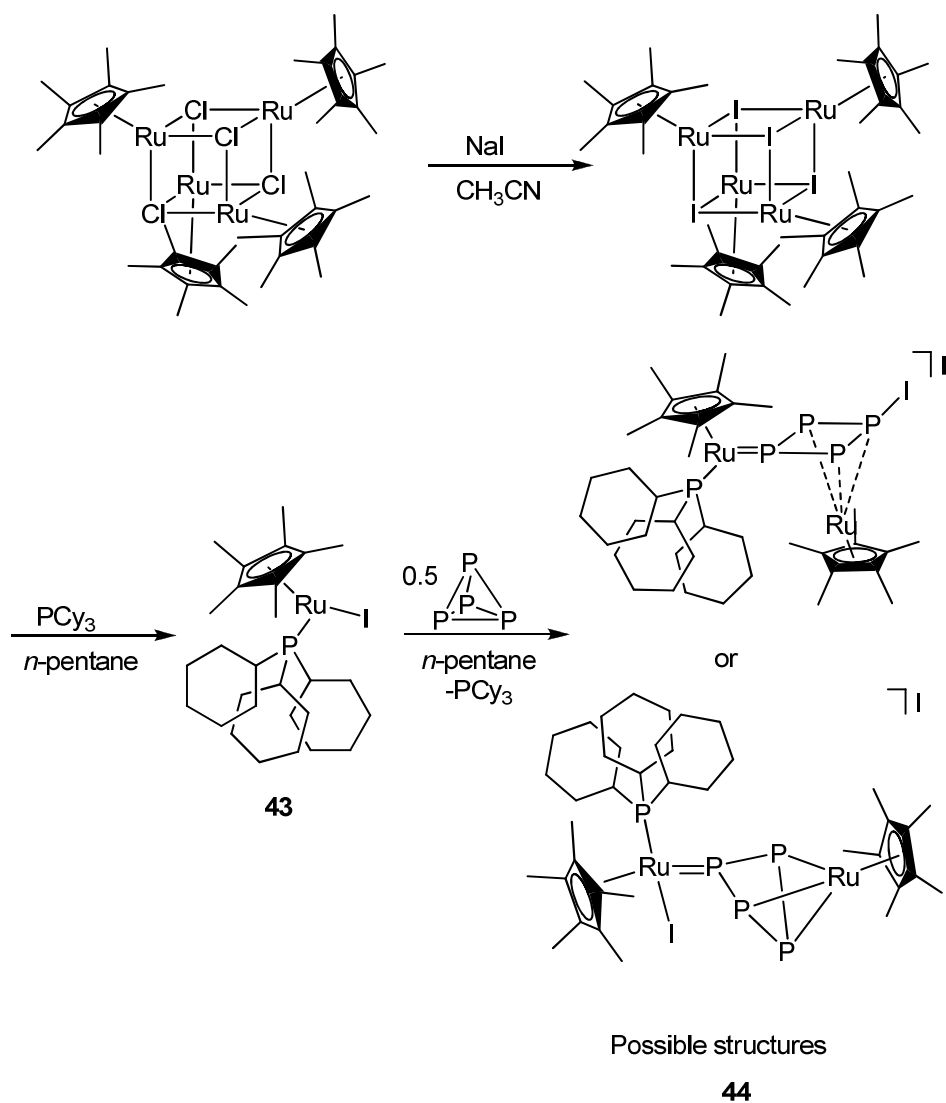
**Figure 3.7.**  $^{31}\text{P}\{^1\text{H}\}$  NMR (red) and  $^{31}\text{P}$  NMR (blue) of the mixture of Br-derivatives. **A** corresponds to **42a** and **B** corresponds to **42b** in experimental part. Impurities are signed with a \*.

Although on the basis of solution  $^{31}\text{P}\{^1\text{H}\}$  NMR spectroscopy only it is hard to propose a putative structure for the two complexes, some considerations can nonetheless be made. First, the strong similarities of the splitting patterns featuring the  $^{31}\text{P}\{^1\text{H}\}$  NMR spectra, suggests that the two compounds are likely isomeric species. Even more significant is the observation that the  $^{31}\text{P}$  NMR spectrum, *i.e.* obtained by turning off the  $^1\text{H}$  decoupler of the spectrometer during the acquisition of the spectrum, see **Figure 3.7.**, indicates the presence of a PH phosphorus atom in both complexes featuring the resonance at 63 and 81 ppm, respectively. The  $^1J_{\text{P-H}}$  coupling constants, 423 and 392 Hz, respectively, are typical of P-H bonds. This observation could indicate the occurrence of the  $\text{P}_4\text{Br}_2$  dianionic ligand functionalization due to the presence of adventitious water on the reaction system hydrolysing the complex **41**. Further studies

are in progress to characterize the solution structure of such pair of isomers.

### 3.3.3 Activation of P<sub>4</sub> with [Cp\***Ru**(PCy<sub>3</sub>)I]

The not yet reported 16-electron complex [Cp\***Ru**(PCy<sub>3</sub>)I] (**43**) was prepared by reacting under inert atmosphere the freshly generated and unstable tetramer [Cp\***Ru**]<sub>4</sub>,<sup>16</sup> with four equivalents of tricyclohexyl phosphine. The solution immediately changed from a dark brown to deep blue colour while the <sup>31</sup>P NMR spectrum of the solution showed a singlet at 47 ppm very close to the signal exhibited by the related complexes [Cp\***Ru**PCy<sub>3</sub>X] (X = Cl, Br). Further addition of half equivalent of solid white phosphorus to the stirred solution of **43** led to the separation of **44** as a brownish precipitate. (see **Scheme 3.7.**)



**Scheme 3.7.** Activation of  $P_4$  with the iodide derivative.

In the absence of good quality crystals of **44** which have not yet been grown in spite of numerous attempts, we could anticipate, since the synthetic procedure used to prepare **44** was the same as for the **38** ( $X = Cl$ ) and **41** ( $X = Br$ ), that the presence of iodide does not affect the reactivity with white phosphorus, thus confidently assigning to the iodo-

### Chapter 3

derivative the formula  $[\{\text{Cp}^*\text{Ru}(\text{PCy}_3)\}(\mu_2, \eta^{2:4}\text{P}_4\text{I}_2)\{\text{RuCp}^*\}]$ . However, while the elemental analysis on the isolated product is consistent with this molecular formula, running the  $^{31}\text{P}$  NMR spectrum of the isolated dark brown product, disclosed a pattern completely different from that exhibited by both **38** and **41** (see **Figure 3.8.**) suggesting that a dramatic change in the reaction pathway have taken place.

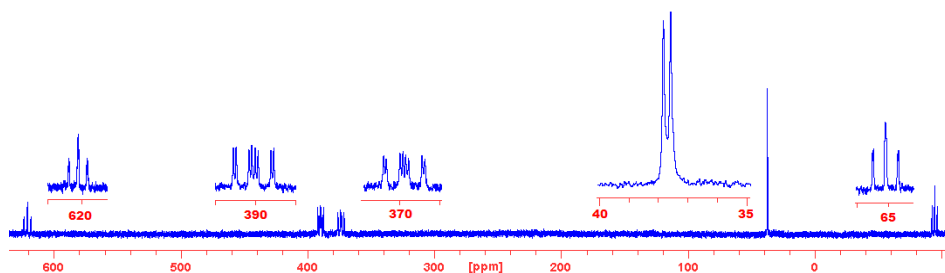


**Figure 3.8.**  $^{31}\text{P}\{^1\text{H}\}$  NMR spectrum of **44** in  $\text{THF-}d_8$  at room temperature.

The  $^{31}\text{P}\{^1\text{H}\}$  NMR spectrum does not show any second order feature and consists of five signals, each of them accounting for one P atom. The doublet at 37.6 ppm is diagnostic and stands for one tricyclohexyl phosphine ligand, meaning that the other  $\text{PCy}_3$  has been lost during the reaction with  $\text{P}_4$ . Therefore, in the final bimetallic complex a  $[\text{Cp}^*\text{Ru}]$  unit is free from  $\text{PCy}_3$  and should be multiply coordinated ( $\eta\text{-}3$  or  $\eta\text{-}4$ ) to a tetraphosphorus unit derived from white phosphorus. Moreover, being the signal at  $\delta = 37.6$  ppm a doublet,  $\eta\text{-}1$  coordination of the  $\text{P}_4$  fragment to ruthenium is reasonably assumed. Product **44** lacks of any symmetry element concerning the  $\text{P}_4$  moiety, so that all the four P atoms are magnetically in-equivalent and a putative structure may be drawn only from the analysis of the coupling constants and chemical shifts of the  $^{31}\text{P}$



### Chapter 3

NMR network. Remarkable is the broad triplet of triplets at very low field,  $\delta = 621$  ppm ( $w_{1/2} = 64$  Hz,  $^1J = 330$  Hz,  $^2J = 31$  Hz), which indicates the presence of a very deshielded P atom likely compatible with a metal-phosphinidene unit. In line with this assumption, a perusal of the literature points out that the chemical shifts for phosphinidenes of group 8 metal complexes vary between 300 and 1000 ppm.<sup>17</sup> For instance, the terminal phosphinidene ruthenium complexes  $[(\eta^6\text{-}p\text{-cymene})\text{Ru}(\text{PR}_3)(\text{PMes}^*)]$  (R = Cy **45**, Ph **46**) show chemical shifts around 840 ppm for the Ru=PMes\* ligand.<sup>18</sup> Further inspection of the  $^{31}\text{P}$  NMR spectrum shows the close proximity of two doublets of doublets at 390 and 370 ppm, which points to a similar chemical environment for these two phosphorus atoms. Finally, a broad triplet of doublets ( $w_{1/2} = 33$  Hz,  $^1J = 240$  Hz,  $^2J = 20$  Hz) around -65 ppm may be tentatively assigned to a P atom bearing a iodide, by analogy to the complex  $[\text{CpRu}(\text{PPh}_3)_2(\text{PI}_2\text{H})]^+$  prepared by us,<sup>19</sup> where the  $\text{PI}_2\text{H}$  ligand resonates at -70 ppm. Alternatively, the iodide ligand could be coordinated to the  $\text{Cp}^*\text{Ru}$  moiety bounded to the highly deshielded phosphinidene-like atom. (see bottom structure in **Scheme 3.7**.)

$^{31}\text{P}\{1\text{H}\}$  NMR studies at low temperature were also performed, as shown in **Figure 3.9**. While the signal at 621 ppm remains unaltered likely due to the rigidity of the Ru=P double bond, the other three signals undergo a dynamic process and broaden as soon as the temperature goes down although the low exchange regime is not attained within the temperature window of THF. In contrast, extensive decomposition of **44** took place on increasing the temperature already to 40 °C.

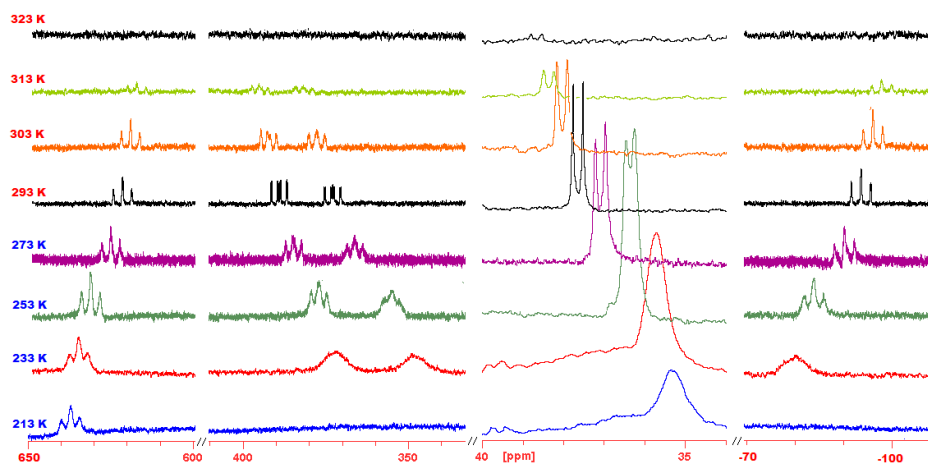


**Figure 3.9.**  $^{31}\text{P}\{^1\text{H}\}$ NMR spectrum of **44** in  $\text{THF-}d_8$  at variable temperature.

High resolution ESI-MS analysis of **44** in the negative ion mode showed the presence of a iodide,  $m/z = 126.9$ , whereas the positive ion mode confirmed the presence of a bimetallic complex containing a water molecule ( $m/z \{[(\text{Cp}^*\text{RuPCy}_3)(\text{P}_4\text{I})(\text{RuCp}^*)]^+ + [\text{H}_2\text{O}]\} = 1023.1$ ), probably due to adventitious water. This unexpected experimental evidence strongly supports the presence of a monocationic complex with an iodide as counteranion. Although we realize that  $^{31}\text{P}$  NMR spectroscopy alone is not sufficient to elucidate the structure of the diiodide derivative **44** in solution, two plausible structures for **44** may be drawn and are shown in **Scheme 3.7.**, based on the NMR studies.

### 3.4. Conclusions

The activation of white phosphorus mediated by the coordinatively unsaturated  $16 e^-$  ruthenium complexes  $[\text{Cp}^*\text{Ru}(\text{PCy}_3)\text{X}]$  ( $\text{X} = \text{Cl}, \text{Br}, \text{I}$ )

## Chapter 3

led to completely unexpected results. New neutral bimetallic Ru complexes containing the unprecedented dianionic  $[P_4X_2]^{2-}$  ligand were isolated in the case of  $X = \text{chloride}$  and bromide. They show fluxional behaviour at room temperature probably due to the opening-closing of the bridges P1-P4 and P2-P3 of the tetraphosphorus moiety. On the other hand, the bulkiness of the iodide atom and its weaker bonding capacity to phosphorus, caused the easy elimination of one iodide atom from the bimetallic  $Ru_2P_4$  moiety and its stabilization as the mononegative counteranion of the monoiodinated  $[(Cp^*RuPCy_3)(P_4I)(RuCp^*)]^+$  cation. Two possible structures have been proposed for the cation of **44** on the basis of elemental analysis,  $^{31}P$  NMR and ESI-MS studies.

## 3.5 Experimental Section

### 3.5.1 Chemicals

All reactions and manipulations were carried out under nitrogen using the drybox or standard Schlenk glassware and techniques. Dichloromethane was purified by distillation over  $CaH_2$ . THF was purified by distillation over sodium wire and benzophenone. MeOH was purified by distillation over Mg and  $I_2$ . Acetonitrile, diethyl ether and pentane were purified by passing them over two columns filled with molecular sieves (LabMaster MBRAUN MD SPS). Ethanol was used without purification. Deuterated solvents (Aldrich) were pre-treated with three freeze-thaw pump cycles before use, and kept over molecular sieves under an inert atmosphere.

The following complexes  $[Cp^*RuCl]_4$ ,<sup>16,20</sup>  $[Cp^*RuBr_2]_2$ <sup>21</sup> and  $[Cp^*RuI]_4$ <sup>16</sup> were prepared according to literature.

### 3.5.2 Characterization methods

#### NMR spectroscopy

Solution multinuclear NMR spectra were recorded on a Bruker Avance 250, 300, 400 and 500 MHz spectrometer.  $^1\text{H}$  chemical and  $^{13}\text{C}$  shifts are referenced to tetramethylsilane (TMS),  $^{31}\text{P}$  chemical shifts are referenced to 85%  $\text{H}_3\text{PO}_4$ .

#### ESI-Mass spectrometry

ESI-MS spectrum were recorded by direct introduction of the samples at 5  $\mu\text{l}/\text{min}$  flow rate in an LTQ-Orbitrap high-resolution mass spectrometer (Thermo, San Jose, CA, USA), equipped with a conventional ESI source. The working conditions comprised the following: spray voltage 4 kV, capillary voltage 3 V, capillary temperature 220  $^\circ\text{C}$ , tube lens 120 V. The sheath and auxiliary gases were set, respectively, at 10 (arbitrary units) and 3 (arbitrary units). For acquisition, Xcalibur 2.0. software (Thermo) and IT analyser were used.

#### Single crystal X-ray diffraction

Diffraction data were collected with a Bruker Smart ApexII diffractometer, using Mo- $K\alpha$  radiation ( $\lambda = 0.71073\text{\AA}$ ) and corrected for Lorentz and polarization effects. All the structures were solved by direct methods using SHELXT<sup>22</sup> and refined by full-matrix least-squared methods against  $F^2$  using the OLEX2<sup>23</sup> software package. All non-hydrogen atoms were refined anisotropically, whereas hydrogen atoms were added at calculated positions and refined applying a riding model with isotropic  $U$  values depending on the  $U_{eq}$  of the adjacent carbon atom.

### Elemental analysis

Elemental analysis were performed by using a Thermo FlashEA 1112 series CHNS-O elemental analyser with an accepted tolerance of  $\pm 0.4$  units.

### 3.5.3 Procedures

#### Synthesis of $[\text{Cp}^*\text{Ru}(\text{PCy}_3)(\mu_2, \eta^{2:4}\text{P}_4\text{Cl}_2)\text{RuCp}^*]$ (38)

A dark blue suspension of  $[\text{Cp}^*\text{RuCl}]_4$  (3.50 g, 3.22 mmol, 1 eq) and  $\text{PCy}_3$  (3.61 g, 12.9 mmol, 4 eq) in *n*-hexane (25 mL) was stirred for 1 hour at room temperature and  $\text{P}_4$  (0.80 g, 6.44 mmol, 1/2 eq) was added as a solid. The dark brown suspension was stirred at room temperature for 20 h. The product was collected by filtration under nitrogen, washed with *n*-hexane (3x10 mL) and dried under vacuum to leave a light brown powder. Yield: 84 %. Single crystals suitable for X-ray diffraction were obtained from a saturated DME solution at  $-30\text{ }^\circ\text{C}$ .  $^1\text{H}$  NMR ( $\text{CD}_2\text{Cl}_2$ , 300 MHz, 293 K):  $\delta = 1.92$  (s, 30H,  $\text{CH}_3$ ), 1.90 – 1.20 (m, 33H,  $\text{PCy}_3$ ) ppm.  $^{31}\text{P}\{^1\text{H}\}$  NMR ( $\text{THF-}d_8$ , 203 MHz, 293 K):  $\delta = 250.8$  (br d,  $w_{1/2} = 325$  Hz,  $^1J_{\text{PP}} = 400$  Hz, 2P,  $\text{P}_1\text{-P}_4$ ), 43.3 (t, 37 Hz, 1P,  $\text{P}_{\text{PCy}_3}$ ),  $-68.8$  (br s,  $w_{1/2} = 3000$  Hz, 2P,  $\text{P}_2\text{-P}_3$ ) ppm.  $^{31}\text{P}\{^1\text{H}\}$  NMR ( $\text{THF-}d_8$ , 203 MHz, 233 K):  $\delta = 253.8$  (ddd,  $^1J_{\text{PP}} = 427$  Hz,  $^1J_{\text{PP}} = 137$  Hz,  $^2J_{\text{PP}} = 32$  Hz, 1P,  $\text{P}_1$ ), 246.8 (ddd,  $^1J_{\text{PP}} = 429$  Hz,  $^1J_{\text{PP}} = 137$  Hz,  $^2J_{\text{PP}} = 34$  Hz, 1P,  $\text{P}_4$ ), 43.3 (t,  $^2J_{\text{PP}} = 32$  Hz,  $^2J_{\text{PP}} = 34$  Hz, 1P,  $\text{P}_{\text{PCy}_3}$ ),  $-62.5$  (dd,  $^1J_{\text{PP}} = 429$  Hz,  $^2J_{\text{PP}} = 378$  Hz, 1P,  $\text{P}_3$ ),  $-80.1$  (dd,  $^1J_{\text{PP}} = 427$  Hz,  $^1J_{\text{PP}} = 378$  Hz, 1P,  $\text{P}_2$ ) ppm.  $^{31}\text{P}\{^1\text{H}\}$  NMR ( $\text{THF-}d_8$ , 101 MHz, 325 K):  $\delta = 252.3$  (dd,  $^1J_{\text{PP}} = 420$  Hz,  $^2J_{\text{PP}} = 37$  Hz, 2P,  $\text{P}_1\text{-P}_4$ ), 43.3 (t,  $^2J_{\text{PP}} = 37$  Hz, 1P,  $\text{P}_{\text{PCy}_3}$ ),  $-64.2$  (br. d,  $^1J_{\text{PP}} = 420$  Hz, 2P,  $\text{P}_2\text{-P}_3$ ) ppm.

### Synthesis of [Cp\***RuBr**]<sub>4</sub> (**39**)

The procedure followed for the synthesis of **39** is analogue to that used for [Cp\***RuCl**]<sub>4</sub>.

A solution of LiEt<sub>3</sub>BH 1M in THF (5.6 mL, 5.049 mmol) was added drop by drop to a suspension of [Cp\***RuBr**]<sub>2</sub> (2.0 g, 5.049 mmol) in 4 ml of THF. The reaction was stirred for 1 hour at room temperature. The light brownish solid was precipitated and the reddish brown solution was removed by syringe. The solid was then washed with 1 mL of cold THF and dried under vacuum. Yield: 60%. <sup>1</sup>H NMR (300 MHz, C<sub>6</sub>D<sub>6</sub>, 293 K):  $\delta = 1.70$  (s, CH<sub>3</sub>, Cp\*) ppm.

### Synthesis of [Cp\***Ru(PCy**<sub>3</sub>)**Br**] (**40**)

To a brown suspension of [Cp\***RuBr**]<sub>4</sub> (300.0 mg, 0.234 mmol) in 10 ml of *n*-pentane, tricyclohexyl phosphine (267.0 mg, 0.936 mmol, 4 eq) was added. The solution became immediately deep blue. The mixture was stirred for 1 hour at room temperature. A small aliquot was taken for NMR characterization. <sup>1</sup>H NMR (300 MHz, C<sub>6</sub>D<sub>6</sub>, 298 K):  $\delta = 1.87$  (m, 6H, CH<sub>2</sub> p-, PCy<sub>3</sub>), 1.68 (m, 12H, CH<sub>2</sub> m-, PCy<sub>3</sub>), 1.46 (m, 18H, CH, PCy<sub>3</sub> + Cp\*), 1.18 (m, 12H, CH, CH<sub>2</sub> o-, PCy<sub>3</sub>) ppm. <sup>31</sup>P{<sup>1</sup>H} NMR (121 MHz, C<sub>6</sub>D<sub>6</sub>, 295 K):  $\delta = 41.9$  (s) ppm. <sup>13</sup>C NMR (75.5 MHz, C<sub>6</sub>D<sub>6</sub>, 298 K) = 74.6 (Cp\*), 34.6 (d, <sup>1</sup>J<sub>CP</sub> = 16 Hz, CH), 30.9 (CH<sub>2</sub> m-) 28.2 (d, <sup>2</sup>J<sub>CP</sub> = 8 Hz, CH<sub>2</sub> o-), 26.8 (CH<sub>2</sub> p-), 11.6 (CH, CH<sub>3</sub>) ppm.

### Synthesis of [Cp\***Ru(PCy**<sub>3</sub>)( $\mu_2, \eta^{2:4}$ **P**<sub>4</sub>**Br**<sub>2</sub>)**Ru**Cp\*] (**41**)

Solid P<sub>4</sub> (58.03 mg, 0.468 mmol, 1/2 eq) was added to the previous solution of **40** and the reaction mixture was stirred for 16 h at room temperature. Afterwards a dark brown solid precipitated and the supernatant

### Chapter 3

was taken off with a syringe. The brownish solid was washed with 3x1 mL of pentane and dried under vacuum. Yield: 70%.  $^1\text{H-NMR}$  (THF- $d_8$ , 300 MHz, 293 K):  $\delta = 1.90$  (s, 30 H,  $\text{CH}_3$ ), 1.84–1.26 (m, 33 H,  $\text{PCy}_3$ ) ppm.  $^{31}\text{P}\{^1\text{H}\}$  NMR (THF- $d_8$ , 121 MHz, 293 K):  $\delta = 261.0$  (br. d,  $w_{1/2} = 255$  Hz,  $^1J_{\text{PP}} = 387$  Hz, 2P,  $\text{P}_1\text{-P}_4$ ), 39.9 (t, 37 Hz, 1P,  $\text{P}_{\text{PCy}_3}$ ),  $-58.0$  (br s,  $w_{1/2} = 1300$  Hz, 2P,  $\text{P}_2\text{-P}_3$ ) ppm.  $^{31}\text{P}\{^1\text{H}\}$  NMR (THF- $d_8$ , 121 MHz, 233 K):  $\delta = 253.8$  (ddd,  $^1J_{\text{PP}} = 415$  Hz,  $^1J_{\text{PP}} = 160$  Hz,  $^2J_{\text{PP}} = 35$  Hz, 1P,  $\text{P}_1$ ), 246.8 (ddd,  $^1J_{\text{PP}} = 417$  Hz,  $^1J_{\text{PP}} = 160$  Hz,  $^2J_{\text{PP}} = 34$  Hz, 1P,  $\text{P}_4$ ), 39.9 (t,  $^2J_{\text{PP}} = 35$  Hz, 1P,  $\text{P}_{\text{PCy}_3}$ ),  $-54.1$  (dd,  $^1J_{\text{PP}} = 417$  Hz,  $^1J_{\text{PP}} = 383$  Hz, 1P,  $\text{P}_3$ ) – 72.4 (dd,  $^1J_{\text{PP}} = 415$  Hz,  $^1J_{\text{PP}} = 378$  Hz, 1P,  $\text{P}_2$ ) ppm.

Identical conditions of solvent, temperature and time were carried out under vacuum line using schlenck techniques obtaining a mixture of complexes.

**42a:**  $^{31}\text{P}$  NMR (162 MHz, THF- $d_8$ , 293 K):  $\delta = 138.1$  (m, 1P,  $\text{P}_A$ ), 65.1 (dm,  $^1J_{\text{PP}} = 200$  Hz,  $^1J_{\text{PH}} = 423$  Hz, 1P,  $\text{P}_B$ ), 41.1 (ddd,  $^2J_{\text{PP}} = 49$  Hz,  $^3J_{\text{PP}} = 13$  Hz,  $^3J_{\text{PP}} = 5$  Hz, 1P,  $\text{P}_{\text{Cy}_3}$ ),  $-36.2$  (ddd,  $^1J_{\text{PP}} = 319$  Hz,  $^1J_{\text{PP}} = 227$  Hz,  $^2J_{\text{PP}} = 10$  Hz, 1P,  $\text{P}_C$ ),  $-97.7$  (ddd,  $^1J_{\text{PP}} = 319$  Hz,  $^1J_{\text{PP}} = 137$  Hz,  $^3J_{\text{PP}} = 5$  Hz, 1P,  $\text{P}_D$ ) ppm.

**42b:**  $^{31}\text{P}$  NMR (162 MHz, THF- $d_8$ , 293 K):  $\delta = 135.9$  (m, 2P,  $\text{P}_A$ ), 82.0 (dm,  $^1J_{\text{PP}} = 239$  Hz,  $^1J_{\text{PH}} = 392$  Hz, 1P,  $\text{P}_B$ ), 40.0 (d,  $^2J_{\text{PP}} = 40$  Hz, 1P,  $\text{PCy}_3$ ),  $-36.6$  (ddd,  $^1J_{\text{PP}} = 319$  Hz,  $^1J_{\text{PP}} = 227$  Hz,  $^1J_{\text{PP}} = 10$  Hz, 1P,  $\text{P}_C$ ) ppm.

#### Synthesis of $[\text{Cp}^*\text{Ru}(\text{PCy}_3)\text{I}]$ (43)

To a suspension of  $[\text{Cp}^*\text{RuI}]_4$  (700.0 mg, 0.482 mmol) in 8 ml of *n*-pentane, tricyclohexyl phosphine (540.5 mg, 1.927 mmol, 4 eq) was

added. The solution becomes immediately deep blue. The mixture was stirred for 1 hour at room temperature. A small aliquot was taken for NMR characterization.  $^1\text{H}$  NMR (300 MHz,  $\text{C}_6\text{D}_6$ , 293K):  $\delta = 1.87$  (m, 6H,  $\text{CH}_2_{\text{p-}}$ ,  $\text{PCy}_3$ ), 1.67 (m, 12H,  $\text{CH}_2_{\text{m-}}$ ,  $\text{PCy}_3$ ), 1.49 (m, 3H, CH,  $\text{PCy}_3$ ), 1.49 (s, 15H,  $\text{Cp}^*$ ), 1.21 (m, 12H, CH,  $\text{CH}_2_{\text{o-}}$ ,  $\text{PCy}_3$ ) ppm.  $^{31}\text{P}\{^1\text{H}\}$  NMR (121 MHz,  $\text{THF-d}_8$ , 293K):  $\delta = 46.3$  (s) ppm.  $^{13}\text{C}$  NMR (75.5 MHz,  $\text{THF-d}_8$ , 293K):  $\delta = 74.7$  ( $\text{Cp}^*$ ), 35.0 (pseudo quartet,  $^1J_{\text{CP}} = 18$  Hz, CH), 30.7 ( $\text{CH}_2_{\text{m-}}$ ) 27.9 (d,  $^2J_{\text{CP}} = 9$  Hz,  $\text{CH}_2_{\text{o-}}$ ), 26.8 ( $\text{CH}_2_{\text{p-}}$ ), 11.9 (CH,  $\text{CH}_3$ ) ppm.

**Synthesis of  $[\{\text{Cp}^*\text{Ru}(\text{PCy}_3)\}(\mu, \eta^1, \eta^3\text{-P}_4\text{I})(\text{RuCp}^*)]\text{I}$  (or  $[\{\text{Cp}^*\text{RuI}(\text{PCy}_3)\}(\mu, \eta^1, \eta^3\text{-P}_4)(\text{RuCp}^*)]\text{I}$  (44)**

Solid  $\text{P}_4$  (119.4 mg, 0.964 mmol, 1/2 eq) was added to a solution of **43** prepared as described above. After two minutes the colour changes from blue to brown. The reaction mixture was stirred for 16 hours at room temperature. Afterwards, a dark brown solid was formed and left to settle down. The supernatant was removed by syringe and the brown product was washed with 3x1 mL of *n*-pentane and 3x2 mL of ethanol and dried under vacuum. Yield: 52%.  $^1\text{H}$  NMR (400 MHz,  $\text{THF-d}_8$ , 293 K):  $\delta = 1.89$ -1.74 (m, 33 H,  $\text{Cp}^* + \text{CH}_2_{\text{m-, p-}}$   $\text{PCy}_3$ ), 1.31 (m, 15H, CH,  $\text{CH}_2_{\text{o-}}$ ,  $\text{PCy}_3$ ) ppm.  $^{31}\text{P}\{^1\text{H}\}$  NMR (162 MHz,  $\text{THF-d}_8$ , 293K):  $\delta = 620.9$  (br. tt,  $^1J_{\text{PP}} = 333$  Hz,  $^2J_{\text{PP}} = 31$  Hz, 1P,  $\text{P}_A$ ), 389.8 (ddd,  $^1J_{\text{PP}} = 333$  Hz,  $^1J_{\text{PP}} = 237$  Hz,  $^2J_{\text{PP}} = 44$  Hz, 1P,  $\text{P}_B$ ), 373.9 (ddd,  $^1J_{\text{PP}} = 333$  Hz,  $^2J_{\text{PP}} = 44$  Hz,  $^1J_{\text{PP}} = 247$  Hz, 1P,  $\text{P}_C$ ), 37.7 (d,  $^2J_{\text{PP}} = 31$  Hz, 1P,  $\text{PCy}_3$ ), -94.4 (br. td,  $^1J_{\text{PP}} = 240$  Hz,  $^1J_{\text{PP}} = 18$  Hz, 1P,  $\text{P}_D$ ) ppm. ESI-MS (acetonitrile):  $m/z = 1023.1$   $[\text{M}+\text{H}_2\text{O}]^+$ . Elemental analysis: calcd.: C, 40.36; H, 5.62. Found: C, 37.47; H, 5.42.



## References

---

- <sup>1</sup> M. Peruzzini, S. Mañas, A. Romerosa, A. Vacca, *Mendeleev Commun.* **2000**, *10*, 134-135.
- <sup>2</sup> V. Mirabello, M. Caporali, V. Gallo, L. Gonsalvi, D. Gudat, W. Frey, A. Ienco, M. Latronico, P. Mastroilli, M. Peruzzini, *Chem. Eur. J.* **2012**, *18*, 11238-11250.
- <sup>3</sup> I. de los Rios, J.-R. Hamon, P. Hamon, C. Lapinte, L. Toupet, A. Romerosa, M. Peruzzini, *Angew. Chem. Int. Ed. Engl.* **2001**, *40*, 3910-3912.
- <sup>4</sup> M. Caporali, L. Gonsalvi, R. Kagirov, V. Mirabello, M. Peruzzini, O. Sinyashin, P. Stoppioni, D. Yakhvarov, *J. Organomet. Chem.* **2012**, *714*, 67-73.
- <sup>5</sup> P. Barbaro, M. Di Vaira, M. Peruzzini, S. Seniori Costantini, P. Stoppioni, *Chem. Eur. J.* **2007**, *13*, 6682-6690.
- <sup>6</sup> M. Di Vaira, P. Frediani, S. Seniori Costantini, M. Peruzzini, P. Stoppioni, *Dalton Trans.* **2005**, 2234-2236.
- <sup>7</sup> M. Di Vaira, M. Peruzzini, S. Seniori Costantini, P. Stoppioni, *J. Organomet. Chem.* **2006**, *691*, 3931-3937.
- <sup>8</sup> P. Barbaro, M. Di Vaira, M. Peruzzini, S. Seniori Costantini, P. Stoppioni, *Angew. Chem. Int. Ed.* **2008**, *47*, 4425-4427.
- <sup>9</sup> M. Baudler *Chem. Rev.* **1994**, *94*, 1273-1297.
- <sup>10</sup> P. Barbaro, M. Di Vaira, M. Peruzzini, S. Seniori Costantini, P. Stoppioni, *Inorg. Chem.* **2009**, *48*, 1091-1096.
- <sup>11</sup> M. P. Mitoraj, A. Michalak, *Inorg. Chem.* **2010**, *49*, 2, 578-82.
- <sup>12</sup> B. K. Campion, R. H. Heyn, T. D. Tilley, *J. Chem. Soc.* **1988**, 278-280.
- <sup>13</sup> D. N. Akbayeva, *Russ. J. Coord. Chem.* **2006**, *32*, 329-334.
- <sup>14</sup> O. J. Scherer, M. Swarowsky, G. Wolmershäuser, *Organometallics* **1989**, *8*, 841-842.
- <sup>15</sup> M. Ouchi, M. Ito, S. Kanemoto, M. Sawamoto, *Chem. Asian J.* **2008**, *3*, 1358-1364.
- <sup>16</sup> P. J. Fagan, W. S. Mahoney, J. C. Calabrese, I. D. Williams, *Organometallics* **1990**, *9*, 1843-1852.
- <sup>17</sup> B. T. Sterenberg, K. A. Udachin, A. J. Carty, *Organometallics* **2003**, *22*, 3927-3932.
- <sup>18</sup> a) A. T. Termaten, T. Nijbacker, M. Schakel, M. Lutz, A. L. Spek, K. Lammertsma, *Chem. Eur. J.* **2003**, *9*, 2200-2208; b) R. Menye-Biyogo, F. Delpech, A. Castel, H. Gornitzka, P. Rivière, *Angew. Chem. Int. Ed.* **2003**, *42*, 5610-5612.
- <sup>19</sup> F. Delgado, M. Caporali, M. Peruzzini, unpublished results.

<sup>20</sup> P. J. Fagan, M. D. Ward, J. C. Calabrese, *J. Am. Chem. Soc.* **1989**, *111*, 1698-1719.

<sup>21</sup> U. Koelle, J. Kossakowski, *J. Organomet. Chem.* **1989**, *362*, 383-398.

<sup>22</sup> G. Sheldrick, *Acta Cryst.* **2015**, *A71*, 3-8.

<sup>23</sup> O. V. Dolomanov, L. J. Bourhis, R. J. Gildea, J. A. K. Howard, H. Puschmann, *J. Appl. Cryst.* **2009**, *42*, 339-341.

## **Synthesis, characterization and preliminary catalytic studies of white phosphorus-based ruthenium phosphide “RuP” nanoparticles**

### **4.1 Overview**

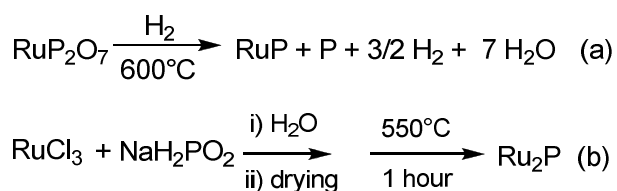
In this chapter the synthesis and characterization of ruthenium phosphide nanoparticles will be described. The novelty introduced is the use of white phosphorus as phosphorus source to react with previously prepared ruthenium nanoparticles. Preliminary results of the catalytic activity of ruthenium phosphide nanoparticles on the hydrogenation of phenylacetylene will be discussed.

## *Chapter 4*

## 4.2 Introduction

Metal phosphide nanoparticles are envisioned as suitable for a wide variety of applications, such as catalysis, transistors, solar cells, electronic and electrochemical devices or batteries.<sup>1</sup> In particular, metal phosphides used as catalysts show excellent activity for a specific class of reactions.<sup>1</sup> A variety of methods for their synthesis have been developed, including solvothermal reactions, high temperature annealing of organometallic and solid-state precursors, and the co-reaction of organometallic reagents with phosphines.<sup>2</sup>  $\text{PH}_3$ ,  $\text{P}(\text{SiMe}_3)_3$ , *tris-n-octylphosphine* or white phosphorus are some examples of the variety of phosphorus sources used for the formation of metal phosphide nanoparticles. Several parameters, such as stoichiometry of the reagents, temperature and nature of the phosphorus precursor are the key points to control the composition, shape, size and crystallinity of the metal phosphide nanoparticles which eventually will determine their applicability.<sup>3</sup>

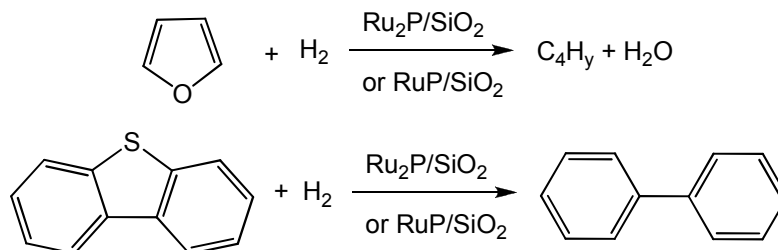
Until now, only two solid state methods have been described for the synthesis of ruthenium phosphide nanoparticles: (a) reduction of pyrophosphates using  $\text{H}_2$ <sup>4</sup> and (b) thermal decomposition of hypophosphites,<sup>5</sup> see **Scheme 4.1**. Noticeably, only two stoichiometries, *i.e.*  $\text{RuP}$  and  $\text{Ru}_2\text{P}$ , respectively, have been achieved.



**Scheme 4.1.** Solid state synthesis of ruthenium phosphide nanoparticles.

## Chapter 4

In 2008, a novel method based on the use of white phosphorus as ‘P’-source was developed by Mézailles *et al.*<sup>6</sup> to synthesize nickel phosphide nanoparticles (Ni<sub>2</sub>P). The method encompasses the reaction of elemental phosphorus with Ni(0) complexes as Ni(acac)<sub>2</sub> or Ni(COD)<sub>2</sub> (acac = acetylacetonate, COD = 1,5-cyclooctadiene) or preformed Ni(0) nanoparticles. Since then, the synthesis of a broad variety of metal phosphide nanoparticles, such as FeP, Cu<sub>3</sub>P, Pd<sub>5</sub>P<sub>2</sub>,<sup>7</sup> InP, Zn<sub>3</sub>P<sub>2</sub>,<sup>8</sup> or Au<sub>2</sub>P<sub>3</sub><sup>9</sup> has been performed in solution using white phosphorus. The discovery of the catalytic activity of metal phosphides nanoparticles in the 1990s led to a great interest for hydrogenation and hydrotreating reactions.<sup>10</sup> Despite large amount of studies on catalytic reactions catalysed by Ru(0) nanoparticles, as hydrogenation reactions,<sup>11</sup> carbon monoxide oxidation,<sup>12</sup> dehydrogenation of ammonia borane (NH<sub>3</sub>BH<sub>3</sub>) and hydrazine borane (N<sub>2</sub>H<sub>4</sub>BH<sub>3</sub>),<sup>13</sup> only very few examples of catalytic activity of ruthenium phosphide nanoparticles have been described. Bussell and co-workers studied the hydrodeoxygenation of furan<sup>5</sup> and the hydrodesulfurization of dibenzothiophene,<sup>14</sup> see **Scheme 4.2.**, using silica supported ruthenium phosphides (Ru<sub>2</sub>P and RuP).



**Scheme 4.2.** Hydrodeoxygenation of furan (a) and hydrodesulfurization of benzothiophene (b).

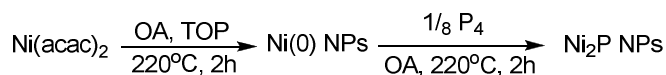
## Chapter 4

Li *et al.*<sup>15</sup> prepared ruthenium phosphide nanoparticles by thermal decomposition of ruthenium chloride and hypophosphite followed by impregnation on MCM-41 support and exhibited higher catalytic activity than Ru/MCM-41 catalyst on the hydrodesulfurization (HDS) of dibenzothiophene and hydrodenitrogenation (HDN) of quinoline. Moreover, RuP nanoparticles were used as electrocatalysts in the oxygen reduction process in acid conditions, being known that RuP has high stability in acid solutions and higher electronic conductivity compared to Ru carbides and nitrides.<sup>16</sup>

Our aim has been the synthesis of ruthenium phosphide nanoparticles through a new route, *i.e.* using white phosphorus as ‘P’-source. Afterwards, RuP nanoparticles have been tested in the form of colloidal dispersion, as unsupported nanostructured catalysts, in the hydrogenation of unsaturated organic substrates. This represents the exploitation of a new application for this material, being known RuP and Ru<sub>2</sub>P as catalysts only for hydrotreating processes.<sup>10</sup>

### 4.3 Synthesis and characterization of RuP NPs

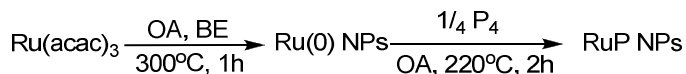
The original procedure by Mézailles<sup>17</sup> to prepare Ni<sub>2</sub>P nanoparticles consists first in the thermal decomposition of Ni(acac)<sub>2</sub> in the presence of oleylamine as reductant and *tris-n*-octylphosphine as stabilising agent to get Ni(0) nanoparticles and afterwards treatment with P<sub>4</sub><sup>6</sup> to afford the desired Ni<sub>2</sub>P as shown in **Scheme 4.3**.



OA = oleylamine  
TOP = trioctylphosphine

**Scheme 4.3.** Synthesis of Ni<sub>2</sub>P NPs.

We tried the same conditions to prepare Ru phosphide nanoparticles. Attempts to reduce Ru(acac)<sub>3</sub> at 220 °C, with different amount of oleylamine in the presence or absence of TOP as ligand, were accomplished without success. Therefore, we prepared ruthenium nanoparticles according to Can and Metin.<sup>18</sup> A mixture of Ru(acac)<sub>3</sub>, oleylamine and dibenzylether was first kept at 120 °C for one hour, then, it was quickly heated up to 300°C and kept at this temperature for an additional hour, see **Scheme 4.4**. After work-up, pure Ru(0) nanoparticles were isolated.



OA = oleylamine  
BE = benzylether

**Scheme 4.4.** Synthetic route to RuP nanoparticles.

**Figure 4.1.** PXRD spectrum of Ru(0) NPs confirming the identity and the purity of the material.



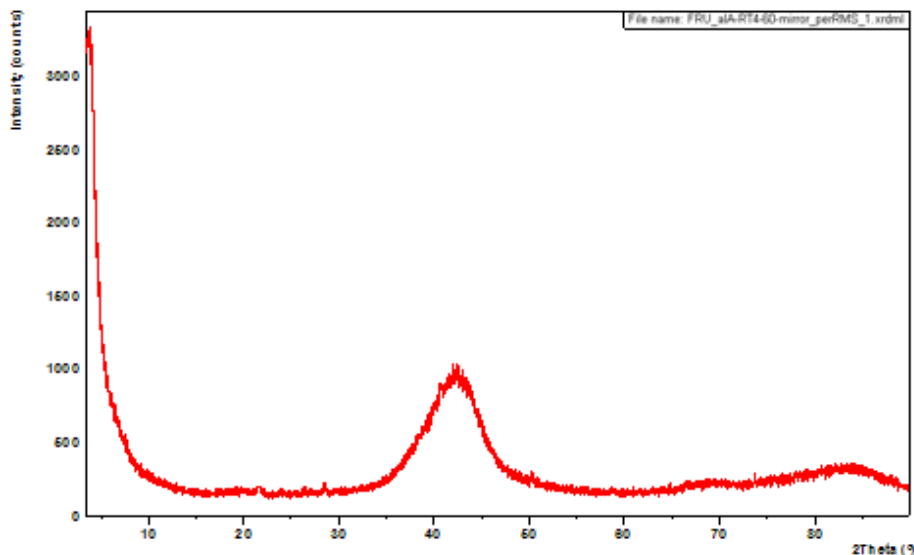


**Figure 4.1.** XRD spectrum of Ru(0) NPs.

Aimed at preparing RuP, we reacted a solution of previously synthesised Ru(0) NPs with the required amount of P<sub>4</sub> in order to have a molar ratio Ru:P equal to 1. As shown in **Scheme 4.4.**, to a mixture of Ru(0) NPs in oleylamine, ¼ P<sub>4</sub> solution in toluene was added. The solvent was then removed under vacuum and the mixture was quickly heated up to 220 °C and kept at this temperature for 2 hours.

The isolated black powder was analyzed by PXRD, see **Figure 4.2.** Although the peaks are very broad, due to the small size of RuP nanoparticles, we could confirm their identity and their purity. The observations of the peak at  $2\theta = 21^\circ$  and the most intense diffraction peaks at  $2\theta = 42^\circ$  and  $2\theta = 46^\circ$  corroborates the presence of the RuP phase, confirming the complete consumption of the precursor, Ru(0) NPs and the absence of any by-product, as for instance Ru<sub>2</sub>P.<sup>12</sup>

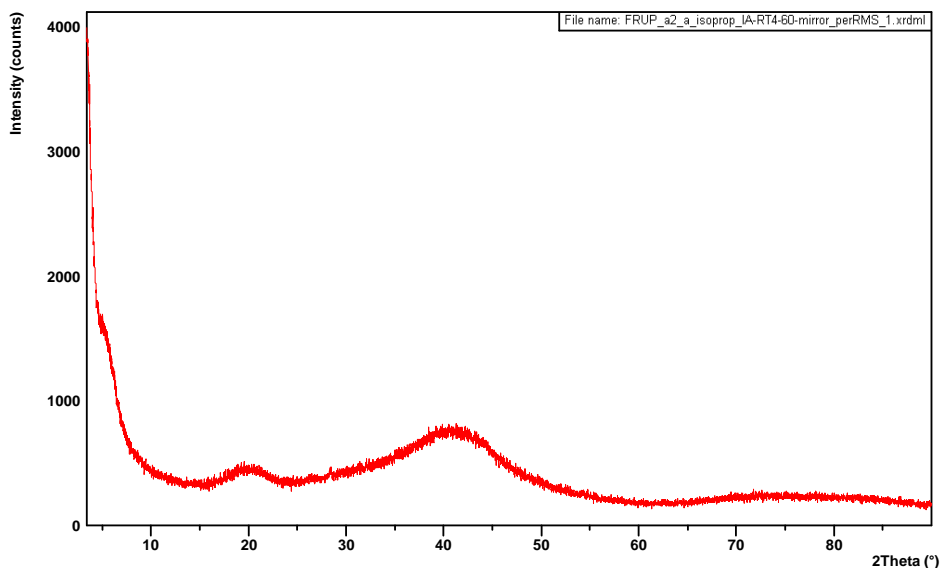


**Figure 4.2.** PXRD spectrum of RuP nanoparticles.

The prepared RuP nanoparticles are well dispersible in organic solvents, especially in THF and are stable in solution under nitrogen for long time at  $T = 4\text{ }^{\circ}\text{C}$ . As solids, they are stable under air for a short time.

To analyse the morphology of the RuP nanoparticles, a colloidal dispersion in THF was drop-casted on a carbon/copper grid and the sample was observed by transmission electron microscopy (TEM). As shown in **Figure 4.3**, RuP nanoparticles looked homogeneous both in the dimension and in the shape and no aggregates were detected.

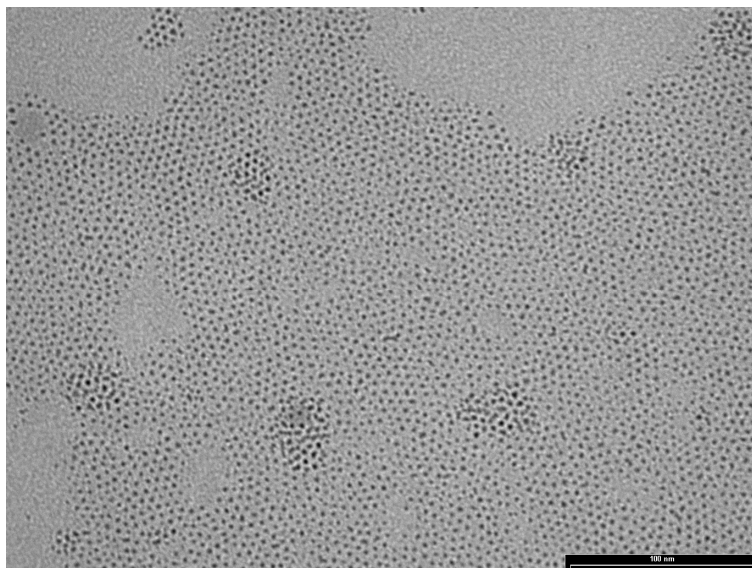


**Figure 4.3.** Bright field TEM image of RuP nanoparticles. Scale bar: 100 nm.

The relative size distribution histogram, see **Figure 4.4.** shows an average mean diameter of  $2.6 \pm 0.4$  nm for the prepared ruthenium phosphide nanoparticles.

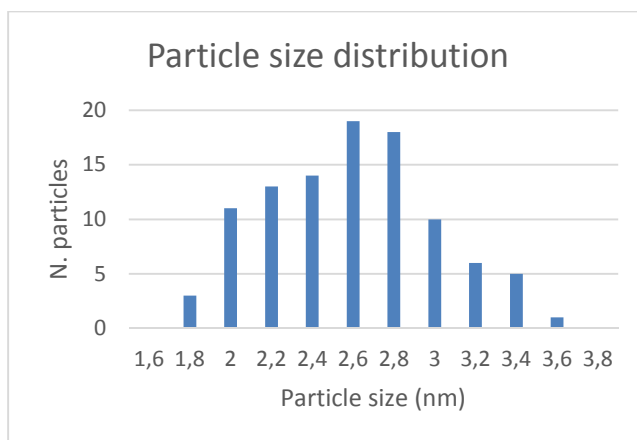


**Figure 4.4.** Particle size distribution of RuP nanoparticles.

## Chapter 4

X-Ray photoelectron spectroscopy is a technique very surface sensitive and allows discerning between elements in different chemical environments. We carried out XPS measurements on a sample of RuP nanoparticles in order to shed some light about the chemical nature and environment of ruthenium, phosphorus and carbon atoms located at the surface of the nanoparticles. **Figures 4.5.**, **4.6.** and **4.7.** display high resolution XPS spectra of C, Ru, O and N atoms, respectively. In **Figure 4.5.** the very intense peak of C at 284.8 eV typical of organic carbon, well agrees with the presence of oleylamine on the nanoparticles surface as stabilising agent. The Ru 3d core transition is characterized by a doublet due to the spin-orbital coupling, namely the 3d<sub>5/2</sub> and 3d<sub>3/2</sub> components, though the latter is covered by the carbon peak. The component responsible for the larger amount of the signal, located at lower values of binding energy (B.E. 3d<sub>5/2</sub> = 279.5 ± 0.1 eV), is attributable, on the basis of literature, either to bulk metallic ruthenium or to ruthenium phosphide. The minor peak (B.E. 3d<sub>5/2</sub> = 281.0 ± 0.1 eV) may be attributed to ruthenium oxide. Indeed, in **Figure 4.6.** we observe the spectrum of oxygen showing two components, the minor peak, at B.E. = 530.4 ± 0.1 eV, is attributable to oxygen in ruthenium oxide species, whereas the major, at B.E. = 532.3 ± 0.1 eV, is characteristic of carboxylate and is probably due to the presence of residual acetylacetonate.

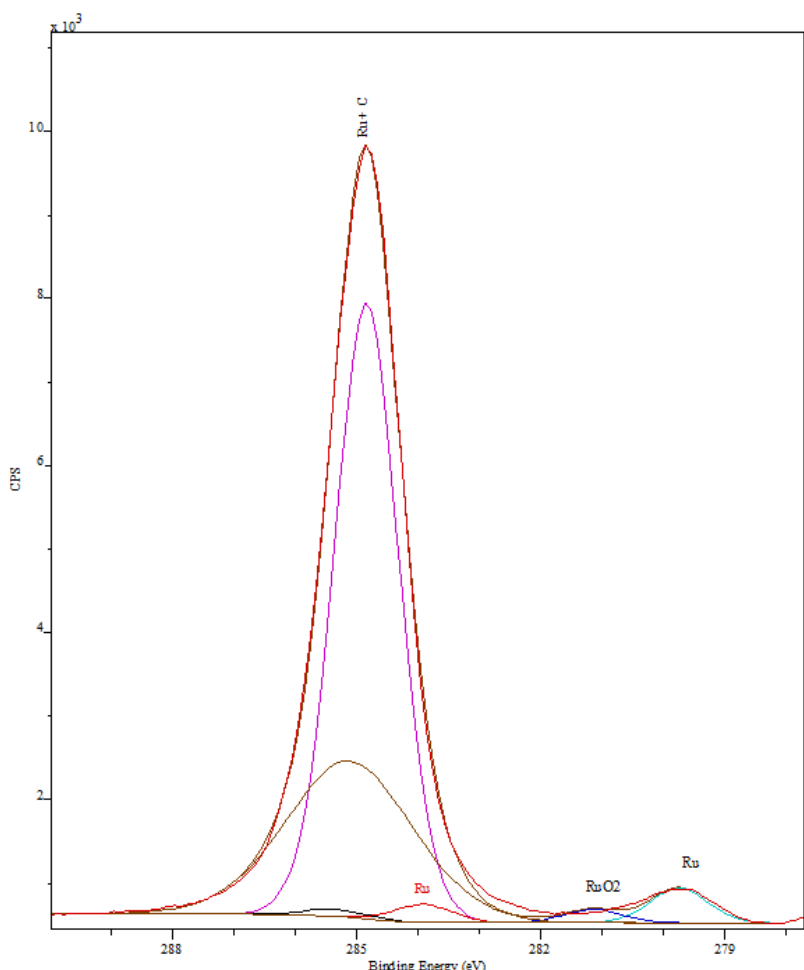


**Figure 4.5.** Curve fitting of C and Ru XPS spectra recorded on a dry sample of RuP nanoparticles.

In **Figure 4.7.** the nitrogen spectrum shows a weak signal at BE = 399.0 eV due to amine group of oleylamine.

Unfortunately, the signal of phosphorus could not be detected, which is not surprising in view of the fact that its sensitivity is nine time less than ruthenium, and the peak of ruthenium is in turn low due to the shadowing effect played by the carbon atoms of organic oleylamine and/or residual acetylacetonate adsorbed on the nanoparticles. In order to remove the

## Chapter 4

surface contaminants, the sample was Ar-sputtered for 30 minutes and afterwards XPS was measured again. The spectra, before and after sputtering (**Figure 4.8**), do not present relevant differences demonstrating that the presence of carbon-rich compounds can not be only ascribed to surface contaminations but it is related to the nature and the structure of the nanoparticles.

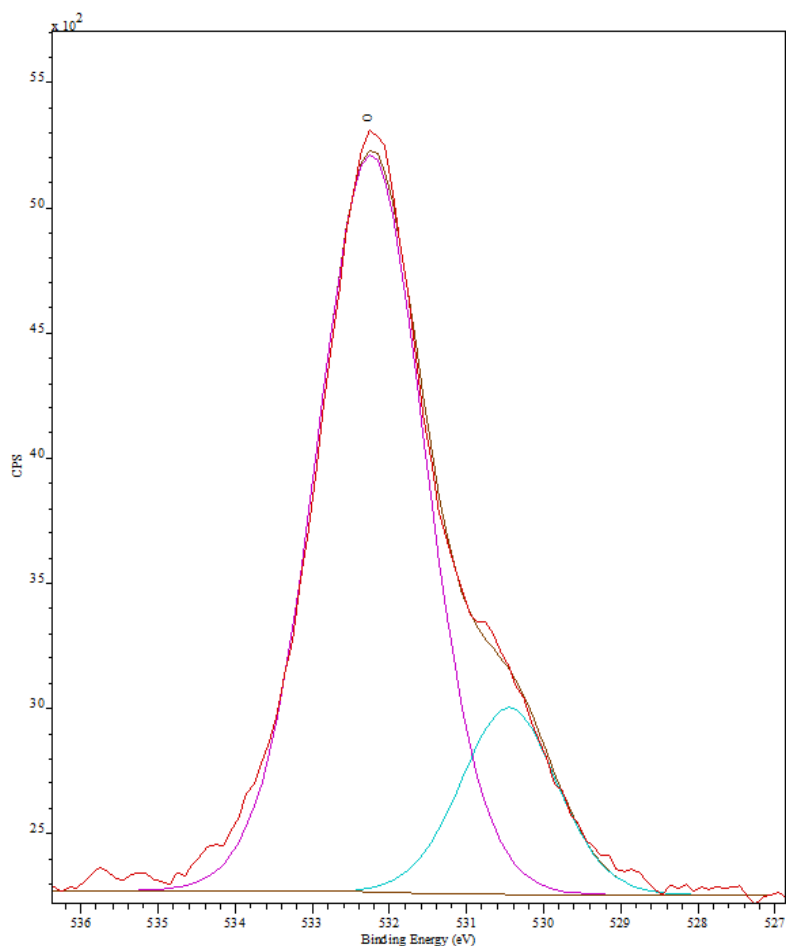


**Figure 4.6.** Curve fitting of the oxygen XPS spectra recorded on a dry sample of RuP nanoparticles.

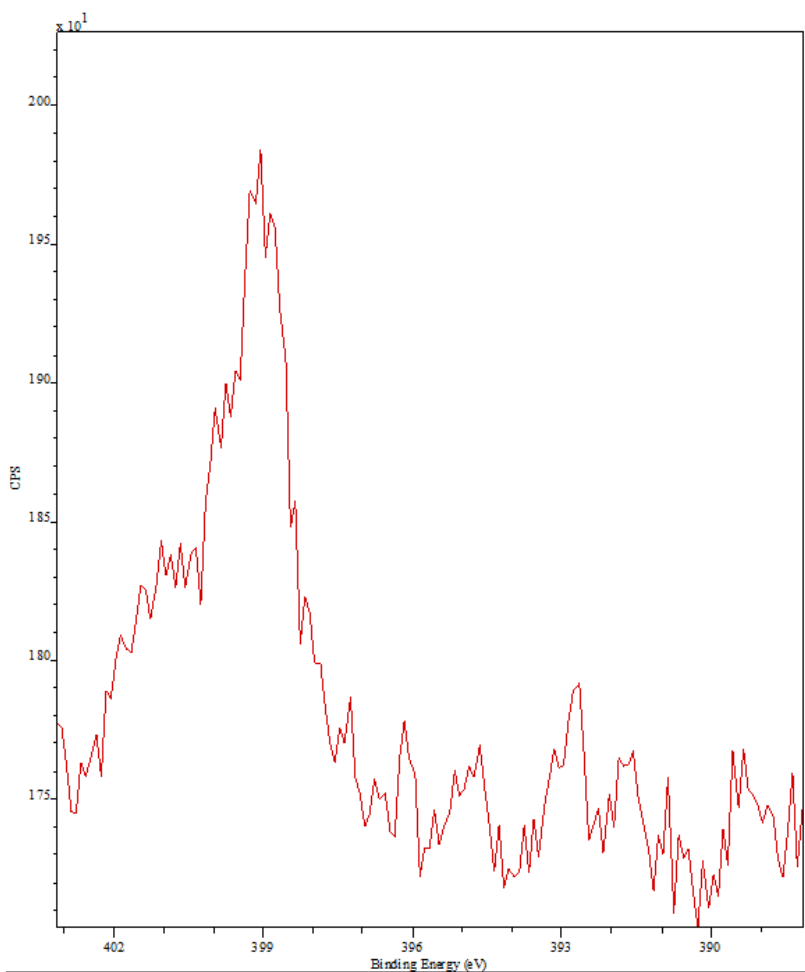


**Figure 4.7.** Curve fitting of the nitrogen XPS spectra recorded on a dry sample of RuP nanoparticles.

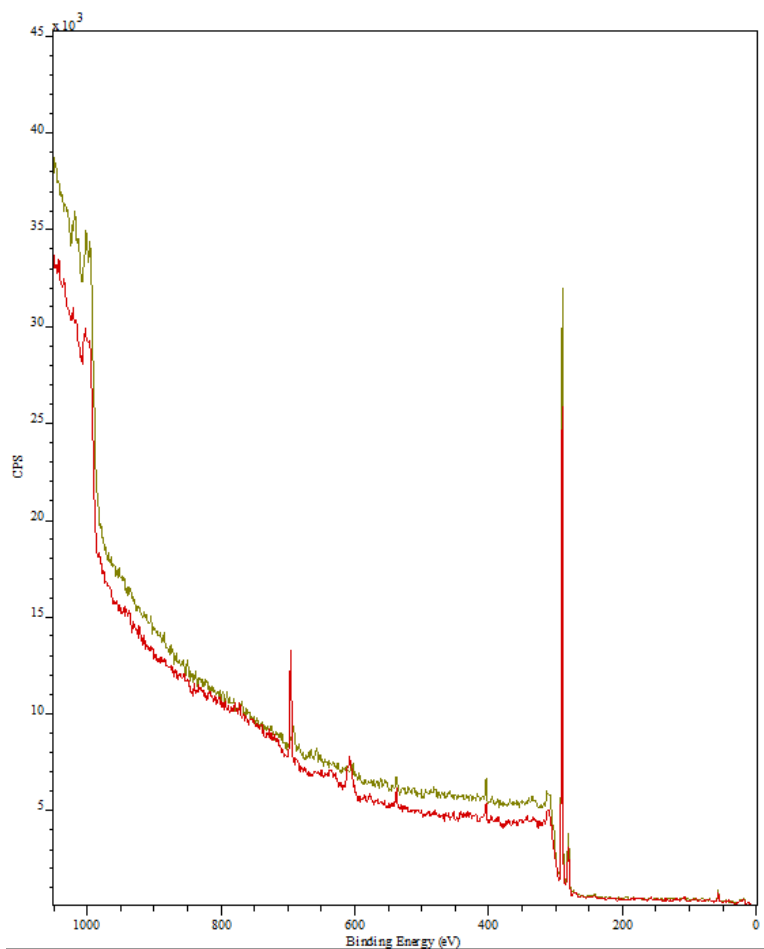
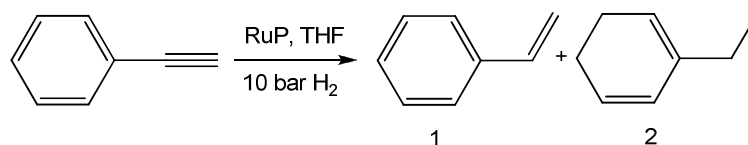


**Figure 4.8.** XPS of RuP before (red) and after (green) sputtering.

## 4.5 Catalytic tests

As preliminary study, RuP nanoparticles were examined as catalysts in the hydrogenation of phenylacetylene, see **Scheme 4.5**.





**Scheme 4.5.** Catalytic hydrogenation of phenylacetylene.

The results of the catalytic tests are summarised in **Table 4.1**. The catalytic activity of RuP nanoparticles was studied using the same conditions reported by Mézailles for the hydrogenation of phenylacetylene catalysed by Ni<sub>2</sub>P NPs (7% mol catalyst in THF at 66 °C).<sup>19</sup> While with Ni<sub>2</sub>P nanoparticles, the conversion of phenylacetylene is only 70%, with 98% selectivity towards styrene and only 2% for ethylbenzene, in the case of RuP, the fully hydrogenated product, *i.e.* ethylbenzene, is formed, with 100% selectivity. Repeating the reaction with an increased ratio RuP:phenylacetylene (7:1000 mol), complete hydrogenation to ethylbenzene was observed again.

Entry	Cat (% mol)	Temp (°C)	Time (h)	Conv. (%)	Select. 2 <sup>[a]</sup> (%)	TON	TOF
1	7	66	16	100	100	14.4	0.9
2	7	66	5	100	100	14.4	2.9
3	0.7	66	5	100	100	144	28.8
4	0.7	66	1	95	39	53	53

**Table 4.1.** General conditions: 10 bar H<sub>2</sub>, 0.0864 M of substrate in THF, [a] measured by GC-MS, TON = mol of desired product/mol of catalyst; TOF = mol of desired product/mol of catalyst / time (h<sup>-1</sup>).

## 4.6 Conclusions

A new procedure for the synthesis of ruthenium phosphide NPs was implemented, involving white phosphorus as “P” source and avoiding harsh conditions, as high temperature. The isolated RuP NPs have been characterised by powder X-ray diffraction which confirms the identity of the compound, the phase purity and the crystallinity. Moreover, TEM measurements show the material is highly homogeneous, constituted by very small nanoparticles, having an average diameter of 2.6 nm. Preliminary tests on hydrogenation of phenylacetylene in mild conditions showed very good catalytic activity and selectivity towards the fully hydrogenated product, ethylbenzene. Further studies on different unsaturated substrates will be carried out in the next months. Moreover, synthesis of Ru<sub>2</sub>P nanoparticles will be also performed and a new series of catalytic studies on hydrogenation reactions will be carried out.

## 4.7 Experimental part

### 4.7.1 Chemicals

All reactions were carried out under argon or nitrogen atmosphere. All the solvents used were of analytical grade and were dried and degassed before use. THF was purified by distillation under Na/benzophenone. RuCl<sub>3</sub>.xH<sub>2</sub>O, acetylacetone, benzylether and oleylamine were used without further purification. Ru(acac)<sub>3</sub> was synthesized according to the literature.<sup>20</sup>

## 4.7.2 Characterization methods

### Transmission electron microscopy

TEM studies were carried out using a Philips instrument operating at an accelerating voltage of 100 kV. Few drops of the palladium colloidal suspension, obtained using either toluene or water, were placed on the TEM lacey copper/carbon grid or copper/formvar grid respectively, air dried and measured.

### Powder X-ray diffraction

PXRD data were collected with an X'Pert PRO diffractometer with Cu-K $\alpha$  radiation ( $\lambda = 1.5418$ ).

### X-ray Photoelectron Spectroscopy

XPS measurements were performed in an ultra-high vacuum (10<sup>-9</sup> mbar) system equipped with a VSW HAC 5000 hemispherical electron energy analyzer and a non-monochromatized Mg-K $\alpha$  X-ray source (1253.6 eV). The source power was 100 W (10 kV $\times$ 10 mA) and the spectra were acquired in the constant-pass-energy mode at E<sub>pas</sub> = 44 eV. The overall energy resolution was 1.2 eV as a full-width at half maximum (FWHM) for the Ag 3d<sub>5/2</sub> line of a pure silver reference. The recorded spectra were fitted using XPS Peak 4.1 software employing Gauss-Lorentz curves after subtraction of a Shirley-type background. The powder sample was introduced in the UHV system via a loadlock under inert gas (N<sub>2</sub>) flux, in order to minimize the exposure to air contaminants and kept in the introduction chamber for at least 12 hours before the measurements.

### 4.7.3 Procedures

#### Synthesis of Ru NPs

The preparation of Ru(0) nanoparticles from ruthenium(III) acetylacetonate was carried out following the procedure by Can and Metin with minor modifications.<sup>32</sup>

A red suspension of Ru(acac)<sub>3</sub> (400 mg, 1.00 mmol) in oleylamine (20 ml, 60.79 mmol) and dibenzylether (16 mL) was degassed with 3 vacuum/N<sub>2</sub> cycles at 120 °C. This temperature was maintained for one hour. Then, the resulted solution was heated up to 300 °C for one hour. The black solution was then cooled down to room temperature, isopropanol and acetone (1:1) were added (100 mL) and after centrifugation at 10000 rpm per one hour, the nanoparticles were isolated and dried under a current of nitrogen.

#### Synthesis of RuP NPs

To a degassed solution of Ru(0) nanoparticles (60.0 mg, 0.594 mmol) in oleylamine (6.0 mL), a solution of P<sub>4</sub> (1.4 mL, 0.149 mmol, 0.11 M, 0.25 eq) in toluene was added. Toluene was removed under vacuum and the solution was quickly heated up to 220 °C and kept at this temperature for 2 hours. The reaction was cooled down, isopropanol and acetone were added (100 mL) and after centrifugation at 10000 rpm per one hour, the nanoparticles were isolated and dried under a current of nitrogen.

#### Catalytic hydrogenations

In a typical experiment, a 100 mL stainless steel autoclave home-built in the mechanical workshop of CNR-ICCOM was equipped with a vial, containing a magnetic stirrer, and charged with a suspension of previously

## *Chapter 4*

prepared RuP nanoparticles in THF under an inert atmosphere. Phenylacetylene was added, then the autoclave was sealed and purged with hydrogen (3 times), before being pressurized with hydrogen up to 10 bar. The autoclave was kept stirring at 25 °C or 66 °C for the required time. After that, the autoclave was cautiously depressurized, the solution was filtered through alumina to remove the catalyst and the filtrate (unreacted substrate and products) was analyzed by GC.

## References

---

- <sup>1</sup> S. Carencó, D. Portehault, C. Boissière, N. Mézailles, C. Sanchez, *Chem. Rev.* **2013**, *113*, 7981-8065.
- <sup>2</sup> Q. Guan, W. Li, M. Zhang, K. Tao *J. Catal.* **2009**, *263*, 1-3.
- <sup>3</sup> S. Carencó, D. Portehault, C. Boissière, N. Mézailles, C. Sanchez, *Adv. Mater.* **2014**, *26*, 371-390.
- <sup>4</sup> J. Gopalakrishnan, S. Pandey, K. K. Rangan, *Chem. Mater.* **1997**, *9*, 2113-2116.
- <sup>5</sup> a) R. H. Bowker, M. C. Smith, M. L. Pease, K. M. Slenkamp, L. Kovarik, M. E. Bussell, *ACS Catal.* **2011**, *1*, 917-922. b) H. Teller, O. Krichevski, M. Gur, A. Gedanken, A. Schechter, *ACS Catal.* **2015**, *5*, 4260-4267.
- <sup>6</sup> S. Carencó, I. Resa, X. Le Goff, P. Le Floch, N. Mézailles, *Chem. Commun.* **2008**, 2568-2570.
- <sup>7</sup> S. Carencó, Y. Hu, I. Florea, O. Ersen, C. Boissière, N. Mézailles, C. Sanchez, *Chem. Mater.* **2012**, *24*, 4134-4145.
- <sup>8</sup> S. Carencó, M. Demange, J. Shi, C. Boissière, C. Sanchez, P. Le Floch, N. Mézailles, *Chem. Commun.* **2010**, *46*, 5578-5580.
- <sup>9</sup> S. Carencó, I. Florea, O. Ersen, C. Boissière, N. Mézailles, C. Sanchez, *New J. Chem.* **2013**, *37*, 1231-1237.
- <sup>10</sup> a) R. Prins, M. E. Bussell, *Catal. Lett.* **2012**, *142*, 1413-1436. b) Y. Kanda, Y. Uemichi *J. Jpn. Petrol. Inst.* **2015**, *58*, 1, 20-32.
- <sup>11</sup> M. J.-L. Tschan, O. Diebolt, P. W. N. M. van Leeuwen, *Top. Catal.* **2014**, *57*, 1054-1065.
- <sup>12</sup> a) S. H. Joo, J. Y. Park, J. R. Renzas, D. R. Butcher, W. Huang, G. A. Somorja, *Nano Lett.* **2010**, *10*, 2709-2713. b) M. Sadakiyo, M. Kon-no, K. Sato, K. Nagaoka, H. Kasai, K. Kato, M. Yamauchi, *Dalton Trans.* **2014**, *43*, 11295.
- <sup>13</sup> Q. Yao, Z.-H. Lu, K. Yang, X. Chen, M. Zhu, *Scientific Reports* **2015**, *5*, 15186.
- <sup>14</sup> R. H. Bowker, M. C. Smith, B. A. Carrillo, M. E. Bussell, *Top Catal.* **2012**, *55*, 999-1009.
- <sup>15</sup> Q. Guan, C. Sun, R. Li, W. Li, *Cat. Commun.* **2011**, *14*, 114-117.
- <sup>16</sup> H. Teller, O. Krichevski, M. Gur, A. Gedanken, A. Schechter, *ACS Catal.* **2015**, *5*, 4260-4267.
- <sup>17</sup> S. Carencó, C. Boissière, L. Nicole, C. Sanchez, P. Le Floch, N. Mézailles, *Chem. Mater.* **2010**, *22*, 1340-1349.
- <sup>18</sup> H. Can, Ö. Metin, *Appl. Cat. B-Environ.* **2012**, *125*, 304-310.
- <sup>19</sup> S. Carencó, A. Leyva-Pérez, P. Concepción, C. Boissière, N. Mézailles, C. Sanchez, A. Corma, *Nano Today* **2012**, *7*, 21-28.

## Chapter 4

---

<sup>20</sup> F. M. A. Geilen, B. Engendahl, A. Harwardt, W. Marquardt, J. Klankermayer, W. Leitner, *Angew. Chem. Int. Ed.* **2010**, 49, 5510-5514.





## Appendix

### Crystal data

**Table 1.** Crystallographic data for  $\{[\text{CpRu}(\text{PPh}_3)_2\{\text{PhP}(\text{OH})_2\}]\text{CF}_3\text{SO}_3\} \cdot 27^{\text{OH}} \cdot \text{CCl}_2$

Formula	$\text{C}_{49}\text{H}_{42}\text{Cl}_2\text{F}_3\text{O}_5\text{P}_3\text{RuS}$
Formula weight	1064.77
Crystal system	Monoclinic
Space group	$P21/c$
$a$ (Å)	12.5099(2)
$b$ (Å)	13.2579(2)
$c$ (Å)	28.0827(6)
$\beta$ (°)	96.283(2)
$V$ (Å <sup>3</sup> )	4629.68(14)
$Z$	4
$T/\text{K}$	150(2)
$D_c$ (g cm <sup>-3</sup> )	1.528
Crystal size (mm)	$0.30 \times 0.25 \times 0.20$
$\mu$ (mm <sup>-1</sup> )	0.662
$2\theta$ range (°)	8.26-57.80
Total reflections	10671
Unique reflections ( $R_{\text{int}}$ )	10653 (0.04)
Observed reflections [ $I > 2\sigma(I)$ ]	9192
Parameters	594
Final $R$ indices [ $I > 2\sigma(I)$ ]	$R_1$ 0.0413, $wR_2$ 0.1066
Max., min., $\Delta\rho$ (e Å <sup>-3</sup> )	1.553, -1.439
Goodness of fit on $F^2$	1.045

**Table 2.** Crystallographic data for  $[(\eta^6\text{-}p\text{-cymene})\text{RuCl}_2\{\text{PhP}(\text{OH})_2\}] \cdot 30\text{H}_2\text{O}$ 

Formula	$\text{C}_{16}\text{H}_{21}\text{Cl}_2\text{O}_2\text{PRu}$
Formula weight	448.27
Crystal system	Monoclinic
Space group	$P2_1/n$
$a$ (Å)	12.4787(2)
$b$ (Å)	11.3676(1)
$c$ (Å)	13.2916(2)
$\beta$ (°)	107.962(1)
$V$ (Å <sup>3</sup> )	1793.56(4)
$Z$	4
$T/\text{K}$	150(2)
$D_c$ (g cm <sup>-3</sup> )	1.660
Crystal size (mm)	$0.20 \times 0.20 \times 0.10$
$\mu$ (mm <sup>-1</sup> )	10.687
$2\theta$ range (°)	10.46-144.12
Total reflections	3481
Unique reflections ( $R_{\text{int}}$ )	3473
Observed reflections [ $I > 2\sigma(I)$ ]	3222
Parameters	210
Final $R$ indices [ $I > 2\sigma(I)$ ]	$R_1$ 0.0429, $wR_2$ 0.1131
Max., min., $\Delta\rho$ (e Å <sup>-3</sup> )	0.987, -0.893
Goodness of fit on $F^2$	1.043

Appendix

**Table 3.** Crystallographic data for  $[\{\text{Cp}^*\text{Ru}(\text{PCy}_3)\}(\mu^2, \eta^2\text{:}^4\text{P}_4\text{Cl}_2)\text{-}\{\text{RuCp}^*\}] \cdot 38\text{-DME}$

Formula	$\text{C}_{42}\text{H}_{72}\text{Cl}_2\text{O}_2\text{P}_5\text{Ru}$
Formula weight	1036.88
Crystal system	Triclinic
Space group	$P-1$
$a$ (Å)	12.7474(2)
$b$ (Å)	13.3991(2)
$c$ (Å)	14.5781(3)
$\alpha$ (°)	70.6590(10)
$\beta$ (°)	79.0950(10)
$\gamma$ (°)	88.9330(10)
$V$ (Å <sup>3</sup> )	2304.44(7)
$Z$	2
$T/\text{K}$	296(2)
$D_c$ (g cm <sup>-3</sup> )	1.494
Crystal size (mm)	$0.02 \times 0.02 \times 0.02$
$\mu$ (mm <sup>-1</sup> )	0.979
$2\theta$ range (°)	3.01-66.35
Total reflections	67593
Unique reflections ( $R_{\text{int}}$ )	17466
Observed reflections [ $I > 2\sigma(I)$ ]	14778
Parameters	490
Final $R$ indices [ $I > 2\sigma(I)$ ]	$R_1$ 0.0355, $wR_2$ 0.0846
Max., min., $\Delta\rho$ (e Å <sup>-3</sup> )	2.077, -1.155
Goodness of fit on $F^2$	1.044

## *Appendix*

# Curriculum vitae

## Personal information

- Data and place of birth: 20/07/1986, Burgos, Spain
- e-mail: fdelgado@iccom.cnr.it  
fuenc86@gmail.com

## Education

- Doctoral candidate in Chemistry (Dottorato in Scienze Chimiche, Ciclo XXVIII) 2015, University of Florence, Florence, Italy. Supervisors: Dr. Maria Caporali, Dr. Maurizio Peruzzini.
- Master degree in Advanced Chemistry specializing in New Materials, 2012, University of Burgos, Burgos, Spain.
- Licenciata degree in Chemistry, 2010 University of Burgos, Burgos, Spain.

## Languages

- Spanish: native
- English: B2
- Italian: B2

## Technical skills

- Standard (vacuum line and Schlenk tube) and glove-box techniques for handling air-sensitive materials.
- Characterization of organic and inorganic compounds (NMR, IR, GC-MS, ESI-MS, elemental analysis, single crystal and powder X-ray diffraction, TEM).
- Standard purification techniques (crystallization, distillation).
- Specific computer programmes (ChemDraw, MestRe, TOPSPIN, ACDLABS) and Office Tools™ (Word™, Excel™, PowerPoint™).

## Research internships

- Collaboration in the group of Dr. Nicolas Mézailles, CNRS, Toulouse, France. 30<sup>th</sup> May - 27<sup>th</sup> June 2015.  
Synthesis and characterization of new ruthenium phosphide nanoparticles ( $\text{Ru}_x\text{P}_y$  NPs) prepared from metal nanoparticles and white phosphorus.
- Collaboration in the group of Prof. Grützmacher, ETHZ, Zürich, Switzerland. 26<sup>th</sup> April - 25<sup>th</sup> June 2014.  
Synthesis, reactivity and characterization of new bimetallic ruthenium complexes containing new  $\text{P}_4\text{X}_n$  ( $\text{X} = \text{Cl}, \text{I}$ ) ligands, coming from the metal-mediated activation of elemental phosphorus.

## Participation in congresses

- Oral communication:  
*“Ruthenium-based materials and their application in phosphorus chemistry”*  
SusPhos Fellows’ meeting, ICIQ, Tarragona, Spain, 6-10 July 2015.
- Oral communication:  
*“XtalFluor-E, a deoxofluorinating reagent for the formation of P-F bonds”*  
12<sup>th</sup> European Workshop on Phosphorus Chemistry (EWPC 2015), University of Kassel, Kassel, Germany, 16-18 March 2015.
- Participation to the First International Conference on Sustainable Phosphorus Chemistry (ICSPC 2014), Florence, Italy, 4-5 December 2014.
- Oral communication:  
*“Mild fluorination of phosphorus oxyacids. Coordination of  $\text{P}_4$  to transition metal complexes”*  
1<sup>st</sup> Annual SusPhos Meeting, Vrije University, Amsterdam, The Netherlands, 24-28 February 2014.

- Poster and Flash Presentation:  
*“Use of diethylaminodifluorosulfonium salt for the fluorination of phosphorus oxyacids”*  
 F. Delgado, V. Mirabello, K. Raltchev, K. Karaghiosoff, M. Caporali, L. Gonsalvi, W. Oberhauser, M. Peruzzini  
 9<sup>th</sup> International School of Organometallic Chemistry (ISOC 2013), Camerino (MC), Italy, 30 August-3 September 2013.
- Oral communication:  
*“Fluorination of phosphorus oxyacids mediated by ruthenium complexes”*  
 F. Delgado, V. Mirabello, K. Raltchev, K. Karaghiosoff, M. Caporali, L. Gonsalvi, W. Oberhauser, M. Peruzzini  
 XXXII Convegno Interregionale delle Sezioni Toscana, Umbria, Marche, Abruzzo della Società Chimica Italiana (TUMA 2013), CNR, Sesto Fiorentino (FI), Italy, 1-2 July 2013.

### **Publications**

- F. Delgado Calvo, V. Mirabello, M. Caporali, W. Oberhauser, K. Raltchev, K. Karaghiosoff, M. Peruzzini *“A straightforward access to ruthenium-coordinated fluorophosphines from phosphorous oxyacids”* (submitted)





## Aknowledgements

First of all, I would like to express my gratitude to my supervisors, Dr. Maria Caporali and Dr. Maurizio Peruzzini, for giving me this opportunity of working with them, within the European SusPhos project. A special thanks goes to Serena Orsi for all her assistance before my arrival and during this period in Florence. Thank Dr. Werner Oberhauser and Dr. Andrea Ienco for their support in single crystal X-ray diffraction and powder X-ray diffraction, respectively.

As part of SusPhos, I want to express my sincerest thanks and appreciation to Marissa de Boer and Prof. Chris Slootweg for their support and continuous interest on my professional evolution.

I would like to thank Prof. Hansjörg Grützmacher, and Dr. Nicolas Mézailles, who provided me an opportunity to join their team, at ETHZ and CNRS, respectively, for short time. Thanks to the lab colleagues, especially Mark Bispinghoff and Sébastien Dreyfuss, for making me easier the stay.

Thanks SusPhos fellows: Deniz, Joanne, Charly, Paul, Mark (again), Laurian, Aike, Frank, Priyanka, Massimo, Emmanuel, Tetiana and Koyel for all the great moments together.

Vorrei anche ringraziare tutti i ragazzi dell' ICCOM, in particolare Manuel, per la sua disponibilità e l'aiuto in laboratorio, Irene, Vanessa e Lapo, per le risate all' ora di pranzo, Antonella, Federica, Gabriele, Alessio, Carmen, Marco, Giulia, Stefano...

Por último, quiero agradecer a mis padres y hermanos que, aunque en la distancia, me han apoyado en todo momento y, que sin su ayuda, no hubiera sido posible realizar este sueño. Y a Enrique, que me ha apoyado y dado ánimos cada día, no dejando venirme abajo cuando, día tras día, los resultados en el laboratorio no eran buenos.

